Analyzing the Magnitude of Drought using Geospatial Technology: The Case of Yabello District, Borane Zone, Oromia Region, Ethiopia.

Abkula Jaldesa Tache

A Thesis Submitted to

The Department of Architecture Engineering

College of Civil Engineering and Architecture

Presented in Partial Fulfillment of the Requirement for the Degree of Master’s in Geo-informatics Engineering

Office of Graduate Studies

Adama Science and Technology University

November, 2024.

Adama, Ethiopia

Analyzing The Magnitude of Drought using Geospatial Technology: The Case of Yabello District, Borane Zone, Oromia Region, Ethiopia.

Abkula Jaldesa Tache

Advisor: Roba Gemechu (PhD)

A Thesis Submitted to

The Department of Architecture Engineering

College of Civil Engineering and Architecture

Presented in Partial Fulfillment of the Requirement for the Degree of Master's in Geo-informatics Engineering

Office of Graduate Studies

Adama Science and Technology University.

November, 2024.

Adama, Ethiopia.

APPROVAL SHEET

I, the advisor of the thesis entitled "Analyzing the magnitude of Drought using Geospatial Technology: The Case of Yabello district, Borane zone, Oromia Region, Ethiopia**.**" and developed by Abkula Jaldesa Tache, hereby certify that the recommendation and suggestions made by the board of examiners are appropriately incorporated into the final version of the thesis.

Advisor: - Roba Gemechu (PhD) Signature _______ Date _________

We, the undersigned, members of the Board of Examiners of the thesis by Abkula Jaldesa Tache have read and evaluated the thesis entitled "Analyzing the magnitude of Drought using Geospatial Technology: The Case of Yabello district, Borane zone, Oromia Region, Ethiopia**.**" and examined the candidate during open defense. This is, therefore, to certify that the thesis is accepted for partial fulfillment of the requirement of the degree of Master of Science in Geo-informatics Engineering.

______________________________	_____________	______________
Chairperson	Signature	Date
______________________________	_____________	______________
Internal Examiner	Signature	Date
______________________________	______________	______________
External Examiner	Signature	Date

Finally, approval and acceptance of the thesis is contingent upon submission of its final copy to the Office of Postgraduate Studies (OPGS) through the Department Graduate Council (DGC) and School Graduate Committee (SGC).

______________________________	_____________	_______________
Head of Department	Signature	Date
______________________________	_____________	_______________
School Dean	Signature	Date
______________________________	______________	________________
Office of Postgraduate Studies, Dean	Signature	Date

DECLARATION

I, Abkula Jaldesa Tache hereby declare that this Master Thesis entitled "Analyzing the magnitude of Drought using Geospatial Technology: the Case of Yabello district, Borane zone, Oromia Region, Ethiopia**.**" is my original work. That is, it has not been submitted for the award of any academic degree, diploma or certificate in any other university. All sources of materials that are used for this thesis have been duly acknowledged through citation.

Abkula Jaldesa Tache	_______________	_______________
Name of the student	Signature	Date

RECOMMENDATION

I, the advisor of this thesis, hereby certify that I have read the revised version of the thesis entitled "Analyzing the magnitude of Drought using Geospatial Technology: The Case of Yabello district, Borane zone, Oromia Region, Ethiopia**.**" prepared under my guidance by Abkula Jaldesa Tache submitted in partial fulfillment of the requirements for the degree of Mater's of Science in Geo-Informatics Engineering. Therefore, I recommend the submission of revised version of the thesis to the department following the applicable procedures.

Roba Gemechu (PhD) _______________ ________________

Advisor Signature Date

ACKNOWLEDGEMENT

First and foremost, I want to express my gratitude to Almighty Allah, the Lord of everything, who has made my entire existence possible and who keeps me well. I would like to express my deepest thanks and gratitude to my advisor Roba Gemechu (PhD) for his supervision, guidance, support and constructive comments throughout the completion of my thesis work. I have special thanks to Adama Science and Technology University (ASTU) for providing me with the financial means to continue my education and engage in relevant research in order to meet my study goals. Additionally, I want to thank the Ethiopian Meteorological Agency for cooperating with my request for rainfall data, which was sent on time.

Finally, I express my honest and sincere gratitude towards my parents, friends, and course instructors for their constant support and thoughtful encouragement throughout the writing of my thesis.

.

TABLE OF CONTENTS

CONTENTS PAGE

LIST OF TABLES

TABLES **PAGE**

LIST OF FIGURES

FIGURES **PAGE**

LIST OF ACRONYMS

ERDAS	Earth Resource Data Analysis System
GIS	Geographic Information System
IDW	Invers distance weighting
RS	Remote Sensing
NDVI	Normalized difference vegetation index
VCI	Vegetation condition index
SPSS	Statistical package for social sciences
CWBAL	Climatic water balance
SPI	Standardized Precipitation Index (SPI)
SPEI	Standardized Precipitation Evapotranspiration Index
USGS	United states geological survey

ABSTRACT

Drought is one of the major environmental disasters, which have been occurring in almost all In the planning and management analyzing drought impacts from the perspectives of environments and agricultural sectors is an essential requirement. Now a day, In addition to using meteorological data to analyze drought in a region, geospatial technologies such as remote sensing (RS) and geographic information systems (GIS) have emerged as important tools for identifying and analyzing agricultural drought because they provide remarkable data across a range of spatial and temporal scales. The district of Yabello in Ethiopia, where this study was carried out, affected by recurring meteorological and agricultural droughts impacts. Therefore, study focused on analyzing the magnitude of Drought through quantifying rain fall data and vegetation variation data in Yabello district by help of Geospatial technology. Monthly total precipitation, maximum and minimum monthly temperatures and landsat5, landsat7, and landsat8 satellite images of 28 years was the data used in the study from 1994 to 2022 years. Standardized Precipitation Index (SPI) and Standardized Precipitation Evapotranspiration Index (SPEI) at the 1, 2, 3, 6, 9, and 12-month scales calculated using Hargreaves method. For this, Pearson correlation coefficient (PCC) and Cohen's Kappa statistics examined the linear relationship and degree of agreement between SPI and SPEI, respectively. Normalized difference vegetation index anomaly(NDVI), DevNDVI, and vegetative condition index(VCI) from Landsat data quantified agricultural drought maps and combined with 2-month and 12-monthSPI / SPEI maps generated by IDW model to obtain overall drought hazard map of district for 28 years of study. Finding of this research revealed the high, positive, and statistically significant correlation between SPI and SPEI, ranged from 0.554 to 0.912 at $p<0.001$ using 95%o confidence interval. Also, Cohen's Kappa Statistics result indicated a statistically fair to substantial ((0.2–0.8) degree of agreement between SPI and SPEI in all investigated time scales at $p < 0.01$. Results indicated, 1998 and 1999 years was absolutely continuous driest year among the others. The overall drought hazards map indicated that, of the entire Yabello district, 30.46418% (9498.978km2), 66.48492% (20730.54km2), and 3.050904% (951.2966km2) were affected by low, moderate, and extreme drought, respectively. Analyzing the magnitude of drought and creating a map of drought hazards will assist to increase preparedness for disasters in regions that are prone to drought, identify areas that are most at risk for drought so that resources may be allocated for risk management, Mitigate the effects of drought (assists in determining the best measures to lessen the effects of drought)

Keywords: analyzing magnitude of drought, *drought index*, geospatial- technology, Yabello

CHAPTER ONE: INTRODUCTION

1.1 Background of the study

Drought is one of the world's worst natural disasters and a recurring issue (Kim et al., 2013). According to broad definitions, a drought is a brief climatic occurrence brought on by an extended period of low rainfall in comparison to normal and average conditions (Mondol et al., 2015). Drought is one of the major environmental disasters, which have been occurring in almost all climatic zones and damaging the environment, agriculture and economies of several countries. In particular, drought poses a threat to food, ecological security, and regional economic development(Queensland, 2021). According to the United Nations convention to combat desertification, which Thiaw (2022) forwarded, D. et al. (2021) reported that over 10 million people died as a result of severe drought events over the previous century, resulting in hundreds of billions of US dollars in economic losses globally, and that the number is still growing.

There are four different forms of drought: meteorological or climatological drought, hydrological drought, agricultural drought, and socioeconomic drought(Wilhite and Glantz, 1985,cited in Durowoju et al., 2022). A period of extended dryness is the simplest way to define meteorological drought. While agricultural drought refers to the impact of meteorological drought on agricultural practices and products, hydrological drought is closely related to the hydrology of a specific region and is commonly defined as the reduction of streamflow and groundwater level. Drought has an impact on people and their enterprises, leading to socioeconomic drought. According to Thomas et al.(2016), as described by Saha et al. (2022), the main effects of the three forms of drought on different socioeconomic activities is known as socio-economic drought.

In Africa drought significantly affects agriculture, human health, and the economy, particularly in Sub-Saharan nations (G. J. G. Gwp, 2016). For example, over 40 million people in Sub-Saharan Africa were said to have suffered as a result of the early to mid-1980s droughts (Office of Foreign Disaster Assistance, 1990, as cited in Wilhite, 2000). The persistent drought in the Horn of Africa, which includes Ethiopia, has a major effect on agriculture, water, food security, and the economy (Thao, 2019, cited in Tesfaye, 2022).

Drought has been recognized as a risk in Ethiopia that impacts the water and agriculture industries, particularly since the 1960s. About thirty significant drought episodes have occurred in Ethiopia over the past century, thirteen of which encompassed the entire nation and previous research indicated that the country's droughts have become more severe and frequent over time, devastating crops and killing a large number of people and animals(Glantz,2019,as cited in Haile et al., 2022). For instance, As indicated by Saha et al.(2022), FAO (2011) and Headey et al.(2012) stated that approximately 80% of the livestock in the pastoral areas along the Ethiopia-Kenya-Somalia border were lost, and many pastoralists moved out of the drought-affected areas.

One of the main causes of Ethiopia's food shortages is drought. Drought and food insecurity have intricate interactions. The most common environmental risk that causes food insecurity is drought (Devereux, 2004). Famines, which often result in population displacement, suffering, and deaths, only occur in developing nations after a drought (Shah et al., 2008). The cyclical drought has a major impact on food security over the long run. This is because the recovery from the previous disaster is hampered by the drought that follows (GAO, 2002). Since rainfall is the primary source of agricultural activity in Ethiopia, drought management requires careful consideration in order to guarantee food security for all. Moreover, regular monitoring of drought conditions can significantly contribute to the sustainable development of the agricultural sector.

Prolonged and recurrent droughts are the most common sign of climate change in the Borana lowland. Further, the risks associated with shorter drought cycles have increased (Oxfam, 2011). According to Herrero et al. (2010), this has led to an increase in livestock mortality and a decrease in animal reproduction performance. As indicated by Duba et al., (2021), Riche et al.(2009) stated that in Borana Zone, drought now happens in every 1-2 years, as comparison to every 6-8 years in the past. This poses a challenge to the livestock production system since it frequently causes livestock to grow smaller in size before full recovering is achieved. In Borana zone dry season occurs from December to February and from June to August (Korecha and Barnston, 2007,cited in Worku, 2024) . In the zone area, yabello district pastoralists' livestock suffered significantly from the drought (Dirriba, 2016; Duba et al., 2021). This district of study (Yabello) repeatedly affected by prolonged meteorological droughts and rain-fed based agricultural drought for many years. Therefore, to mitigate the negative consequences of the drought on agriculture and the economy, accurate drought monitoring is required.

Examining the effects of drought from the viewpoints of the agricultural and environmental sectors is crucial for planning and management. Although it is challenging to precisely track when droughts occur, it is possible to track and examine their features, including intensity, using various drought indices.

. Information about the characteristics of the drought, which is mostly based on the drought indices, is crucial for monitoring the conditions of the drought. By combining data from various indicators, such as temperature, precipitation, soil moisture, vegetation condition, stream flow, groundwater, evapotranspiration, and so forth, drought indices are a single number used in drought monitoring to define drought features, such as spatial extent, duration, and severity (Amalo et al., 2017; Qamer et al., 2019; Zargar, 2011).

This can be done either through climatic drought indices from meteorological data sets or modern remote sensing-based drought indices. In comparing with conventional weather data, remote sensing approaches are relatively better suited for monitoring vegetation conditions and as well as agricultural drought (Domenikiotis et al., 2004,cited in Wondimu et al., 2022)

Before, during, or after a disaster, the current situation can be monitored using satellite or remote sensing techniques. They can serve as a source of baseline data that can be used to compare changes in the future, and GIS techniques offer an appropriate framework for integrating and analyzing the various kinds of data sources needed for disaster monitoring. The overuse of natural resources due to population growth, soil erosion, declining water supplies, and potential future climate change scenarios have all become major causes for concern in recent years. Using satellite images is a better option to reduce the issue of area targeting because they are readily available, reasonably priced, and helpful in identifying the beginning, length, and severity of droughts. The assessment system can reduce the effects of losses related to drought by providing timely information on the scope and severity of the drought. Beside the use of meteorological data to characterize meteorological drought with in an areaThese days, remote sensing (RS) and geographic information systems (GIS) play a crucial role in agricultural drought identification, assessment, and management because they provide remarkable data across a range of spatial and temporal scales that are hurried and time-consuming when done using traditional methods(Sruthi & Aslam 2015, cited in Amin et al., 2020). Calculating several vegetation indices, such as the Normalized Difference Vegetation Index (NDVI), Vegetation Condition

Index (VCI), Temperature Condition Index (TCI), and Vegetation Health Index (VHI), among others, makes it feasible to track agricultural droughts.

1.2 Statement of the problems

Severe drought affects Africa more than any other continents, with more than 300 events recorded in the past 100 years, accounting for 44 percent of the global total, and more recently, Sub-Saharan Africa has experienced the dramatic consequences of climate disasters become more frequent and intense(Taylor et al., 2017; Guha-Sapir, D. et al., 2021, cited in Thiaw, 2022).

Ethiopia which is one of sub-Saharan African country is currently undergoing under one of the worst droughts caused by La Niña in the past forty years, after four unsuccessful rainy seasons in a continuous since late 2020. Prolonged drought worsens food insecurity and malnutrition and jeopardizes vulnerable livelihoods largely dependent on livestock. Ethiopia's Drought impacts also characterized by changes in wet lands, decreased biomass or vegetative cover and over all damage to the land (land degradation) in all ecologies due to excessive dryness. In pastoralist and in agro-pastoralist areas this situation results in damage and loss of rangelands and agricultures(Mera, 2018).

The agricultural sector is very important in the rural areas of the Borona zone of Ethiopia region, in which study area of the Yabello district is included. In the zone, agriculture is rain-fed and has a low productivity due to sub-optimal rainfall characteristics. In the highlands people predominantly grow (cash) crops with some livestock for additional income. The people in the lowlands keep livestock as major economic activity, based on traditional pastoralist systems. The pastoralist grow some crops for own use. These activities are stressed by factors like drought. For instance, the rural people are very vulnerable to droughts, such as the events in 2000 and 2008 years and during the drought of 2000, 80% of livestock died and in 2008 a relief program was executed supplying water and fodder to the communities(Vries, 2010).

The district of Yabello in Ethiopia, where this study was carried out, has also seen more difficulties due to recurring drought effects. The Yabello district in the Borana Zone of Southern Oromia was occasionally submerged in drought. In this region of the country, drought is manifested by the irregularity of rainfall. This results in temporally and spatially inadequate amount of moisture to support agricultural products in the district. Agriculture is vulnerable to climate change. The sector is sensitive and it is seriously affected by the recurrent drought which is mostly related to climate change. These prominent realities clearly emphasize the degree of vulnerability of agricultural sector products of the district to sever drought hazards. Drought is currently more pronounced in the study area which results in the loss of rangeland vegetation and water scarcity, shortages of food, and nutrition as well as the death of people and livestock in particular. For example, according to PDO (2017), as described by Boru (2017), 26,232 cattle were died and 18,823 of peoples were dependent on food aid under safety net program in Yabello district.

In relation to the drought issues in this and the surrounding areas, numerous studies have been conducted in the last few decades in the study areas of Yabello and El-woye, as well as in various pastoralist areas (Abera and Aklilu, 2012; Paul, 2013; Opiyo et al., 2014; Dirriba and Jema, 2015; Argaw et al., 2015; Dirriba, 2016, as cited in Duba et al., 2021). The majority of research has focused on examining how pastoralists and agro-pastoralists have dealt with the effects of drought. As they clarified, Paul (2013) also looked at the socioeconomic effects of droughts, coping mechanisms, and governmental initiatives in Kenya's Marsabit County. Furthermore, they reiterate that, Dirriba (2016) investigated the effects of droughts and traditional coping mechanisms of the Borana community in the districts of Yabello and Dirre, Ethiopia, where survey results indicated that drought had a significant negative impact on the pastoralists' livestock. Ultimately, though, they came to the conclusion that those studies were unable to pinpoint the degree of yearly rainfall variability in the main and short seasons, as well as the patterns and fluctuations of drought in the study area spanning more than thirty years. Their study's primary objective was to evaluate the meteorological drought that occurred between 1987 and 2017 by taking into account both the main and short rainy seasons as well as the distribution of annual rainfall using various indices and two meteorological stations located in Ethiopia's Oromia Region's Borana Lowlands. Regarding these, later study also fail in that they did not use remote sensing satellite data that can cover large area and give huge meaningful information wisely rather than using traditional method (only they used rainfall stationed data during their study).Having these problems in hand, also there is no evidences of the research conducted spatially on Agricultural issues of the study area. Therefore, this study aimed to fill these gaps by focusing on the assessment of Meteorological and Agricultural droughts using both rainfall and remotely sensed data and it analysis drought severity on Yabello district’s Environments from 1994 to 2022 years.

1.3 Objective of the study

1.3.1 General Objective

General objective of this study is to analysis the magnitude of Drought in Yabello district through quantifying rain fall and vegetation variation from 1994-2022 using Geospatial technologies for the recognition of the recurring droughts with in study area.

1.3.2 Specific objectives

- ✓ Determine magnitude of Drought through quantifying rain fall data of yabello district from 1994-2022.
- ✓ Detects changes in vegetation due to variation in rainfall between1994-2022 using GIS and RS.
- ✓ Quantify drought affected area in magnitude between1994-2022 by help of GIS and RS.
- ✓ Produce a drought hazard map of the years from 1994-2022 using GIS and RS.

1.4 Research questions

Research questions from the above specific objectives are:

- ✓ Can magnitude of the Drought determined through quantifying rain fall data?
- ✓ How can changes in vegetation due to variation in rain fall between1994-2022 can be detected using GIS and RS?
- ✓ How quantify drought affected area in magnitude between 1994-2022 by help of GIS and RS?
- ✓ Can drought hazard map of the years from 1994-2022 produced Using GIS and RS?

1.5 Significance of the study

Study allows data, methods, temporal and spatial way of studying drought for researchers, policy makers, community, and other stakeholders working on the issue of drought.

In this research, Analyzing the magnitude of drought and creating a map of drought hazards will assist to increase preparedness for disasters in regions that are prone to drought, identify areas that are most at risk for drought so that resources may be allocated for risk management, Mitigate the effects of drought (assists in determining the best measures to lessen the effects of drought). Study supports the possible means of studying and identifying drought hazard area in different periods of time by help of the Remote sensing technique using satellite and rain fall data. The primary goals of this research are to determine how a protracted drought impacts the study region and to improve our knowledge of how to analyze the effects of drought on the environment through the use of conventional and remote sensing techniques. Additionally, the techniques employed in this study such as the Standardized Precipitation Evapotranspiration Index (SPEI), which is no longer used for drought studies in our nation will be used as a resource for any interested parties or individuals to use in future research.

1.6 Scope of the study

In order to monitor drought risks within this study area, the current study work on Yabello District uses rainfall data and satellite data to identify and quantify drought risks using geospatial technologies. The Standard Precipitation Index (SPI), the Standardized Precipitation Evapotranspiration Index (SPEI) derived from rainfall data, and the Normalized Difference Vegetation Index (NDVI) anomaly, DevNDVI and Vegetation Condition Index (VCI) derived from various Landsat platforms (Landsat 5, 7, and 8) with a few common spatial resolutions are the drought indices used in this study.

1.7 Limitation of the study.

Despite the fact that the drought has affected the entire Borana zone, this study's focus was on the analysis of the drought in the Yabello district due to constraints on time and funding. A limitation of this research was the utilization of a single meteorological station for assessment of drought, even four other stations out of study area used only for interpolation. Station of study area leading to the omission of certain point data related to fundamental climate variables like temperature and precipitation. But these omitted data were filled in and did not adversely affect the study's conclusion. More indices, such as the Temperature Condition Index (TCI) coupled with the Vegetable Health Index (VHI) to produce a vegetation health index (VHI) as an indicator of drought, should have been included in the study in order to increase its scope and produce robust results.

1.8 Organization of the Study

The study has organized in to five chapters. The first chapter contains brief description of introduction. The second chapter deals with literature review and addresses the relevant literature that was associated with the study. . The third chapter has described the materials and methods. The fourth chapter was concerned with results and discussion of the study finally, the fifth chapter covers the conclusion and recommendations.

1.9 Operational definition of Terminologies

Drought index: single number that is used to measure how severe drought events.

Hazard: a severity event, material, human activity, or state that has the potential to result in death, serious injury, negative health effects, property damage, disruption of social and economic life, or environmental harm.

Impact: Changes in bio-geophysical and social systems usually modulate impacts, which are quantifiable outcomes of (or system reactions to) climate dynamics and hazards.

Magnitude of drought: the cumulative severity of a drought event over a period of time

Pastoralists: are individuals/communities derive their food and resources primarily from herding domesticated animals or live stocks.

Geospatial technologies: tools like that create datasets to analyze and map the area (Earth), remote sensing and Geographic information systems etc.

CHAPTER TWO: LITERATURE REVIEW

2.1 Concept and Types of Drought

A drought is a natural occurrence that happens when runoff, soil moisture, and seasonal precipitation fall below the long-term or normal average (Mera, 2018). Normally, when an area experiences unusually dry weather, lesser rainfall, and inadequate soil moisture, drought occurrence a phenomenon associated with climate change—becomes apparent. Sometimes it causes rivers, ponds, and lakes to have lower water levels, which has long-term effects on cattle, agriculture, and general economic activity(Shaheen and Baig, 2011; Akhtar, 2014, cited in Negassa, 2017).

Drought is classified into four primary categories depending on its causative reasons or as a hazard: hydrological, meteorological, socio-economic, and agricultural drought(Legesse & Suryabhagavan, 2014).

2.1.1 Meteorological Drought

A meteorological drought is primarily brought on by a lack of precipitation relative to normal conditions for a certain area and time frame. Additional factors that are thought to contribute to the incidence of meteorological drought include high evaporation, low humidity, desiccating winds, and elevated temperatures. Rainfall has been frequently utilized in meteorological drought assessments.

. Actually, a number of research have focused on using monthly precipitation data to analyze droughts. These methods concentrated on examining the length and severity of droughts in connection to precipitation deficits. In order to explain meteorological drought, several authors compare the length of the dry period and the degree of dryness in a particular area to the average or usual quantity. Bayarjargal et al. (2006), for example, defined drought as a recurrent extreme climate event over a specified territory, marked by below-normal precipitation over a period of months to years, as mentioned in Negassa (2017).

2.1.2 Agricultural Drought

Agricultural drought occurs when some of the consequences of hydrological and meteorological dryness cause the soil moisture availability to drop below the ideal level needed for plants to grow properly throughout crucial stages of the growth cycle.

Around the world, people have been losing their lives due to agricultural drought, which is characterized by irregular rainfall patterns and a lack of moisture. In the truest meaning of the word, the largest hazard to life in the majority of developing nations worldwide is agricultural drought.

. Therefore, it would appear that the study of agricultural droughts is receiving more attention now than it has in the past. Agricultural drought is defined by many local researchers as essentially connecting different aspects of weather and hydrological drought impacts on agricultural conditions by emphasizing factors such as low precipitation, discrepancies between actual potential evapotranspiration, soil type, soil water deficit, and decreased ground water or reservoir levels that lead to lower crop yields. Drought in agriculture has a wide range of effects on many economic sectors.

2.1.3 Hydrological Drought

A hydrological drought is characterized by a consistently low water volume and/or discharge in streams and reservoirs that lasts for months or years.

Hydrological drought was caused by deficiencies in reservoirs, groundwater levels, stream flow, or surface runoff (Legesse and Suryabhagavan, 2014). The frequency and severity of hydrological droughts can be impacted by changes in land use and the resulting soil degradation. The use of stream flow data for hydrological drought analysis is quite common. To evaluate hydrological drought, however, data sets such as surface-water area and volume, surface runoff, stream flow measurements, infiltration, water-table changes, and aquifer characteristics are typically needed.

2.1.4 Socio-economic drought

The demand and supply of certain economic items, together with aspects of agricultural, hydrological, and meteorological droughts, are tightly linked to socio-economic definitions of drought (Hazaymeh and Hassan, 2016, quoted in Wondimu et al., 2022). It is distinct from the other kinds of droughts in that supply and demand determine when it occurs. The climate's inherent fluctuation causes the water supply to be plenty in some years but insufficient in others to meet environmental and human demands. Economic drought is a serious problem that affects many facets of human life, according to Goddard et al. (2003) and Nagessa (2017). It can lead to a number of environmental and economic issues, particularly in the agricultural industry.

Human and animal population and growth rate, water and feed needs, crop failure severity, industrial type, and water requirements are among the data types needed to evaluate socioeconomic drought.

2.2 Causes of Drought

Soil, land cover, and hydrologic systems are expected to be significantly impacted by climate change due to rising temperatures, evapotranspiration, and rainfall variability (Hazaymeh and Hassan, 2016; Panu and Sharma, 2002)

. Drought phases have a unique natural component in Africa, where they are partially impacted by geophysical occurrences that alter the humidity of the continent. Drought patterns were altered by climate variability and human impacts on the environment in the context of population growth (Masih et al., 2014). These consequences include mining, burning, deforestation, land degradation, and changes in land use. Human activities such as excessive use of water resources, growing urbanization and settlement, and the extension of pasture and agricultural areas also have an impact on droughts (Zeng, 2003). The primary causes of drought are generally understood to be anthropogenic factors, including mining, deforestation, land degradation, land use change, fire, and changes in air movement brought on by multi-decadal variations in the global sea surface temperature (Dai 2011; Zeng, 2003).

2.3 The Impact of Drought

According to Kogan (1997) and Tadesse et al. (2004), drought is seen as a complex and powerful environmental disaster that has an impact on the environment, society, and economy globally because of its gradual start, long duration, cumulative effects, and wide geographic distribution. When there is less water available in dry and semi-arid regions, droughts are most severe. In addition to the severity of the hazard, the sensitivity of a sector or activity also affects the repercussions of drought. Due to geographical differences in agriculture, the impact and vulnerability to the same drought are therefore different. Numerous important effects are caused by drought, both directly and indirectly. Increased rates of animal and wildlife death, as well as decreased productivity in forests, rangelands, crops, and water levels, are direct r. epercussions of drought. These direct impacts' consequences are referred to as indirect impacts. Additionally, the effects of drought can be categorized by the sector that is impacted, resulting in social, economic, or environmental impacts. In particular, losses either directly from drought or indirectly, like damage to plant and animal species caused by wildfires, are referred to as environmental impacts. Similar to this, agriculture and associated industries are impacted by numerous economic factors. Lastly, public safety, health, quality of life, water-use conflicts, and geographical disparities in effect distribution and relief are also considered social repercussions. The use of contemporary remote sensing and geographic information systems improved the work of numerous researchers by enabling them to efficiently monitor, evaluate, and analyze specific area drought behaviors such as its onset, frequency, duration, and severity levels. This approach also seemed to be successful in characterizing drought in terms of its specific local events. Consequently, scientists are now able to effectively further deconstruct droughts according to their effects on a specific geographic region (Figure 1).

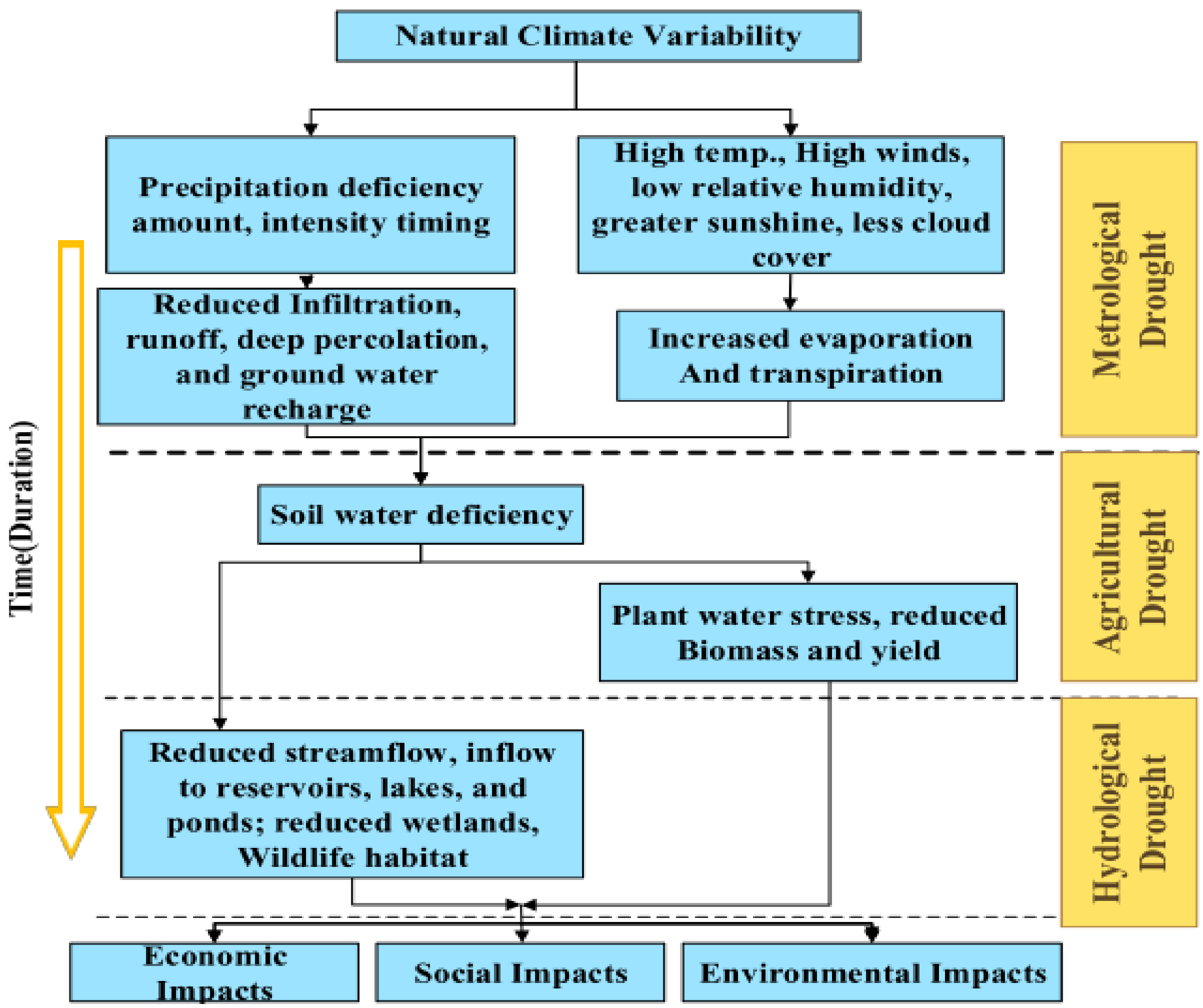

Figure 1: Categories of drought impacts (Jeyaseelan, 2004, cited in Negassa, 2017)

2.4 Drought in Ethiopia

Climate variables that herald the onset of drought include high temperatures, strong winds, and comparatively low humidity. Drought breaks out in Ethiopia during the several seasons that occur in different parts of the nation when seasonal rainfall falls by roughly 30% to 50% below normal (Mera, 2018). This indicates that because to a decrease in soil moisture and seasonal rainfall unpredictability, dryness strikes arid regions more frequently. One of the sub-Saharan African nations most vulnerable to drought is Ethiopia. There have been several severe droughts in Ethiopia. For example, there have been roughly 30 significant drought periods in the last century. Thirteen of these drought episodes were deemed severe and are known to have impacted the entire nation.

(Gebrehiwot et al., 2011). Over the past three decades, drought has been Ethiopia's most significant natural calamity (Asheber, 2010; Gebrehiwot & Van Der Veen, 2013). Mera (2018) claims that Ethiopia's drought had a particularly negative impact on all areas, including water resources, hydropower (insufficient water for industry and decreased electricity production), and agriculture (loss of crops and livestock). These factors led to disease, famine, population migration, malnutrition, and a host of other issues for farm families.

Agriculture continues to be by far the most significant sector of the Ethiopian economy since the vast majority of the people makes their living from rain-fed agriculture and other commercial activities. However, because to the country's extremely low rainfall, even a small alteration has a profoundly detrimental impact on agricultural output generally and seasonal crop yields specifically. According to Sadoff (2006), as indicated by Legesse & Suryabhagavan (2014), Since rain-fed agriculture provides for 80% of Ethiopia's population, fluctuating rainfall is correlated with both economic production and welfare. Because of its reliance on rain-fed agriculture, the nation's economy is particularly susceptible to the effects of climate change and variability, which are typically exhibited by irregular rainfall and frequent droughts.

The spatiotemporal scope of a drought must be established in order to study and lessen its detrimental consequences. This is why different interpolation techniques should be used to build basin-by-basin drought maps based on appropriate drought indicators.

. In drought mapping, kriging and inverse distance weighting (IDW) are the most popular interpolation techniques. Kriging is a method that uses the values of neighboring places to estimate the value of a variable at an unknown location. This linear model predicts values in the spatial field by utilizing statistical correlations between the observed points while inverse distance weighting (IDW) a spatial interpolation technique that uses a weighted combination of nearby measured values to estimate values at unmeasured places.

Comparing different statistical elements can help identify which of these approaches is most successful (Ali et al. 2011; Rahman & Lateh, 2016, quoted in Yuan et al. 2016). The literature has a number of studies that use interpolation techniques to determine the spatiotemporal distribution of meteorological droughts. For instance, Bagheri (2016) employed kriging interpolation, natural neighbor interpolation, and inverse distance weighting (IDW) interpolation for meteorological mapping in order to extrapolate computed SPI values for 17 stations to the entire study region. However, he chose to use the inverse distance weighting (IDW) interpolation technique for the spatial characterization of meteorological drought in order to get better results about the research area.

Ethiopia has employed drought monitoring systems based on meteorological data from ground stations, including rainfall, weather, agricultural performance, and water availability, to adjust livelihood systems to the changing climate. To put it another way, ground stations were the primary national information sources for agricultural drought evaluation until recently.

This dependence on ground data, however, might not produce fruitful outcomes since, for example, a low density of weather stations might make it challenging to obtain adequate spatial and temporal climatic data. In addition to the remote-sensing approach for identifying drought-prone areas, Jeyaseelan et al. (2002) give spatial information on drought-prone areas using historical vegetation index data obtained from satellite series. Agricultural drought-prone areas can be identified and mapped with the help of satellite data and sophisticated methods like remote sensing and Geographic Information System (GIS). The decision-making process for drought monitoring and determining the best location for particular adaptation and mitigation is aided by agricultural drought hazard mapping(Legesse & Suryabhagavan, 2014).

Drought has a more serious and immediate effect on agricultural crops, which lowers output and causes food shortages, unemployment, and other problems. Effective monitoring of agricultural drought, including its start, progression, and effects on crops, is therefore necessary to reduce damage. Drought monitoring is a continual analysis process that encompasses the impact and spatial extent of drought, as well as a variety of indicators of drought severity utilizing drought indices. Agricultural drought monitoring comprises the measurement and evaluation of various agro-climate factors in agricultural regions to create suitable indicators for agricultural drought assessment. These evaluations are then translated into drought reports that precisely and impartially define the features of drought conditions. Typically, early warning systems may use this combined data before drought events begin.

Drought monitoring has the objective of warning about a possible incoming drought, providing adequate information for an objective drought declaration and for avoiding severe water shortages. Since the 1960s, various techniques and drought indices have been put forth to recognize and track drought events. Certain of these indices are oriented to refer to hydrological or agricultural drought, or water shortages in urban water supply systems, while others describe meteorological drought, which is based on precipitation series. Drought indices combine thousands of data points about stream flow, precipitation, snowpack, and other indicators of the water supply into a coherent overall picture. Usually expressed as a single figure, a drought index value is far more helpful for making decisions than raw data.

The expected outcome is the characterization of the meteorological and agricultural drought periods in the historical record in the geographical unit. Decision-makers can measure the abnormality of historical rainfall variability and its effects on a district by accurately characterizing the drought. While certain indices are more appropriate for specific applications than others, none of the indices is fundamentally better than the others under all conditions. Various indices for tracking droughts. There are the two methods currently in use for monitoring droughts: 1) conventional approach and 2) the remote sensing-based approach of drought monitoring.

2.5 Conventional approach of drought monitoring

Conventional approaches are also known as traditional or ground based approaches. There are indices in this approach to track drought in agriculture, hydrology, and meteorology. The Standardized Precipitation Index (SPI), Rainfall Anomaly Index (RAI), Palmer Drought Severity Index (PDSI), and other indices are among the Meteorological Drought indices. In addition, there are several agricultural drought indices such as the Crop Moisture Index (CMI), Palmer Moisture Anomaly Index (z-index), and Computed Soil Moisture Index, and several hydrological drought indices such as the Total Water Deficit Traditional (TWDT), Palmer Hydrological Drought Severity Index (PHDS),. The lack of spatial detail and their reliance on data gathered at ground stations, which is occasionally dispersed, are two significant disadvantages of these indices that affect their dependability as drought indicators (F. J. Brown, and B. C. Reed, 2002, H. Legesse, 2010).

Some of the indices are discussed below.

2.5.1 Standardized Precipitation Index (SPI)

The primary purpose of the Standardized Precipitation Index (SPI) is to monitor and define drought. It is an index determined by the likelihood of precipitation over any given period of time. Drought intensity is arbitrarily defined for values of the SPI with the following categories as Table 1(Iwata et al., 2012):

Using historical data from any rainfall station, SPI enables the determination of the rarity of a drought at a specific time scale (temporal resolution) of interest. It gives a precipitation a single numerical value that can be compared across areas with distinctly different climates.

Table 1 SPI values adopted from (Iwata et al., 2012; Qaisrain et al., 2021).

SPI Values	
2.0+	Extreme wet
1.5 to 1.99	Very wet
1.0 to 1.49	Moderately wet
-0.99 to 0.99	Near normal
-1.0 to -1.49	Moderately dry
-1.5 to -1.99	Severely dry
-2.0 to less	Extremely dry

2.5.2 The Standardized Precipitation Evapotranspiration Index (SPEI)

Another drought index that is based on temperature data for maximum and minimum values as well as precipitation is the Standardized Precipitation Evapotranspiration Index (SPEI). Utilizing the cumulative difference between precipitation and potential evapotranspiration, this index is computed similarly to the SPI. Because of these features, the SPEI is a particularly useful index for research on how global warming affects drought and drought monitoring. The package "SPEI" in R-Studio 4.0.3 software was used to calculate both drought indices, SPI and SPEI for a 12-month scale(Montes-Vega et al., 2023).

There is no direct way to measure drought, and it is generally calculated based on its impacts using different indices (Svoboda and Fuchs, 2017). There are a lot of indices available for this use, but since they are region-specific and rely on the availability of input data, index selection is crucial. When monitoring and categorizing drought, it's also critical to take time-scale into account (Gurrapu et al., 2014). For instance, a drought lasting less than a month may be classified as meteorological, one lasting three to six months as an agricultural drought, one lasting twelve months as a hydrological drought, and any lengthier than twelve months as a socio-economic drought (Homdee et al., 2016; Jasim and Awchi, 2020). Drought durations of 1, 3, 6, 9, and 12 months were taken into consideration in their study. According to Adnan et al. (2018), as described by Qaisrani et al.(2021), the SPI,SPEI and the Reconnaissance Drought Index (RDI) are the indices most suitable for Pakistan. The study employed the SPI and SPEI indices due to their standardization, flexibility, and ease of calculation across various time scales. SPI views precipitation as the only input variable, whereas SPEI takes global warming into account in addition to the impact of temperature on water demands. Due to its consideration of the water balance in evapotranspiration, SPEI is also significant for arid and semi-arid zones (Saeidipou et al. 2019). Both indices have comparable time scales and drought classifications, which are displayed in Table 2.

Table 2 SPI/SPEI values with description (Qaisrain et al., 2021).

SPI/SPEI values	Categories
> or =2.00	Extremely wet
1.50 to 1.99	Very Wet
1.00 to 1.149	Moderately wet
-0.99 to 0.99	Near normal
-1.00 to -1.49	Moderately drought
-1.50 to -1.99	Severe drought
< or =-2.00	Extreme drought

A number called a drought index is used to quantify the severity of drought occurrences. The drought indices track changes in temperature, river discharge, precipitation deficit over time, and other measurable variables. The most popular and widely used drought monitoring index, the SPEI, looked into the drought events for this study. The SPEI is a multi-scalar index that is more expressive and appropriate for characterizing droughts, climate variability, and global warming than other indices. For example, a study carried out in northern Ethiopia and East Africa demonstrated that SPEI could be used to assess the drought in Ethiopia. (Haile et al., 2022).

Due of the abundance of drought indices, comparison studies have frequently been conducted to determine which index, or combination of indices, and associated timelines best characterize a particular form of drought in a particular location. The ability of the various indices to accurately characterize the features (onset, duration, severity, etc.) of past drought events or their association with hydrological or agricultural impacts in a particular region are typically the basis for evaluating the performances. Analyses often focus on assessing how similar the indices are to one another, and they are nearly always based on the Pearson correlation coefficient (r) between the related severity time series. When assessing how similar the temporal dynamics of two indices are, the correlation coefficient (r) can be used as a measure of the strength of the linear link between two generic variables. It is commonly understood, therefore, that the correlation does not convey the degree of agreement between two variables. When two drought indices show the same severity classifications over a specific time period, they are said to be in agreement. The Cohen's Kappa test, one of the most popular ways to examine the agreement between two different raters or analytic approaches, can be used to efficiently get evaluation (Cohen1960, 1968, as cited in Todisco & Lena, 2021).

2.6 Remote sensing-based approach of drought monitoring

The process of remote sensing involves detecting and logging the energy reflected from a target, then handling, evaluating, and utilizing the data. A sensor needs to be positioned on a stable platform that is apart from the target being observed in order to gather and record the energy that the target reflects or emits. Satellites, planes, and the ground can all have platforms for remote sensors. Remote sensing in space is typically carried out from satellites that orbit the planet. We concentrate on satellites for remote sensing in this work.

Satellites measure solar energy's energy intensities, or radiations, at various electromagnetic spectrum wavelengths. Everything, including the earth, oceans, atmosphere, clouds, rain, vegetation, cities, people, etc., emits energy at certain wavelengths and absorbs energy at others, which makes this information helpful.

A combination of current advancements in technology, remote sensing can assist with drought monitoring, prediction, and mitigation. For this purpose, data from multiple satellites can be used, regardless of the agricultural, meteorological, or hydrological perspective that a researcher may have on drought. Compared to traditional methods, it allows one to more directly and efficiently comprehend the effects of drought over a wider area and in a shorter amount of time (A. Sharma, 2006, H. Legesse, 2010).

In 2010, Svoboda in his research stated that satellite based vegetation monitoring plays an important role in drought monitoring and early warning, since vegetation condition reflects the overall effect of rainfall, soil moisture, weather and agricultural practices. Due to this fact, our focus is on vegetation condition monitoring and prediction.

The condition of vegetation can be evaluated through remote sensing by analyzing reflectance values at different wavelengths of energy. Micrometers (µm) and nanometers (nm) are the units used to measure wavelengths. 1,000 nm is equal to one µm. The electromagnetic spectrum's visible region spans approximately 400 nm to 700 nm. The wavelength of the green color linked to plant health is centered around 500 nm. The visible portion of the electromagnetic spectrum is depicted in Figure 2.

The infrared region contains wavelengths up to approximately 25 µm longer than those in the visible region. The near infrared (NIR) region is the infrared region that is closest to the visible region. Agricultural remote sensing uses both visible and infrared wavelengths.

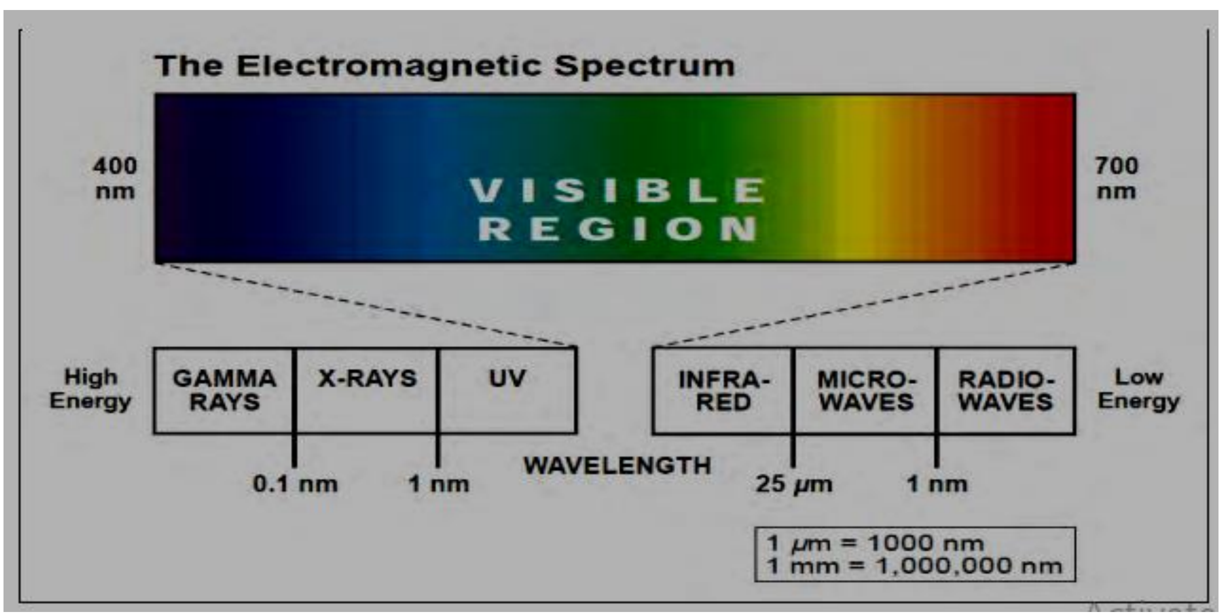

Figure 2: The visible region of the spectrum ranges from about 0.4 µm to 0.7 µm (kogan, 1965).

The comparison of reflectance values at various wavelengths, or vegetation indices, is a widely used method to assess the health of vegetation. An indicator of plant productivity, density, and health is called a vegetation index. In order to perform photosynthesis, plant leaves both reflect and absorb visible light. A healthy plant emits a lot of near-infrared light and very little reflected visible light (red region) according to a light-measuring sensor. Stressed or unhealthy vegetation reflects more in the red portion of the spectrum and less in the infrared portion. A plant's vegetation index rises with the number of healthy green leaves it possesses and the strength of the difference in light reflection between visible and near-infrared wavelengths.

The NDVI is the most widely used vegetative index. Based on variations in the quantity of visible (red) and near-infrared light reflected from plants on Earth's surface, the NDVI index, or scale, represents the state of the vegetation.

The range of NDVI values is +1.0 to -1.0. Areas of bare rock, sand, or snow are typically visible at very low NDVI values (0.1 or less). Shrubs, grasslands, and senescing crops are examples of sparse vegetation with moderate NDVI values (0.2 to 0.5). Furthermore, dense vegetation, like that found in temperate and tropical forests, or crops at the height of their growth cycle are associated with high NDVI values (0.6 to 0.9). The near-infrared (NIR) and red wavelength bands can be used to calculate the NDVI using the following algorithm:

$$NDVI = NIR\text{-}RED \,/\, NIR + RED$$

Where, NIR and RED is the reflectance in the near infra-red and red bands, respectively. NDVI is a nonlinear function that ranges between -1 and +1. However, in practice, NDVI measurements generally range between -0.1 and +0.7. Cloud, water, snow, ice and non-vegetated surfaces have negative NDVI values. Bare soils and other background materials produce NDVI values ranging from -0.1 to +0.1. Low values indicate poor vegetation conditions and possibly adverse weather impacts; values greater than 0.5 indicate healthy vegetation conditions. The NDVI values for vegetation are positive and range from 0.1 to 0.7. Drought conditions are more common in areas with lower NDVI values (Prathum Chaiet al., 2001).

2.6.1 NDVI anomaly

By calculating various vegetation indices, such as the Normalized Difference Vegetation Index (NDVI), Dev NDVI, and Vegetation Condition Index, it is possible to monitor agricultural droughts (VCI)(Legesse & Suryabhagavan, 2014).

Utilizing NDVI values, the NDVI anomaly is a vegetation index that is used to evaluate the severity of agricultural droughts. Based on this anomaly, the degree of drought can be classified and expressed as a percentage. Its values range from -50 to -25 (severe drought), -25 to -10 (moderate drought), -10 to 0 (slight drought), and values greater than 0 (no drought). Less than -50 indicates a very severe drought.

2.6.2 NDVI Deviation (DevNDVI)

As stated in Sisay et al. (2013), Jones et al. (1997) state that the NDVI does not, by itself, represent drought or non-drought conditions. However, the difference between the current NDVI values and the corresponding long-term mean NDVI values can be used to describe the effects of drought severity on vegetation. Using the NDVI value determined from each image as follows, the NDVI deviation (DevNDVI) from each image was calculated. (Tucker, 1979 , as cited in Wondimu et al., 2022)):

$$DEVNDVI = NDVIi - NDVI\ mean,$$

Where, NDVIi is the NDVI value for the year i and NDVImean is the long term average of NDVI.

When DEVNDVI is negative, it indicates below normal vegetation conditions and therefore suggests prevailing drought conditions; the greater the negative value, the greater the magnitude of drought severity.

2.6.3 Vegetation Condition Index (VCI)

The Vegetation Condition Index (VCI), which is in good agreement with precipitation patterns, was formerly used to assess the spatial characteristics of drought as well as its duration and severity. It was measured in percent provider (Chopra, 2006). It serves as a gauge of the vegetation cover's condition based on the NDVI minima and maxima that are experienced over an extended period of time for a particular ecosystem. It makes the NDVI more comparable and enables the comparison of various ecosystems. According to Kogan (1995), this makes it a more accurate indicator of water stress conditions than the NDVI. The quantity and caliber of images that are available for the determination of the absolute minimum and maximum determine the VCI.

$$VCI = (NDVIi - NDVI\ min) / NDVI\ max - NDVImin*100$$

Where, NDVi is the current NDVI value, NDVImin and NDVImax are a multi-year minimum and maximum NDVI.

Values of the VCI below 50% indicate varying degrees of drought severity. Kogan (1995) demonstrated how extreme drought conditions can be determined using a VCI threshold of 35%. When the NDVI value is nearing its long-term minimum, it indicates an exceptionally dry month, as indicated by the VCI value close to 0% (zero percent). Low VCI values over a number of consecutive time intervals point to the beginning of a drought.

Kogan (1997) states that a VCI of less than 50% indicates varying degrees of drought severity, while a VCI of less than 50% indicates an extreme drought. Moreover, the VCI values for east Africa below 35% were arbitrarily categorized as follows:

1. <10% extreme drought
2. 10% - 20% severe drought
3. 20% -35% moderate drought
4. 35% -50% no drought
5. >50 wet

Normalized Difference Vegetation Index (NDVI) and Vegetation Condition Index (VCI) are the most widely used indices among those used to evaluate drought.

Based on input data from drought indices, drought indices provide distinct images of the severity of the drought throughout the study region. A composite image of the drought hazard throughout the study region can only be created by combining data from all variables onto a single layer. By highlighting common information from all drought indices brought on an equal scale, weighted overlay analysis in geographic information systems (GIS) offers a way to generate composite response of drought hazard and gives a clear picture of drought severity. (Shah & Iqbal, 2023)**.** A useful method for producing integrated analyses with various and dissimilar inputs based on several criteria is weighted overlay analysis(Aziz et al., 2018). In addition to describing how Shahid et al. (2008) created composite drought hazard maps for Bangladesh using various drought monitoring indices, Shah and Iqbal (2023) also explained how Shaheen and Baig (2015) used weighted overlay analysis to generate composite drought hazard maps at meteorological and agricultural scale in the arid region of Thal Doab, Pakistan. In light of these researchers' theories, this study also employed the NDVanomaly, DevNDVI, and VCI drought severity layers to create a combined drought-severe map at the agricultural scale using weighted overlay analysis in GIS.

2.7 Empirical reviews

Drought analysis is challenging because of the wide spatial and temporal variability exhibited by each drought events. It is impossible to sufficiently characterize and track drought with a single technique. Techniques for analyzing droughts should be modified to account for the characteristics of drought that are unique to a certain sector, time, and place.

Rainfall and socioeconomic indicators played a significant role in tracking the start and progression of the Ethiopian drought. However, obtaining adequate and trustworthy meteorological and socioeconomic data on time continues to be difficult because meteorological stations are still sparsely spaced throughout the nation's drought-prone regions, and the ones that are do so with a track record of inadequate data collection(Mera, 2018).

These days, the identification, assessment, and management of agricultural droughts has come to rely heavily on remote sensing (RS) and geographic information systems (GIS). This is because these tools provide exceptional data across a range of spatial and temporal scales, which conventional techniques rush and time-consume (Amin et al., 2020).

Duba et al.(2021) examined the meteorological droughts in the Borana, Ethiopia's Oromia Region, in the Yabello and El-Woye Areas between 1987 and 2017. The purpose of the study was to look into the magnitude, frequency, and patterns of drought occurrences in the studied area. The rainfall data in the study were analyzed using the Mann Kendal test, the standard precipitation index, and the drought index calculator. Additionally, SPIs for the annual period, short rainy season, and main rainy season were calculated. The years 1998, 2002, 2003, 2006, 2015, and 2016 were drought times in the research area, based on their findings. Additionally, they indicated that about 50% of the 1987–2017 timeframe was affected by drought, with the most severe and extreme drought episode occurring in the research area in 2006, with SPI values of -2.14 at El-Woye and -2.01 at Yabello.

Haile et al.(2022) Analysis of drought in the Bilate Watershed: Sub-Basins of the Ethiopian Rift Valley using Standardized Evapotranspiration and Aridity Index He looked at the Bilate watershed's spatiotemporal patterns of drought from 1981 to 2016. The study's examination of the drought made use of monthly rainfall and temperature data. Additionally, SPEI-12 and SPEI-03 timelines were used to assess the patterns of drought. Additionally, his findings showed that there were ongoing drought occurrences in both timelines from 1988 to 2016, with a drought value of (SPEI = −2.5 to −1.2). Once more, he noted in his study that the SPEI is the most useful and favored index for studies on drought because it takes temperature into account more so than other indices when comparing drought over time and location.

Worku(2024) investigated the use of SPI and SPEI for spatiotemporal study of drought severity in the semi-arid Borana region in southern Ethiopia.

To describe drought during these times and rainy seasons in space and time, the Standardized Precipitation Index (SPI) and Standardized Precipitation Evapotranspiration Index (SPEI) at 3- and 12-month timescales were used in the study. The findings showed that, at different locations, moderate to severe drought conditions commonly affected the months of March through June and September through November. The driest years have been identified as 1984, 1985, 1992, 1999, 2000, 2001, and 2011, among other years.

Tefera et al.(2019) Analyzes SPI and SPEI in comparison as instruments for assessing drought in Northern Ethiopia's Tigray Region. The primary goal of their study was to compare the degree of agreement between SPI and SPEI when employed as drought assessment instruments during time periods of one, three, six, twelve, and twenty-four months. Cohen's Kappa statistics were used for the SPI and SPEI agreement test. SPI and SPEI were computed using gridded monthly temperature and precipitation Climatic Research Unit time-series data version 4.01 for the years 1901 through 2016. The study reported that across all time scales, there was a positive linear association ($r > 0.7$, $p < 0.001$) between the assessments of SPI and SPEI. At all timescales, the study also discovered an acceptable level of agreement between SPI and SPEI ratings in the studied area. Similar to this, their analysis's Cohen's Kappa statistics, which indicate how well two approaches agree, revealed a fair amount of agreement (0.2–0.6)

Birhanu Gedi.f et al.(2014) evaluated the risk of drought in Ethiopia's Tigray Region's southern zone. This study made use of satellite sensor data, which are continuously available, reasonably priced, and capable of identifying the beginning, lengthening, and intensity of droughts. Using eight-year time series rainfall data and decadal satellite SPOT NDVI (Normalized Difference Vegetation Index), drought risk zones are identified that are experiencing both meteorological and agricultural drought. Once more, they employed remote sensing and geographic information systems (GIS) to detect and track droughts. They did this by comparing the NDVI deviation with the long-term mean NDVI and the Vegetation Condition Index (VCI), which was obtained from the SPOT.

Legesse & Suryabhagavan, (2014) used remote sensing and geographic information systems to analyze the agricultural drought in Ethiopia's East Shewa Zone. Using the Water Requirement Satisfaction Index (WRSI), Standard Precipitation Index (SPI), and Normalized Difference Vegetation Index (NDVI) anomalies, the researcher evaluated the spatiotemporal variance in agricultural drought pattern and severity. Based on the results obtained, he concluded that there was a regional variation in the severity level of the agricultural drought throughout the cropping seasons of 2000 to 2005, which resulted in a drop of grain yield. He further clarified that the year 2000 was the second most terrible year ever, behind 2002. In the study, he divided the combined agricultural risk map of the East Shewa zone into subzones with slight, moderate, and severe agricultural drought risk, which, respectively, covered 17.18%, 41.32%, and 41.50% of the entire area. Finally, he concluded that decision-making processes related to drought monitoring can be aided by agricultural drought risk mapping.

2.8 Identified Research gaps

In Ethiopia, Numerous studies and real-world experiences attest to the fact that the nation has been afflicted for many years by severe droughts that can be destructive.

Many local and international academics have been working tirelessly to comprehend the nature of the recurring drought and develop potential strategies to mitigate its severe effects on the local ecosystem in an attempt to effectively alleviate the situation. Unfortunately, the majority of the attempts undertaken up to this point have not been able to yield outcomes that would allow the intended aims to be effectively achieved. This was mostly due to the fact that the county's traditional research practices used to exclusively rely on ground-based data gathering and processing methods, with the exception of a few recent attempts to integrate contemporary satellite resource data and remote sensing techniques.

However, it is clear that there are several shortcomings with the traditional methodologies in comparison to the modern research approaches. The traditional approach was not time-effective, mostly due to inefficient access, aside from its inefficiency in obtaining the necessary data for the intended reasons. Furthermore, past studies have not adequately taken into account agriculture, particularly in the lowland areas of the Borana zone under study. Furthermore, in spite of the severity of the drought conditions, no indication of notable studies pertaining to the drought that have been undertaken spatially on agricultural concerns in the Yabello district has been found.

The current study aims to improve district drought hazard management efforts by utilizing modern satellite data resources, remote sensing, and geographic information systems to analyze meteorological and agricultural droughts using both rainfall and remotely sensed data. This is done in recognition of the existing research gaps and the need to carefully consider the current features of the severe drought problems in the district. Moreover, the Standardized Precipitation Evapotranspiration Index (SPEI), which was used in this study to quantify meteorological droughts but is no longer in use in our country for drought studies, is available for use by anyone with an interest in conducting future research.

CHAPTER THREE: METHODS AND MATERIALS

3.1 Description of the study area

3.1.1 Location of study area.

The study conducted in Yabello district found in pastoral areas of Borena Zone of Oromia Regional state, Ethiopia. Astronomically, the district is located between 4°30′55.81″ and 5^0 23' 12.7" North Latitude and the 37°44′14.70" and 38^0 32' 52. 6" E Longitude and relatively the district is bounded by Arero district of Borena Zone in east, Dubuluqi districts of Borena Zone in the south; Elwaye district of Borena zone in the west and Gomole of Borena zone in the north. Yabelo is the capital of the district which is 565 km far from country's capital city Addis Ababa.

The district is roughly 31,4180 km2 in total. The range of altitudes is 500–1500 meters above mean sea level. The study region is subject to a bi-modal monsoon rainfall type, with 60% of the yearly rainfall falling in Ganna (March to May) and 40% in Hagaya (September to October). About 24.5°C is the average annual temperature. About 24.5°C is the average annual temperature. Maximum and minimum temperatures are correspondingly 26.4°C and 26.83°C, respectively (Wako Duba et al., 2021).

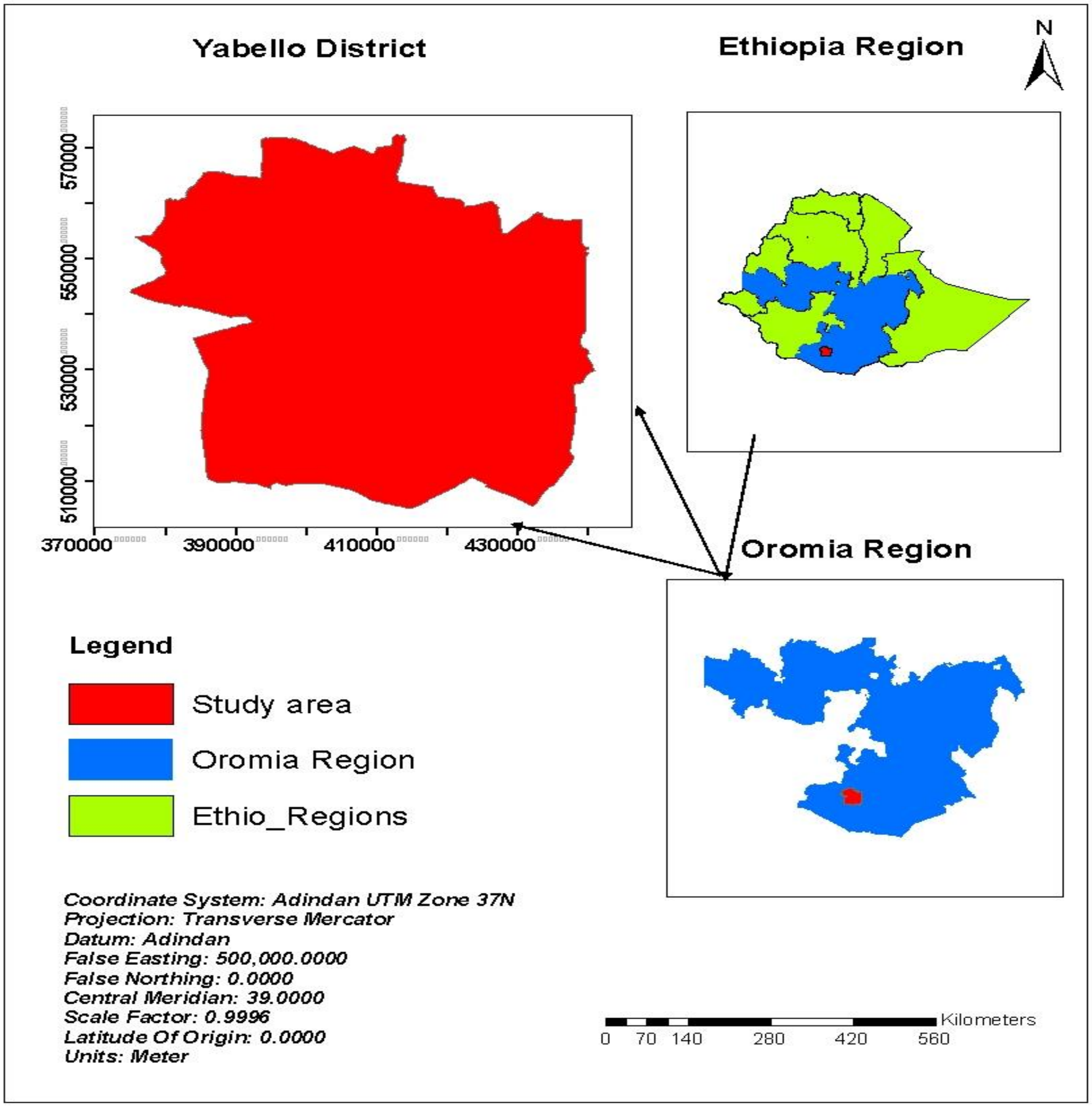

Figure 3: Location map of the yabello district.

3.1.2 Topography

Altitude of Yabello district varies from 1206 meter to 2361 meter throughout the area. Lower elevations and higher elevations seen at south west and middle of the district above mean sea level. The area has no rivers or streams, and the land is divided into arable or cultivable: 10%, Pasture: 60% , Forest: 10%, Swampy, degraded, or unusable: 20%.

3.1.3 Land use

The Yabelo District Agriculture and Natural Resource Office estimates that 11,971 ha (2.19), and 292,028 ha (52.62), are used for cultivation and grazing, respectively. The district's remaining area is divided into a variety of land use patterns, including urban land, uncultivated land, open wood land, exposed sand soil surface, bushlands, shrublands, and forests, both natural and man-made. The land use and cover of the Yabello district has changed significantly; the amount of forest and grassland land has drastically decreased, croplands have grown fivefold, and bushed-grasslands and bush lands have both significantly risen (Mesele et al., 2006).

3.2 Data Types and Data Source

3.2.1 Data Sources

The data used in this study came primarily from secondary sources. Satellite data, rainfall data, and temperature data were gathered in order to determine the severity of the drought. Since it defines the quality of the research, the most important factor in each study was the collection of correct and reliable data.

Table: data sources

No	Data required	Source	Data type	Year	Data format
1	Monthly total Rainfall data	Ethiopian Meteorological Institute(EMI) and (https://power.larc.nasa.data-access-viewer/)	Secondary	1994 - 2022	Excel
2	Monthly total minimum and maximum temperature	Ethiopian Meteorological Institute(EMI) and (https://power.larc.nasa.data-access-viewer/)	Secondary	1994 - 2022	Excel

3	Landsat Satellite images	USGS	Secondary	1994 - 2022	TIFF

3.2.2 Meteorological Data

This study depends on the information/ data obtained from Ethiopian Meteorological Institute (EMI) this consists ofbasic climate elements of rainfall and temperature record of the past past 28 years. Monthly total Rainfall data, Monthly total minimum temperature and Monthly total maximum temperature data for the Yabello station was obtained from Hawasa branch of the Ethiopian Meteorological Institute(EMI) for the years 1994–2022,and used to create the Standard Precipitation Index (SPI) and Standard Precipitation Evapotranspiration Index (SPEI). The study area's rainfall data was collected for 28-year periods. This investigation involved five metrology stations in total. Only one of those stations is located inside the research area. In order to transform the point data into continuous raster surfaces and improve the study's consistency and dependability, the remaining four nearby stations were employed for interpolation.

Researcher also used other data that downloaded from the Power Access Climate Data website (https://power.larc.nasa.data-access-viewer/), to fill in some data gaps. Appendix I, Appendix II and Appendix III indicates Rainfall data, minimum and maximum temperature used in this study.

3.2.3 Quality control of Meteorological data

Quality control was conducted on the temperature and precipitation data that were acquired from the Ethiopian Meteorological Institute (EMI). The researcher uses SPSS software to fill in the missing values in the data and determines if the minimum temperature recorded during that time was higher than the maximum temperature.

3.2.4 Data Reliability Test

The Cronbach's alpha coefficients were used by the researcher to ensure the reliability of the study. The Cronbach's alpha is the standard.70 regarded as trustworthy(reliable) and lower are.60 regarded as untrustworthy(unreliable)(Keith, 2017).

Table below indicates that variables in this study have Cronbach's alpha values above o.70, indicating the reliability of the data and their ability to measure the intended goal. With the aid of SPSS software, the Cronbach's Alpha value for variables in the study were calculated, and each factor underwent factor analysis.

Table: Reliability Statistics

Reliability Statistics		
Cronbach's Alpha	Cronbach's Alpha Based on Standardized Items	N of Items
.937	.939	3

3.2.5 Satellite Image data

Three satellite images (two decadal and one satellite image covering 8 years) of the study area were downloaded from the USGS Earth Explorer website, https://earthexplorer.usgs.gov/ using the place name of the study area and its Path-168 and Row- 57. By selecting the "Additional Criteria" option and ensuring that the cloud cover is less than 10%, the datasets used were downloaded with the consideration of the years 1994 -2004, 2004 -2014 and from 2014 – 2022 years. The study used images with a spatial resolution of 30 m and less than 10% cloud cover. The LANDSAT data that were used for this study are listed in table 3 below.

Table 3 Summary of spatial data sets used in this study.

Dataset type	Acquisition year	Pixel Resolution (m)/Scale	Path/Row	Producer	Purpose
Satellite data Landsat8 OLI/TIRS C1 level-1	2014/01/18	30m	168/57	USGS	For-generation of drought indices like NDVI, and VCI
Landsat5	1994/01/11	30m	168/57	USGS	For-generation of drought indices NDVI, and VCI.
Landsat7	2004/01/10	30m	168/57	USGS	For- generation drought indices NDVI, and VCI

The TM and ETM+ instrument on Land sat 5 and 7 observe the Earth with 7 different filters or bands. Bands 1, 2, 3, 4, 5, and 7 on TM and ETM+ are sensitive to light energy from the sun reflected by the surface of the earth. Each band is sensitive to a different part of the reflected electromagnetic energy. The parts of the reflected energy are defined by the length of energy waves. The human eye sees reflected light in that band of wavelengths as the color blue, green and red; hence, band one is usually observed as the blue band. In a similar manner, bands two and three of the TM and ETM+ instruments record reflected green and red light, respectively. TM and ETM+ bands four, five, and seven record reflected light in wavelengths that human eyes cannot detect. The band 4 referred to as near infrared, bands 5 and 7 referred to as short wave infrared. Band 6 of the TM and ETM+ instruments is different from all the other bands because it doesn't record reflected light energy, but rather energy emitted by the Earth's surface. It is sometimes called as the thermal infrared band (TIR band) or just the thermal band.

Additionally, the following data also used for the study.

Table 4 Ancillary and other spatial data used in study.

Ancillary and other data	Producer	Purpose
Administrative boundaries	Taken from Yabello district land administration office	Boundary demarcation for study
Meteorological data/Rainfall and temperature data	Hawassa Meteorological agency	Generation of drought indices like SPI and SPEI, rainfall analysis.

3.3 Software/Materials Used

Table 5 Shows Software used in the course of the study

Software	Application
ARCGIS 10.8	Map preparation drought indices generation and data processing to obtain out put
ERDAS EMAGINE 2015	Image preparation and processing
Rstudio-2023.12.1-402/ R.4.3.3 Software	Used to generate drought indices such as SPI and SPEI

SPSS Software 29.0.2.0.	To analysis correlation between generated drought indices.
MS EXCEL	Statistical analysis and graphical preparation
MS WORD	Word document processing

3.4 Data processing and analysis methods

The study uses quantitative research methodologies to address its purpose. Using meteorological (temperature and rainfall) and remote sensing data, the methodology uses geographic information systems and remote sensing technology to analyze the extent of the drought over the research area.

Data on temperature and rainfall quality were examined. Collected temperature and rainfall data Were used to calculate conventional based drought indices such as the Standardized Precipitation Index (SPI) and the Standardized Precipitation Evapotranspiration Index (SPEI) using Rstudio software. Additionally, the Pearson correlation coefficient (PCC) and Cohen's Kappa statistics were used to examine the linear relationship and degree of agreement between SPI and SPEI, respectively. Inverse distance weighting interpolation method used for meteorological drought mapping using calculated values of SPI and SPEI at 3and 12 month scales. Researcher looked at the preprocessing needs for the Landsat satellite image, which include layer stacking, re-projection, and shape file extraction of the research region. Landsat images were used to compute the remote sensing-based drought indices to produce drought maps from 1994-2004, 2004- 2014 and from 2014-2022 years.

Drought was measured using remote sensing-based indicators such as the Normalized Difference Vegetation Index (NDVI), DevNDVI, and Vegetable Condition Index (VCI), which was created with ArcGIS 10.8. Afterwards, a weighted overlay analysis was conducted in the research area to evaluate agricultural drought using the NDVI anomaly, DevNDVI and vegetation condition index (VCI) which was created with ArcGIS 10.8.

3.4.1 Meteorological data Processing

The agency's long-term temperature and rainfall records for the study area's station contain some gaps or missing values. One disadvantage of using these data types is that station data has missing values. Researcher used a different version of the data that downloaded from the Power Access Climate Data website (https://power.larc.nasa.data-access-viewer/), to fill in some data gaps. Using the multiple imputation method, it was determined that the missing data in the time series was less than 5%(Das, 2021). The general solution to the missing data problem is called multiple imputation, and it can be found in a number of widely used statistical packages. It fills in the missing values by producing believable numbers from the distributions of and relationships between the observed variables in the data set, then combining the results from each of them in the right way. In meteorology, straightforward method (arithmetic averaging of multiple imputation) is frequently used to fill in the gaps in meteorological data. The missing data is obtained by calculating the dataset mean corresponding to the closest rainfall stations, as shown in the equation below (Wangwongchai et al., 2023):

$$R_o = \frac{\sum_{i=1}^{n} R_i}{N} \tag{1}$$

Ro is the missing data at the target station Ri is monthly rainfall at the nearest stations and N is the total number of rain fall stations closest to the point of interest.

R o is the missing data at the target station, R i is the daily rainfall at the nearest stations, and N is the total number of rainfall stations closest to the point of interest.

According to the researcher's above theory, the remaining missing values in the study area's meteorological data were thus found using the multiple imputation method and SPSS Software 29.0.2.0: Figure5: depicts the SPSS software's interface for computing missed values in meteorological data.

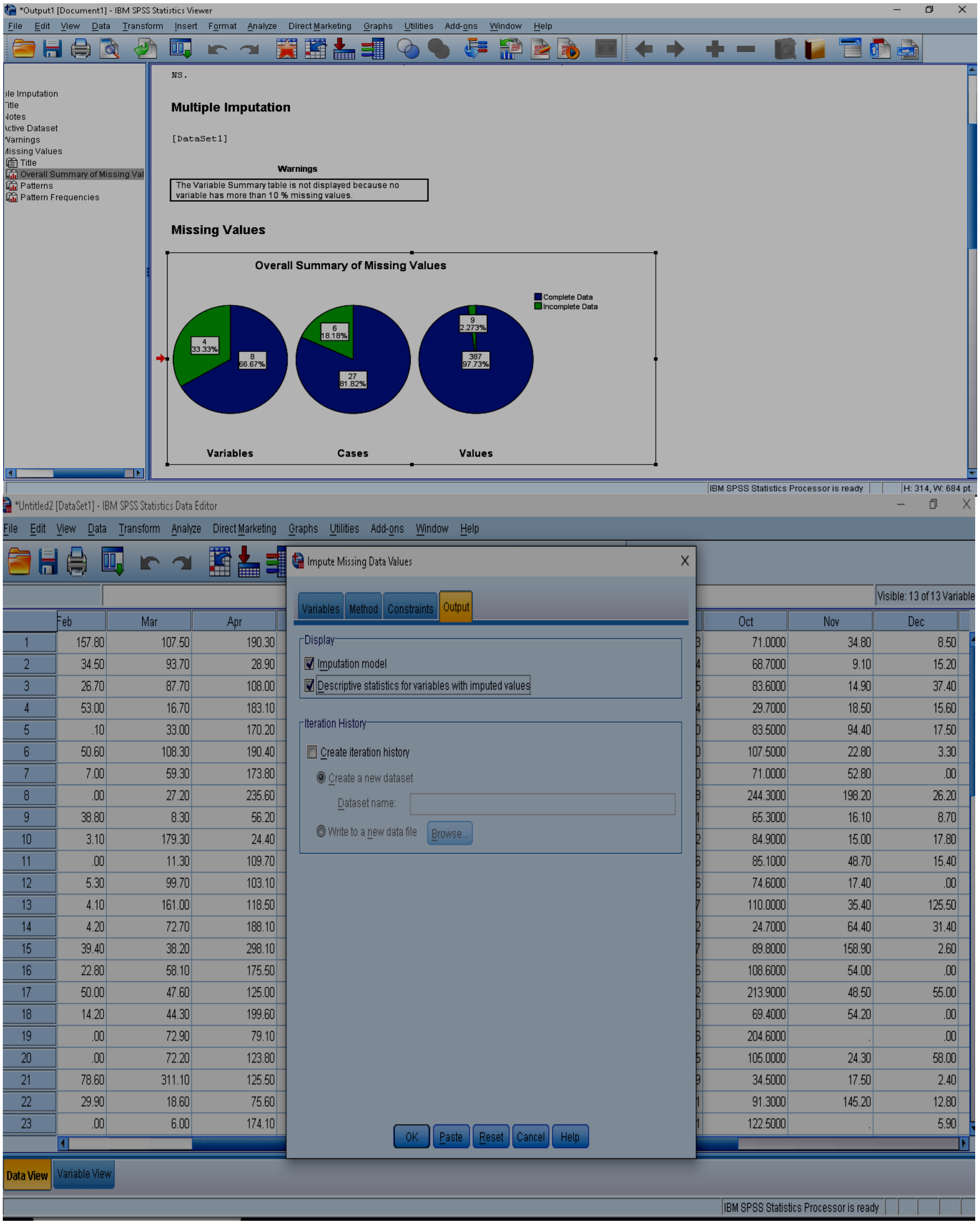

Figure 4: Inter face of SPSS software for Computation of missed values of meteorological data.

Meteorological data collected for 28 year period, from 1994 to 2022, was used specifically to obtain SPI and SPEI output values for analysis. SPI and SPEI were generated using data processed in Rstudio-2023.12.1-402/ R.4.3.3 software (http://cran.r-project.org/web/packages/SPEI).

3.4.2 Satellite Image Data Processing

After the data were downloaded, ERDAS Imagine was used to process the satellite images for 1994–2004, 2004–2014, and 2014–2022. Picture Pre-processing is done in the ERDAS Imagine 2015 and ArcGIS 10.8 environments. This includes coordinate system adjustment (projection from geographic coordinate system to projected coordinate system), layer stacking, clipping, and generation of the drought indices.

3.4.3 Meteorological Data Analysis methods.

Every month, data on rainfall, minimum and maximum temperatures, and other variables were entered into a Microsoft Excel 2016 spreadsheet. For the purpose of creating the Standardized Precipitation Index (SPI) and Standard Precipitation Evapotranspiration Index (SPEI), two drought indices, these meteorological data were sorted and stacked in the desired order before being imported into the Rstudio software.

According to Vicente et al. (2010) and Wondimu et al., (2022), the indexes should be calculated using at least 30 years' worth of data. But, due to unavailability of data, study computed SPI and SPEI using 28-years rainfall and temperature data from the Ethiopian Meteorological institute's Hawassa branch. Both indices were computed using Rstudio-2023.12.1-402/ R.4.3.3 software and the SPEI Package. These indices used to characterize (map) meteorological drought with in the study area using IDW interpolation method.

Using rainfall data, the Standardized Precipitation Index (SPI) was created to characterize the Meteorological drought in the study area. The SPI values are obtained by the package using the monthly total rainfall, while the SPEI values of the necessary time scales of 1, 2, 3, 6, 9, and 12 months and the characterization of the drought magnitude in the study area were calculated using the monthly minimum and maximum temperatures, the total rainfall, and the latitude of the stations. SPI and SPEI are the reliable indices that are most frequently used to calculate drought conditions based on climatic data, as suggested by Haile et al., (2022). SPEI is a widely used and recent index for drought analysis.

Researchers employed a number of statistical techniques, including the Cohen's Kappa statistics and the Pearson correlation coefficient, to determine the relationship and level of agreement between SPI and SPEI.

3.4.4 Standard Precipitation Index (SPI) based drought analyses

The SPI has been widely used over the past 20 years since it was first proposed by McKee et al. (1993; 1995). Worku, (2024)in his research explained Viste et al. (2013) suggested this index for countries like Ethiopia with limited data access.

The station under study's meteorological drought or precipitation deficit is determined over a number of timescales using the Standard Precipitation Index. The SPI value allows one to compare the total amount of rainfall for all the years in the historical record for a given period of time with the rainfall over that same period. An extended precipitation record at the target station is first fitted to a probability distribution (such as the gamma distribution) in order to calculate the SPI. This is subsequently converted into a normal distribution so that the mean SPI is zero (McKee et al., 1993; Edwards and McKee, 1997, cited in Duba et al., 2021). (Svoboda et al., 2012)

A drought event occurs any time the SPI is continuously negative and reaches an intensity of -1.0 or less; the event ends when the SPI becomes positive. Each drought event, therefore, has a duration defined by its beginning and end, as well as an intensity for each month that the event continues, as described in Svoboda et al.'s study as well as McKee and others' (1993) use of the classification system shown in the SPI value table (Table 1). They also defined the criteria for a drought event for any of the timescales. The "magnitude" of a drought is defined as the positive sum of the SPI for each month during the drought event.

The Standardized Precipitation Index (SPI) is a widely accepted index that is computed for multiple time periods, including 1, 2, 3, 6, 9, or 12 months, using rainfall as a single input. Previous research has demonstrated that the numerical measurements of precipitation are converted into standard units, normalized, and computed using Eq. 1 (Tefera et al., 2019 and Qaisrani et al., 2021).

$$SPI = \frac{X-Xm}{\sigma} \tag{1}$$

Where: X= recorded rainfall at the station

Xm = mean of rainfall, σ = standard deviation

Although equation (1) was utilized in numerous previous studies, more recent research employed the gamma distribution function as a continuity test and calculated SPI using the SPI package version 1.1 and the "precintcon package" version 2.3.0 in the RStudio application. This allowed for a comparison of rainfall with the total rainfall over a comparable time period in earlier records (Uddin et al., 2020, cited in Qaisrani et al., 2021).

Similarly, SPEI Package (Danandeh Mehr & Vaheddoost, 2020) in R environment evolved the SPI time series calculations in this study. That is to say, SPEI package (1.8.1) loaded in Rstudio-2023.12.1-402/ R.4.3.3 Software's environment used to calculate SPI values at 1, 2, 3, 6, 9, and 12 time scales. By default, the package uses Gamma distribution to standardize the SPI values. The SPI values that were obtained were classified in accordance with table (1) that was previously shown. The steps required to calculate SPI values using the SPEI Package loaded in the console portion of Rs tudio Software were explained in appendix (VI)after precipitation data were organized and imported into Microsoft Excel 2016. Figure 6 below shows interface of RStudio software while computing SPI.

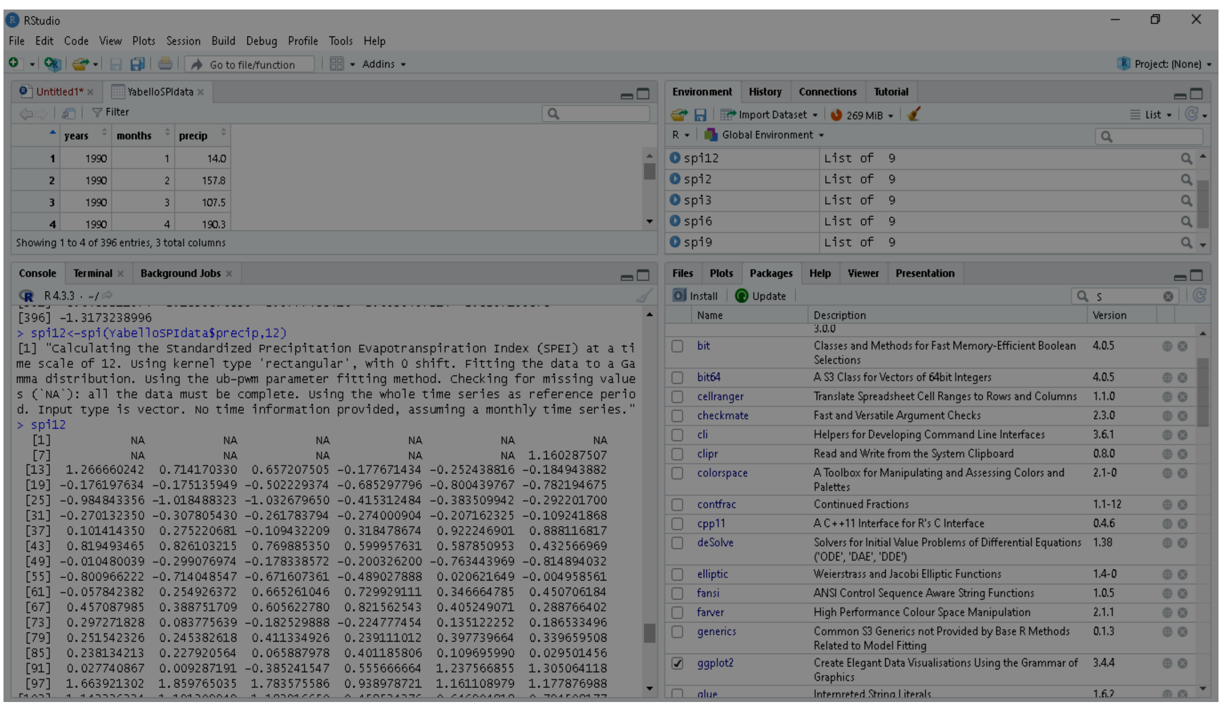

Figure 6 Interface of RStudio software while computing SPI

3.4.5 Standard Precipitation Evapotranspiration Index (SPEI) based drought analyses

Another drought index that is based on temperature data for maximum and minimum values as well as precipitation is the Standardized Precipitation Evapotranspiration Index (SPEI). As explained by Haile et al. (2022), Mishra et al. (2010) state that the SPEI is a multiscalar index that is more expressive and appropriate for characterizing droughts, climate variability, and global warming than other indices. Like SPI, this index also used to characterize meteorological drought in study area.

The first step to calculate the SPEI is the estimation of monthly potential evapotranspiration (PET). Potential evapotranspiration (PET) is the amount of evaporation and transpiration that would occur if a sufficient water source were available.

As stated in Qaisrani et al. (2021), the researchers (Thornthwaite 1948; Hargreaves 1994; Anderson and French 2019) claim that various approaches, such as the Penman-Monteith, Hargreaves, and Thornthwaite methods, exist to compute PET depending upon the data available. Vicente et al. (2010) state that while the estimated SPEI is not greatly affected by the PET method employed, there are times when certain approaches yield better PET quantification results than others. However, Beguería et al. (2014) discovered significant variations in SPEI calculated using various PET methodologies in dry and semi-arid environments. Penman-Monteith was suggested by Beguería et al. (2014) as the optimal choice for estimating PET for the computation of SPEI, with the Hargreaves and Thornthwaite methods coming in second and third. However, in addition to temperature data, the Penman-Monteith method requires data on sunshine, humidity, and wind speedall of which are insufficient in the study area, both temporally and spatially. The only parameters that the Hargreaves method seeks for are precipitation, maximum and minimum temperatures, latitude, and extraterrestrial radiation (Ra). Beguería et al. (2014) suggested the Hargreaves method as it is more effective than other methods at accounting for potential evapotranspiration, particularly when data is limited. As a result, the Hargreaves technique was applied in this study, which requires rainfall, maximum and minimum temperatures, and the station's latitude as a proxy for solar radiation. The R Studio SPEI package was utilized to compute SPEI based on temperature and precipitation data spanning from 1990 to 2022. (Beguería and Vicente-Serrano 2017; Montes-Vega et al., 2023 ; Minas et al., 2022). The Hargreaves method of calculating the PET is given in Eq. (2)

(Hargreaves and Samani 1985, as cited in Qaisran etal., 2021). See Obtained data under (s Appendix IV).

$$PET= cH.0.408Ro.(T+17.8)\sqrt{Tmax - Tmin} \quad (2)$$

Where, cH is the Hargreaves coefficient with a value of 0.0023, an inverse of the latent heat flux of vaporization gives constant value of 0.408 at 20 °C, Ro denotes solar radiation calculated as a function of latitude, and the mean temperature is given as T.

Then, the water balance equation is used to calculate the difference in monthly water balance of a given month (i.e. deficit Di) is by subtracting PET from precipitation value of a given month (Pi).

$$D_i=P_i-PET_i \quad (3)$$

Where, Pi is the total precipitation value at the month i. Finally, the evolved deficit values are s tandardized and fitted to a log-logistic distribution function. The SPEI value at the month i is t he standardized values of the exceeding probability (p) of a given Di and is calculated by Eq. (4) (see also Appendix VII).

$$SPEI_i = Wi \ \frac{2.515517+0.802853Wi+0.010328Wi2}{1+1.432788Wi+0.1892689Wi2+0.001308Wi3} \quad (4)$$

While for p≤ 0.5, Wi =$\sqrt{-2\ln p}$ whilst, if P> 0.5

W_i = $\sqrt{-2\ln p}(1-p)$, and the sign of the resultant SPEI is reversed for p>0.5(Danandeh Mehr et al. 2019; cited in Danandeh Mehr & Vaheddoost, 2020).

Where, p is the probability of exceeding a given Di. Di is the climatic water balance (CWB) in a given period (mm), Pi is the precipitation in a given period (mm), and PET is the potential ev apotranspiration in a given period (mm) calculated using the Hargraves method.

In this research, the software created by Berguer et al. (2014), as described in Abara et al.(2020) which uses above formula was utilized for the SPEI calculation. R package SPEI version 1.8. 1 (http://cran.r- project.org/web/packages/SPEI) was used to apply the software. The Hargreav es method is used by the package to calculate SPEI values. Refer to Appendix VIII for the calc ulation steps Table 1 was used to classify computed SPEI values.
Figure 5 below shows interface of RStudio software while computing SPEI.

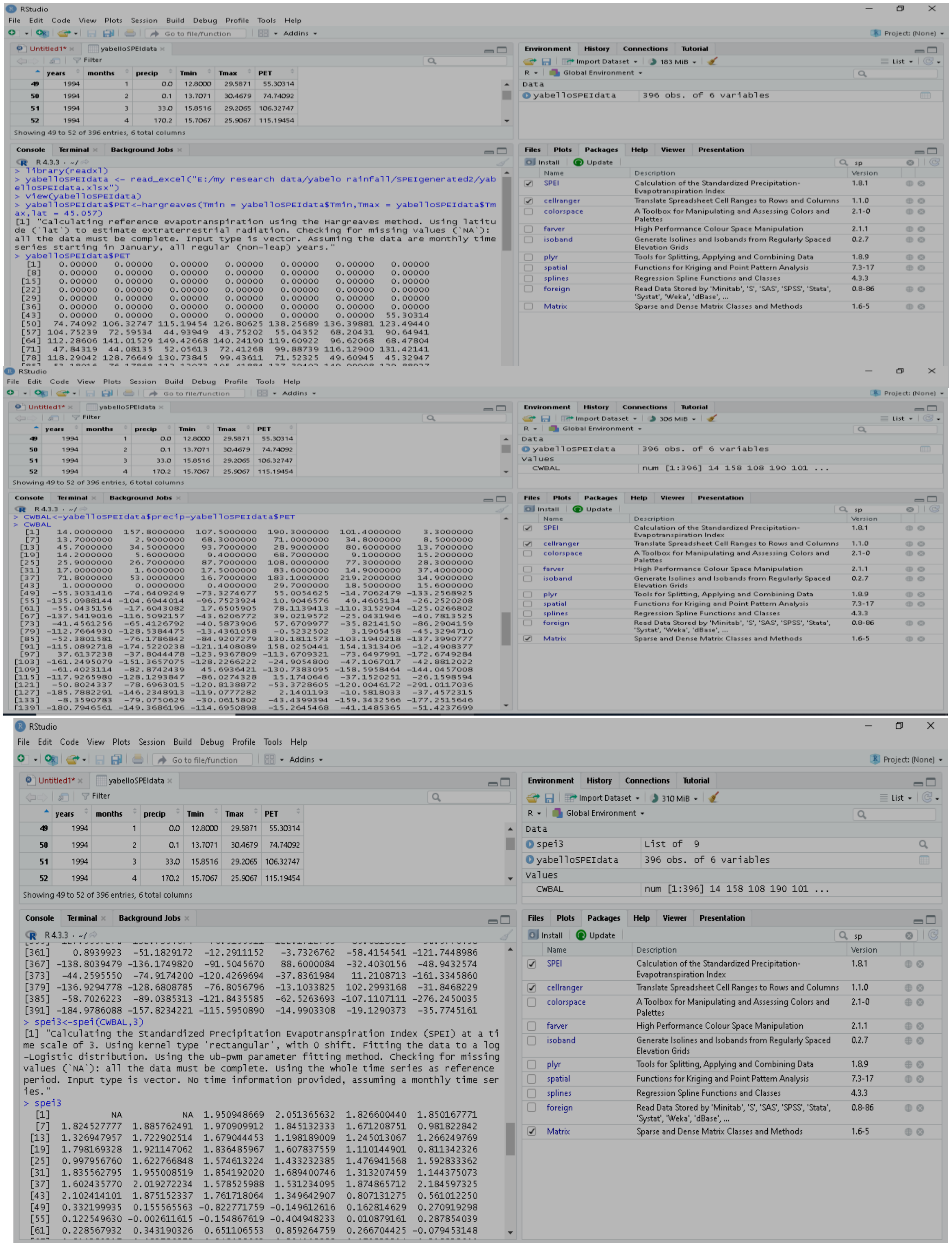

Figure 6 interface of RStudio software while computing SPEI

3.4.6 Drought Characteristic Analysis using SPI and SPEI

Characteristics of drought are explained by factors related to frequency, duration, intensity, and severity of the drought (Dilawar et al., 2021).

SPEI measures the frequency, duration, and severity of droughts using both evapotranspiration and precipitation. The duration, frequency, and severity of a drought are among the characteristics that can be ascertained and its impact evaluated using a drought index. The SPEI and SPI drought index were utilized in this study to identify the characteristics of the drought.

The drought and non-drought events are denoted, respectively, by the negative and positive values of SPEI. When the SPI value first drops below zero, the drought begins, and it ends when the SPI value rises. When SPEI values are negative and fall below zero, it is referred to as a drought event (Abara et al., 2020).

The maximum intensity of dry events is calculated using drought indices in accordance with table 1's classification. Drought caused by weather patterns and hydrological factors is assessed based on its length and intensity. When the drought indices (SPI, SPEI) for any given time period are less than zero, that period is considered to be the length of the drought. The indices that show a few dry events with longer duration are determined by the increasing time scale, whereby each new month has less of an impact on the total precipitation (McKee et al. 1993, as cited in A & A, 2020). The extreme drought duration is highlighted in the current paper.

i. Drought Duration

The number of months between the beginning and end of a drought was used to define its duration. In this study, the length of time that the SPEI and SPI values were consistently negative is known as the drought duration (D). When the drought indices (SPI and SPEI) for any given time period are less than 0, that period is considered to be the length of the drought. It is calculated using formula provided (Xu et al., 2018, cited in Worku, 2024)).

$$D = \sum_{i=1}^{n} d_i \tag{5}$$

Where, di is duration of ith drought event in an area and n is the total number of drought events in the area.

ii. Drought frequency

Drought frequency, according to Yu et al. (2014) as stated in worku (2024), is the quantity of drought events in a specific period of time. Wang et al. (2018) estimated it as the ratio of the number of months in a time series that were drought-free to the total number of months in the time series.

$$F = (n_m / N_m) * 100 \tag{6}$$

Where, n m is the number of drought months and Nm is the total number of months over study period. Total number of months for 28 years = 28*12 = 336 months

iii. Drought magnitude (DM)

The positive total of the negative drought indices over a series of months is the drought magnitude. SPI and SPEI may be substituted in the drought magnitude formula instead. The following formula

was provided by (McKee et al.1993, as cited in A & A, 2020) and was used to determine the drought magnitude (DM) for both SPI and SPEI:

$$DM = -\left(\sum_{j-1}^{x} SPI_{ij} \right) \tag{7}$$

Where, j is the first month when SPI or SPEI becomes negative and x is the last consecutive month with the negative value of the index.

3.4.7 Assessment of linear relationship between SPI and SPEI

The Pearson correlation coefficient (PCC), also known as the product-moment correlation coefficient, was used to test for a linear relationship between SPI and SPEI. PCC is the most widely used statistical method for displaying the strength of relationship between two variables. Furthermore, when two sets of continuous data are available on the same experimental unit and follow a bivariate normal distribution, PCC is used to test for a linear relationship. The PCC only measures correlation. PCC has a range of + 1 (perfect positive linear relationship) to − 1 (perfect negative linear relationship). The PCC value of 0 indicates that the variables do not have any linear relationship(Adler & Parmryd, 2010). However, as explained in Tefera et al.(2019), it would be misleading to use PCC to characterize the degree of agreement between variables. Hence in this study, PCC was used only to test the strength and direction of the linear relationship between the two drought indices at selected time scale. Pearson correlation(r) can presented by the equation (Faheem et al., 2024):

$$r = \frac{\sum (x_i - \bar{x})(y_i - \bar{y})}{\sqrt{\sum (x_i - \bar{x})^2 \sum (y_i - \bar{y})^2}} \tag{8}$$

Where, xi and yi are the variables and x and y are the mean of variables.

3.4.8 Cohen's Kappa statistics

It is common in many disciplines to evaluate the level of agreement between two or more assessment methods. In order to quantify the nominal scale agreement between two assessment methods, kappa statistics were introduced. Kappa statistics is said to be one of the most often used statistics for this purpose because of its ability to solve this problem. A standardized scale of -1 to 1, where 1 represents perfect agreement, 0 represents exactly what would be expected by chance, and negative values indicate agreement less than chance, which is a rare occurrence, is used to measure this difference (Viera & Garrett, 2005). Refer to Table 6 for an interpretation.

Table 6 Interpretation of Kappa Values

Kappa Value	Degree of agreement
<0	Agreement equivalent to chance
0.1-0.2	Slight agreement
0.2-0.4	Fair agreement
0.4-0.6	Moderate agreement
0.6-0.8	Substantial agreement
0.8-0.99	Near perfect agreement
1	Perfect agreement

Cohen's kappa (J.A., 1960) can be used to calculate kappa statistics. Fleiss J. (1972) stated that Kappa statistics can also be obtained using Fleiss' Kappa, as Tefera et al. (2019) also explain. Fleiss's Kappa is an extension of Cohen's Kappa for three or more ratters (measurements), and

Cohen's Kappa is used to determine the degree of agreement when there are either two assessment methods with one trial or one assessment method with two trials. Furthermore, unlike Fleiss' kappa, Cohen's kappa makes the assumption that the assessment techniques are predetermined and carefully chosen. In light of these presumptions, Cohen's Kappa Statistics was determined to be appropriate for this research and was employed to evaluate the level of agreement between SPI and SPEI as instruments for assessing drought. Since Kappa statistics performs well on ordinal or nominal data, each assessment method's continuous values (SPI and SPI, for example) can be used and the formula for Cohen's Kappa statistics is given as below. (Tefera et al., 2019).

$$k = \frac{\rho_O - \rho_e}{1 - \rho_e} * 100 = 1 - \frac{1 - \rho_O}{1 - \rho_e} \qquad (9)$$

Where, Po is the relative observed agreement and Pe is the predicted probability of chance agreement.

3.4.9 Spatial analysis of Meteorological drought hazards based on calculated SPI and SPEI values.

The accuracy of spatial representations of drought conditions is influenced by interpolation in addition to the selection of drought indices. Several interpolation techniques that are frequently employed in drought monitoring have been assessed in earlier research.

According to Yuan et al.(2016), Rhee et al. (2008) examined the effects on droughts across space by comparing two interpolation techniques used for mapping drought indices: spatial interpolation (IDW) plus aggregation and simple unweighted average.They discovered that the best approach is spatial interpolation and aggregation. Generally speaking, using interpolation techniques prior to determining drought indices may result in greater error than doing so after the drought index has been determined.

Yuan et al. (2016), in their study indicated that Inverse Distance Weighting (IDW) and Ordinary Kriging are the most widely utilized interpolation techniques in the environmental sciences, Li and Heap (2011) employed them. The technique known as inverse distance weighting interpolation makes use of the presumption that nearby points are more similar than far-off ones. It estimates the value of any point that has not been measured using the values that are known around the prediction point. The influence of values nearer the prediction point will be greater than that of values farther away. As a result, it depends on the local influence at each measured place decreasing with distance. Because it gives greater weight to points that are closer to the forecast, this technique is known as the reverse distance weighting approach. The main formula for the procedure is as follows(Johnston et al. 2001, cited in Yuan et al., 2016):

$$x = \frac{\sum_{i=1}^{n} z_i \; w_i}{\sum_{i=1}^{n} w_i} \qquad (10)$$

Where, x is unknown point to be estimated, Zi represents the control value for the i-th sample point and Wi a weight that define the relative importance of the individual control value, n is number of stations or points, Zi is the interpolation procedure.

But, in this study IDW interpolations between SPI and SPEI at both 3-months and 12-months was carried out using ArcGIS 10.8 software. Computed values of SPIand SPEI at these timescale were interpolated using five stations (Yabello, Taltale, Dire, Arero and Surupha stations). SPEI and SPI at selected time scale was computed for each stations. But, interpolation output was only masked to yabello district using study area shapefile (boundary obtained) because of the study targeted to it.

Note that: The remaining four stations used only to generate spatial view (interpolation area coverage) in yabello district, analysis did not performed on them. Therefore, spatial analysis of meteorological drought was taken with in district boundary of the study area.

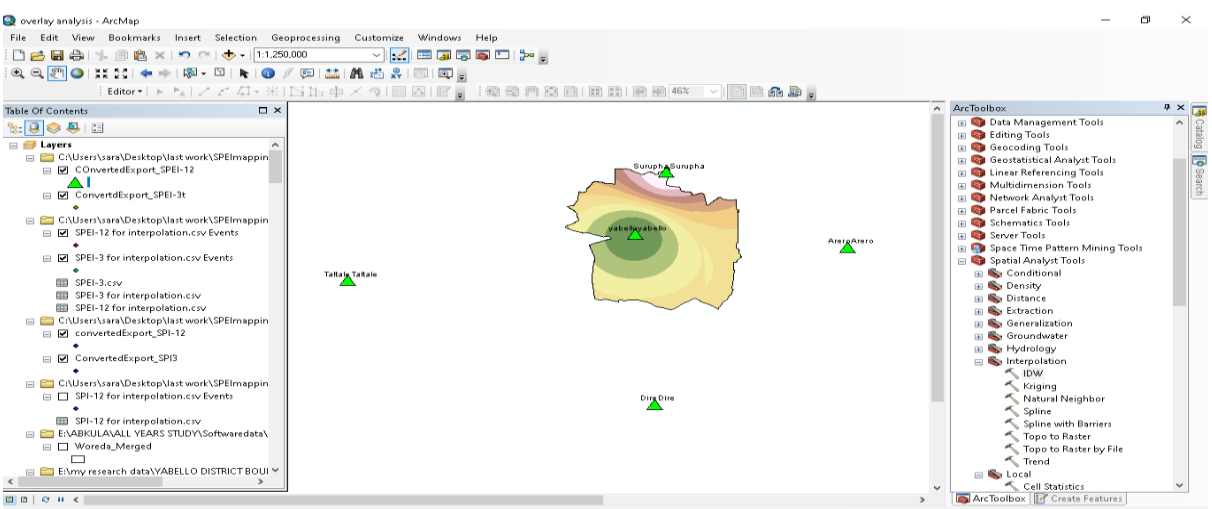

Figure: interface of ArcGIS10.8 during interpolation process

3.5 Satellite Image based spatial analysis of agricultural drought.

The task of monitoring drought in remote sensing images is both crucial and difficult. The specific work involved in this task is analyzing multiple temporal remote sensing images for the same target area quantitatively in order to determine the extent of surface changes. This is accomplished by applying layer stack, subset, and projection image preprocessing to all downloadable LANDSAT-8 data in order to perform drought analysis. Three drought indices were created for the analysis of LANDSAT images of the study area: the Vegetation Condition Index (VCI), the NDVI deviation (DevNDVI), and the Normalized Difference Vegetation Index (NDVI). Since there is a negative correlation between vegetation density and rainfall amount and duration, on the one hand, and vegetation cover on the other, vegetation cover is a very powerful environmental indicator of drought. Based on the generated index, the condition of the study's vegetation was evaluated.

The following three drought indices were used to analyze the spatiotemporal variation of agricultural drought patterns and agricultural drought severity:

3.5.1 NDVI anomaly analysis

By analyzing NDVI anomalies, one can use the NDVI as a vegetative drought index to evaluate drought (Murali et al. 2008, cited in Legesse & Suryabhagavan, 2014). Equations (6) were utilized to classify the NDVI anomaly index into distinct classes of drought severity, as indicated in Table 1 (Amin et al., 2020). and to compute the NDVI anomaly index for the chosen study periods.

$$\text{NDVI anomaly} = 100\ (\text{NDVi} - \text{NDVIavg}) \,/\, \text{NDVIsd} \qquad (12)$$

Where, i particular value of NDVI, avg = average value, sd = standard deviation.

Table 7 NDVI anomaly classification.

No.	NDVI anomaly values	Drought severity classes
1	< -50	Very severe drought
2	-50 to -25	Severe drought
3	-25 to -10	Moderate drought
4	-10 to 0	Slight drought
5	>0	No drought

3.5.2 The NDVI deviation

The NDVI value obtained from each image was used to calculate the NDVI deviation (DevNDVI) (Tucker, 1979, as cited in Wondimu et al., 2022)):

$$DEVNDVI = NDVIi - NDVI\ mean, \quad (13)$$

Where NDVIi is the NDVI value for the year i and NDVImean is the long term average of NDVI.

The NDVI deviation values were classified based on(Hill & Atnafu, 2011) at range of > -0.05 to <=0.1(near normal) followed by > -0.2 to<= -0.05 (drought) using the Nearest Neighbor Rule classification while he was studying whole Ethiopia. Table 8 shows this classification.

Table 8 NDVI deviation classes and range of values

No	Drought classes	Range of Dev NDVI values
1	Severe drought(extremely dry)	<= -0.2
2	Drought(moderately dry)	>-0.2 and <=-0.05
3	Near normal	>-0.05 and <=0.1
4	Above optimum(extremely wet)	>0.1

3.5.3 Vegetation Condition Index (VCI) analysis

The highest amount of vegetation appeared during a year with ideal weather. Conversely, the year with the least favorable climate exhibit a drought, for example, it will have the least amount of vegetation because it will directly impede the growth of vegetation. As a result, it serves as a gauge for the health of the vegetation cover and is expressed as a percentage when assessing the spatial characteristics of drought, its duration, and its severity based on the NDVI minima and maxima experienced over an extended period of time for a particular ecosystem. Equation 7 and Table 9, respectively, present the VCI calculation and classification (Uttaruk & Laosuwan, 2017).

$$VCI = (NDVIi - NDVI\ min) / NDVI\ max - NDVImin*100 \quad (14)$$

Where, NDVImax and NDVI min defined as the maximum NDVI and minimum NDVI for all time intervals of the study years.

Furthermore, Kogan (1997) noted that VCI below 50% indicates varying degrees of drought severity and that VCI of 35% is a threshold for extreme drought, as reported in Birhanu Gedi.f et al. (2014). Additionally, he arbitrarily categorized the East African VCI values below 35% as follows (Birhanu Gedi.f et al., 2014):

Table 9 VCI drought Classification

VCI value (%)	Drought classes
<10%	extreme drought
10% - 20%	severe drought
20% -35%	moderate drought
35% -50%	no drought
> 50%	wet

3.6 Weighted overlay analysis

With the aid of the previously mentioned, weighted overlay analysis is carried out to determine the susceptible drought-prone areas (drought hazard map). A useful technique for producing integrated analyses with different and dissimilar inputs based on multiple criteria is weighted overlay analysis. In this study, drought-prone areas from 1994 to 2022 were evaluated by combining the results of 2-months and 12- Months of SPI/SPEI and landsat data, including NDVI, Dev NDVI, and VCI (Aziz et al., 2018):

$$A = W_1A_1 + W_2A_2 + \ldots + W_n A_n \tag{15}$$

Where, W_{n} = Criteria/weight, provided that sum of all Wn is100. A_{n} = Input raster

Aziz et al. (2018) gave the NDVI and VCI 40% and 30% weight, respectively. Since the long-term mean is unavailable in the case of Dev NDVI, the actual drought situation could not be represented by Dev NDVI. As a result, it is given a 20% weight. Amin et al. (2020) contributed 20% for VCI and 40% for SPI to the creation of a final combined drought risk map during their study, in addition to Aziz et al. (2018). The total weights add up to 100 percent. As indicated in Legesse & Suryabhagavan (2014), Lemma (1996) states that the probability of drought occurrence in a given area can be classified into high, moderate, and low drought probability zones based on the percentage of years that drought occurs: >50%, 30-50%, and <30%, respectively. Based on this, study used drought severity layers of NDVI anomaly, DevNDVI and VCI to generate composite drought severe map at agricultural scale through weighted overlay analysis in GIS10.8.

Weights were assigned to each parameter based on their importance and from a comprehensive literature review, as shown in Table 10.

Table 10 Numerical weights and ranked value assigned to the subclasses of drought severity

No	parameter	classes	Reclassified ranked value	Weight
1	SPI	Moderately dry Severely dry Extremely dry	1 2 3	24
2	SPEI	Moderately dry Severely dry Extremely dry	1 2 3	26
3	NDVI anomaly	Very severe drought Severe drought Moderate drought Slight drought No drought	1 2 3 4 5	15
4	DevNDVI	extremely dry moderately dry Near normal extremely wet	1 2 3 4	15
5	VCI	extreme drought severe drought moderate drought no drought wet	1 2 3 4 5	20

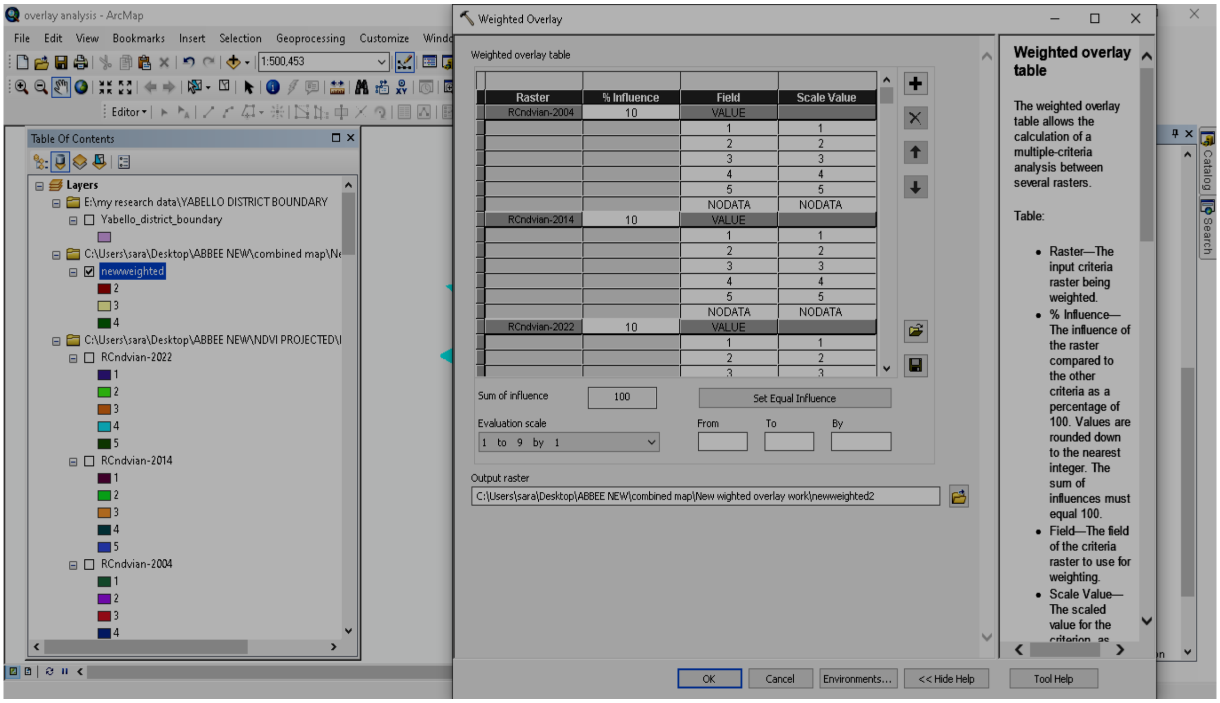

Figure: interface of ArcGIS while overlaying layers

So, researcher followed above criterion to show the severity of drought in study area. But, the area of the drought classes were calculated using the below formula:

Area (sq-km) = Count *30* 30 / 100000 (16)

Where ,Count = no of Cells and the cell size of landsat images were 30*30.

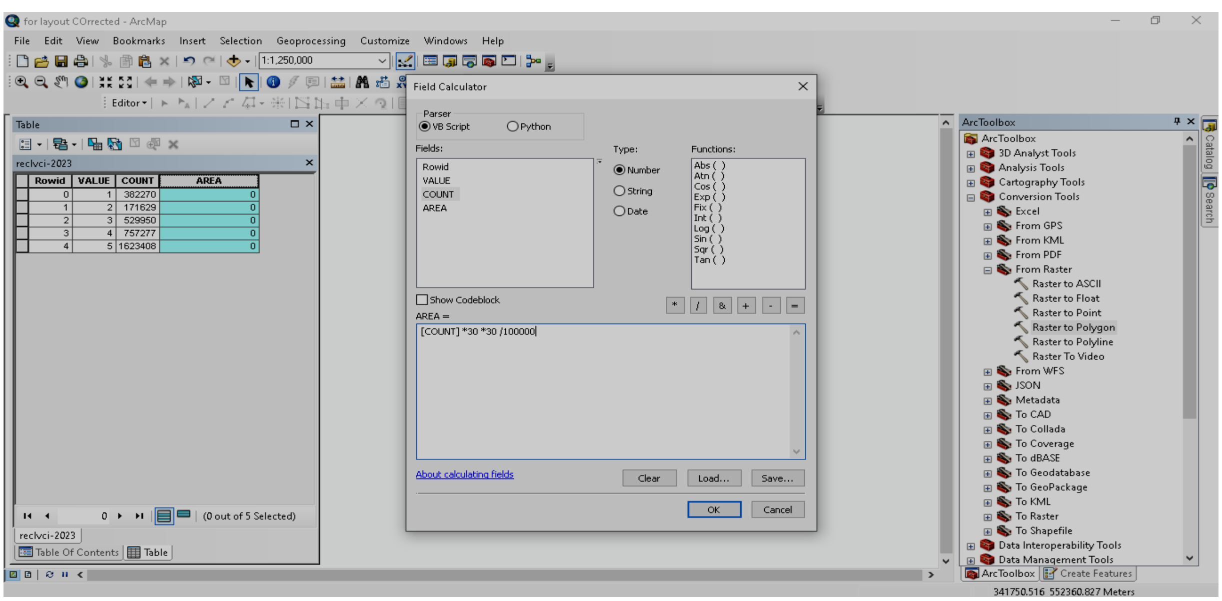

Generally, Rainfall data based drought indices and Satellite based drought indices for drought characterization was used to study droughts. Techniques and the data inputs that was used throughout this study explained briefly in the methodological Scheme of the Study displayed here below:

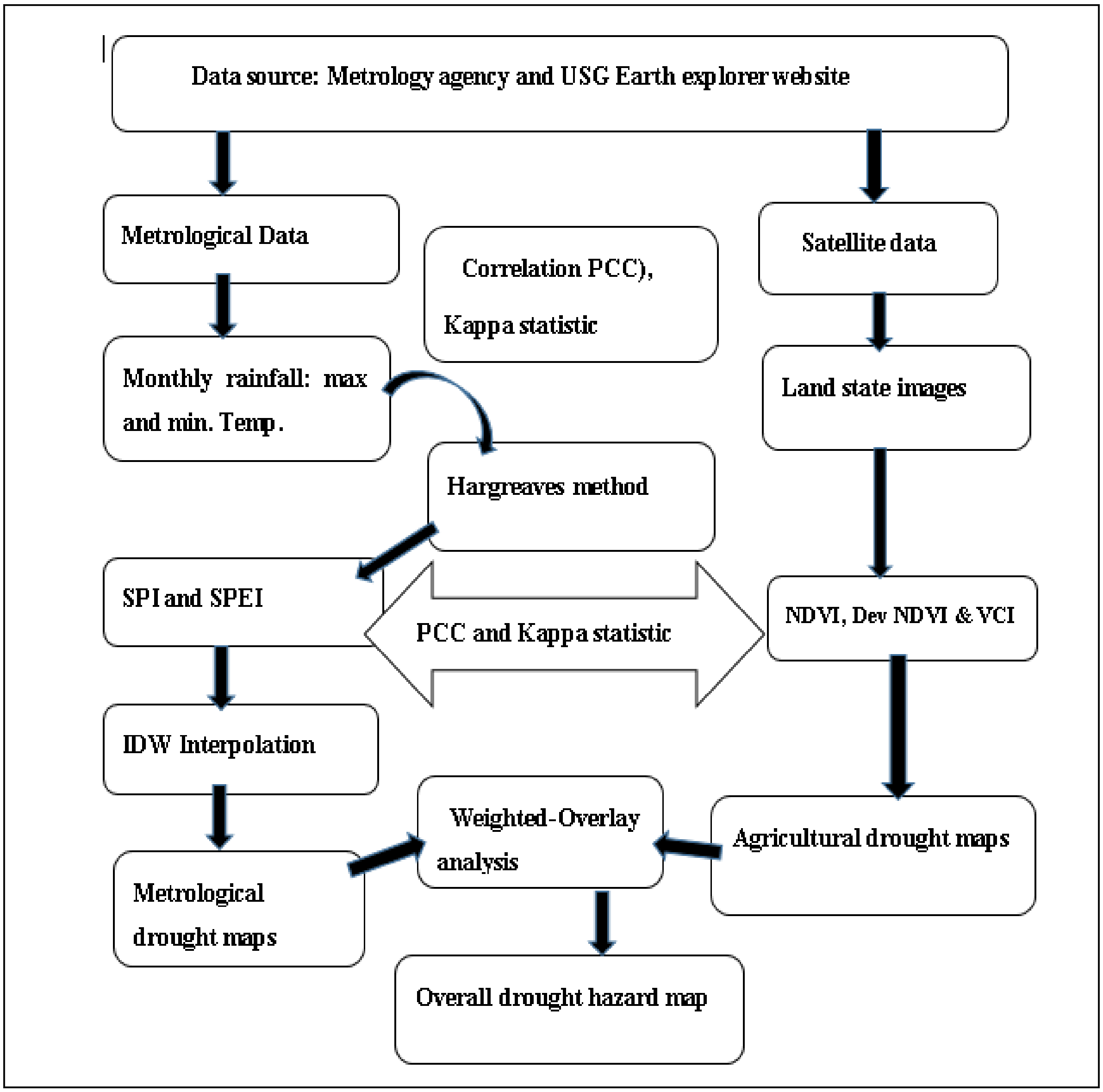

Figure 7: Methodological Scheme of the Study

CHAPTER FOUR: RESULT AND DISCUSION

4.1 Results

In this study, meteorological data based two drought indices(SPI and SPEI) and three Remote sensing data based drought indices(NDVI, DevNDVI and VCI) used to assess severity of the Meteorological and Agricultural drought from 1994 to 2022 in yabello district area of study. Using the SPEI Package (1.8.1) that was loaded into the Rstudio-2023.12.1-402/ R.4.3.3 Software environment, the SPI and SPEI time series computations are evolved. The package standardizes the SPI and SPEI values by default using the log-logistic and gamma distributions, respectively(Beguería and Vicente-Serrano 2017,as cited in Danandeh Mehr & Vaheddoost, 2020). Using the Hargreaves approach, the monthly PET and monthly Climatic water balance were estimated. SPI and SPEI time series at 1, 2, 3, 6, 9, and 12-month timescales were computed using temperature and rainfall data for the meteorological station for the period 1994–2022 in order to evaluate the state of the drought in the research area.

4.1.1 Standardized precipitation index (SPI) Standard Precipitation Evapotranspiration Index (SPEI) based drought analyses results

Standardized precipitation index and Standardized Precipitation Evapotranspiration index are two indices that are used to detect drought occurrences at timeframes of 1, 2, 3, 6, 9, and 12 months. At these various time scales, varying drought magnitudes were noted.

Figure 1. Shows, SPI and SPEI graph of yabello station at 1 time scales. When looking at these lower time scales, both indexes displayed comparable patterns. The results of a 1-month drought investigation showed that the station experiences frequent meteorological droughts. The start and finish of the study period are marked by drought in both indicators. At the 1-month SPI time scale, the extreme values of the SPI obtained are as follows: 2.72 in 2017 and -2.496 in 1994, which indicate extreme meteorological drought episodes, and 2.76 in 2019 which indicates exceptionally wet study period. Furthermore, the maximum 1-month SPEI values that indicate an extreme meteorological drought event were found to be -3.322 in 2000 and -3.18 in 2022. This one-month SPEI indicates a continuous drought in the station from the end of 2021 to the end of 2022. Table 11, which displays SPI and SPEI at a 1-month time scale, demonstrates that greater frequencies of meteorological droughts with durations ranging from 7 to 12 months

occurred in 1994, 1998, 2000, 2001, 2008, 2011, 2012, 2014, 2015, 2016, 2018, and 2022. Additionally, SPEI-1 shows that there was meteorological droughts in 2005, 2006, and 2021 year.

Table 11 SPI and SPEI at 1-Month time scale.

1-month SPI														
years	jan	feb	mar	apr	may	jun	jul	aug	sep	oct	nov	dec	negat_SUM	Frequency
1994	-1.47	-2.50	-0.45	0.57	0.61	-0.43	-1.24	0.61	-0.74	-0.22	0.87	0.03	-7.04	7
1995	0.45	0.84	0.77	0.80	-1.34	0.59	-0.79	-0.36	0.97	0.23	-0.62	-1.05	-4.16	5
1996	-0.21	-0.73	0.10	0.61	0.32	0.82	0.73	-0.50	1.61	-0.49	0.18	-0.55	-2.47	5
1997	-1.45	-1.76	-0.61	1.27	-1.20	0.10	0.64	-1.45	-0.46	1.98	1.99	0.38	-6.93	6
1998	1.79	0.57	-1.44	-1.32	0.45	0.04	-0.03	0.00	-1.16	-0.62	-0.90	-0.48	-5.94	7
1999	-1.79	-1.18	1.46	-2.39	-2.21	-1.45	0.55	-0.76	-0.12	-0.19	-0.95	0.05	-11.03	9
2000	-0.70	-1.32	-1.25	-0.26	-0.21	-2.13	-0.58	0.49	-0.41	-0.19	0.09	-0.07	-7.11	10
2001	1.13	-0.89	0.67	-0.37	-2.34	-0.80	0.36	0.57	-0.24	-0.41	-0.84	-0.58	-6.47	8
2002	0.33	-1.03	1.31	-0.12	0.66	0.00	-0.17	-1.27	0.79	0.27	-0.23	2.31	-2.82	6
2003	0.06	-1.02	0.31	0.78	1.39	-1.87	-1.38	1.05	-1.49	-1.95	0.40	0.55	-7.71	5
2004	1.26	0.58	-0.32	1.83	0.84	-0.58	-0.56	-0.58	1.05	-0.09	1.62	-1.17	-3.30	6
2005	0.22	0.09	0.08	0.63	1.07	0.28	0.23	-0.86	-1.09	0.25	0.20	-0.58	-2.53	3
2006	-1.20	0.83	-0.12	-0.02	-2.35	-0.75	-1.05	1.01	-1.14	1.66	0.09	1.15	-5.43	6
2007	-0.58	-0.27	-0.19	0.90	0.14	0.28	1.88	0.55	0.82	-0.52	0.21	-0.58	-2.14	5
2008	-0.29	-0.58	0.31	-0.80	-1.54	-0.58	0.81	-0.58	1.46	1.56	-0.58	-0.58	-5.53	8
2009	0.60	-0.58	0.30	-0.04	1.14	-1.32	-1.05	-0.54	0.76	0.19	-0.56	1.22	-3.51	5
2010	0.15	1.35	2.39	-0.02	1.28	-0.60	-0.12	0.94	0.13	-1.53	-0.83	-1.21	-4.30	6
2011	-0.58	0.32	-0.90	-0.88	0.08	0.39	0.84	-0.58	-0.44	-0.06	1.48	-0.21	-3.65	7
2012	-0.58	-0.58	-1.63	0.62	0.39	0.35	-1.33	-0.62	0.31	0.47	-0.58	-0.72	-6.04	7
2013	0.63	-0.58	0.91	0.23	-1.87	0.20	-0.24	0.22	1.48	0.53	-0.58	-0.58	-3.84	4
2014	-1.70	-0.58	0.52	-1.35	-0.13	-0.36	-1.83	2.49	-0.84	0.80	-0.36	-1.57	-8.71	9
2015	-0.58	-1.03	-0.06	-0.05	0.01	1.30	-0.58	-0.07	-0.85	0.32	0.66	1.04	-3.22	7
2016	-0.93	0.74	-0.85	1.88	-0.50	1.26	-0.58	-0.58	-0.44	-1.96	0.46	-0.06	-5.88	8
2017	-1.29	-0.26	0.01	-2.72	0.07	-0.58	0.64	1.00	1.52	1.68	-0.16	-0.58	-5.59	6
2018	-0.58	0.78	1.31	1.19	0.42	-0.39	-2.39	-0.45	-0.85	-0.63	-0.45	0.60	-5.75	7
2019	-0.91	-1.10	-1.05	-0.64	-0.10	2.77	0.64	-0.62	0.40	1.37	1.36	1.47	-4.43	6
2020	1.25	0.42	0.90	0.30	0.24	0.67	1.44	0.51	0.75	1.18	-0.50	-0.82	-1.31	2
2021	0.07	-0.48	-1.29	-0.11	1.43	0.04	1.79	1.31	0.83	-0.29	1.70	0.05	-2.17	4
2022	-0.58	-0.58	-1.25	-0.26	-0.21	-0.58	-0.58	0.49	-0.41	-0.19	0.09	-0.07	-4.70	11

1- month SPEI														
years	jan	feb	mar	apr	may	jun	jul	aug	sep	oct	nov	dec	negat_sum	Frequency
1994	-0.86	-0.52	-0.55	0.39	0.45	-0.15	-0.15	0.39	-0.63	-0.44	0.81	-0.01	-3.30	8
1995	-0.84	0.83	0.76	0.65	-1.00	-0.02	-0.23	0.08	0.70	0.12	-0.41	-0.41	-2.90	6
1996	-0.03	-0.23	-0.01	0.42	0.17	0.57	0.47	-0.30	1.20	-0.68	0.06	-0.53	-1.77	6
1997	-0.65	-0.57	-0.76	1.17	-0.88	-0.21	0.42	-3.17	-1.44	1.77	2.17	0.36	-7.69	7
1998	1.66	0.46	-1.52	-1.63	-0.40	-0.77	-1.25	-1.28	-1.70	-1.19	-0.75	-0.46	-13.15	12
1999	-1.38	-0.81	1.04	-1.81	-1.83	-0.32	0.35	-0.28	-0.31	-0.35	-0.60	-0.01	-7.70	11
2000	-0.54	-0.66	-1.46	-0.93	-1.17	-2.37	-3.32	-1.02	-1.37	-0.62	-0.17	-0.32	-13.96	12
2001	1.00	-0.67	0.15	-0.81	-1.84	-0.84	-2.63	-1.18	-1.22	-0.98	-0.66	-0.69	-11.54	10
2002	0.31	-0.37	1.19	-0.28	0.46	0.02	-0.16	-0.13	0.50	0.22	-0.26	2.35	-1.21	5
2003	0.21	-0.34	0.04	0.58	1.04	-0.14	0.03	0.74	-0.83	-1.82	0.23	0.42	-3.12	4
2004	1.34	0.65	-0.52	1.65	0.55	-0.23	-0.41	-0.40	0.59	-0.30	1.74	-0.35	-2.22	6
2005	0.33	0.20	-0.09	0.37	0.76	0.18	0.24	-0.27	-0.65	0.12	0.11	-0.55	-1.56	4
2006	-0.58	0.84	-0.23	-0.10	-1.31	-0.30	-0.05	0.75	-0.56	1.68	0.05	1.07	-3.14	7
2007	-0.53	0.04	-0.40	0.67	0.06	0.19	0.82	0.54	0.64	-0.73	0.11	-0.54	-2.20	7
2008	-0.09	-0.39	0.11	-0.64	-0.99	-2.18	0.54	-0.02	1.06	1.36	-2.16	-0.55	-7.02	8
2009	0.74	-0.26	0.09	-0.10	0.81	-0.29	-0.32	-0.23	0.44	0.11	-0.42	1.13	-1.61	6
2010	0.34	1.28	2.11	-0.09	0.99	-0.07	0.32	0.74	0.06	-1.43	-0.56	-0.46	-2.60	5
2011	-0.68	0.40	-0.80	-0.95	0.03	0.13	0.18	-0.47	-0.26	-0.24	1.59	-0.03	-3.43	7
2012	-0.69	-0.46	-1.16	0.43	0.21	0.06	-0.18	-0.39	0.11	0.41	-2.15	-0.29	-5.33	7
2013	0.75	0.79	0.83	0.14	-1.13	0.06	-0.04	0.20	1.02	0.47	-2.14	-2.73	-6.04	4
2014	-0.75	-0.30	0.35	-1.05	-0.28	-0.28	-0.09	1.76	-0.34	0.84	-0.25	-0.50	-3.84	9
2015	-0.89	-0.35	-0.25	-0.18	-0.07	0.46	-0.47	-0.57	-0.97	0.22	0.58	0.89	-3.76	8
2016	-0.50	0.68	-0.43	1.68	-0.39	0.62	-0.40	-0.26	-0.51	-1.71	0.32	-0.11	-4.31	8
2017	-0.87	0.08	-0.28	-1.54	-0.16	-0.32	0.27	0.65	1.21	1.69	-0.13	-2.54	-5.84	7
2018	-0.84	0.79	1.26	1.06	0.24	0.06	0.15	-0.10	-0.73	-0.81	-0.36	0.39	-2.83	5
2019	-1.38	-0.74	-1.44	-1.11	-0.18	1.88	0.07	-0.45	-0.04	1.39	1.40	1.40	-5.34	7
2020	1.18	0.16	0.40	-0.32	-0.16	0.04	-0.28	-0.59	-0.47	0.96	-0.52	-0.62	-2.96	7
2021	-0.17	-0.53	-1.45	-0.75	0.76	-0.59	-0.21	-0.30	-0.05	-0.94	1.56	-0.16	-5.16	10
2022	-1.13	-1.05	-1.48	-1.04	-0.95	-2.20	-3.18	-1.65	-1.25	-0.98	-0.31	-0.27	-15.49	12

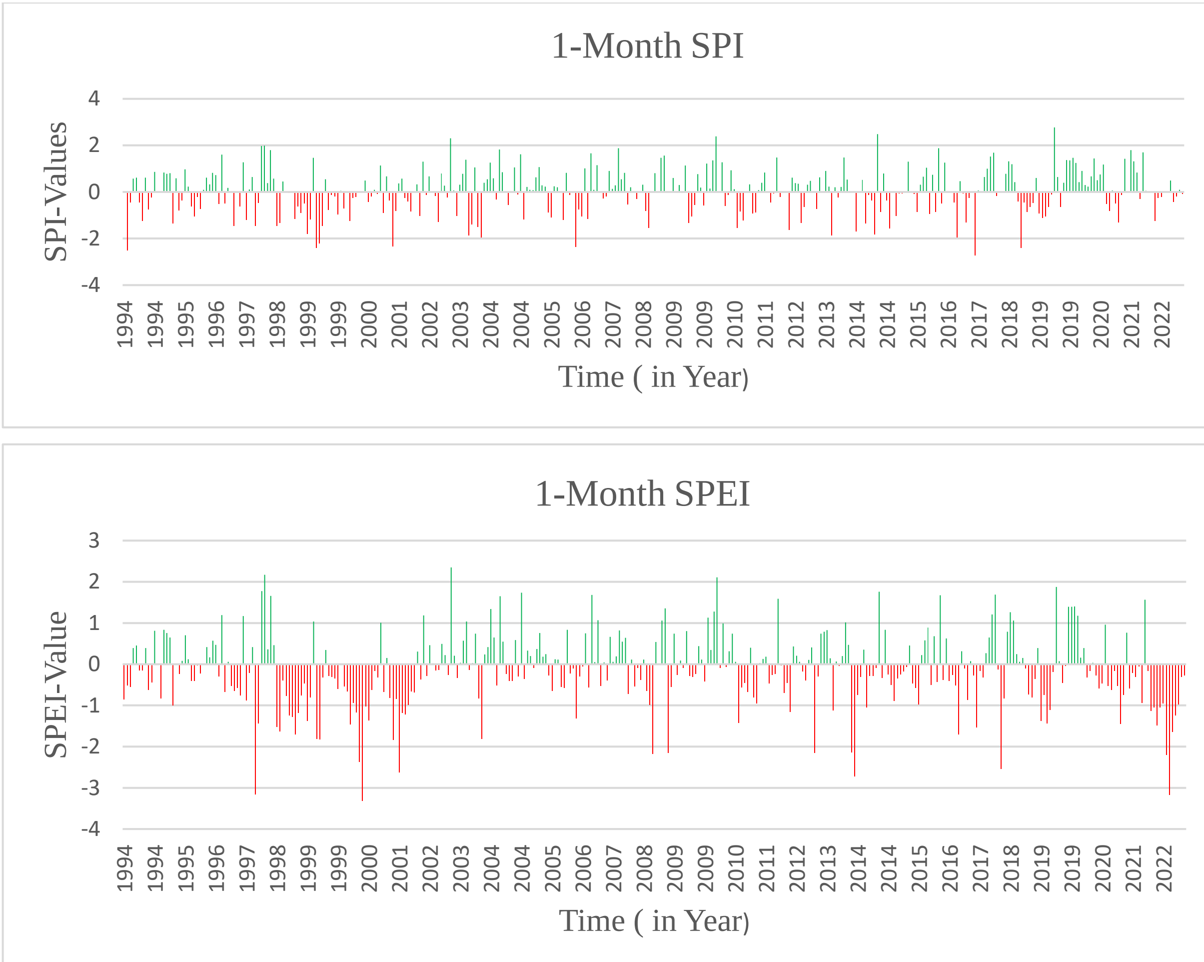

Figure 8. SPI and SPEI graph of yabello station at 1 time scales.

Different drought magnitudes and severities were detected at the station at 1-month SPI/SPEI, as shown above (Table 11 and Figure 9). In the research region, extreme drought (SPI/SPEI ≤ −2) was regularly recorded in February 1994, May (2001,1999), June 2000, and July 2018 at 1-month SPI. The severity of the extreme drought was also recorded in July 2022 (3.18) and August 1997 (3.12) using 1-month SPEI (Yabelo station). Furthermore, there were instances of severe and moderate drought in January, February, and August of various years. The driest years within the study periods were 1999, 2000, 2002, and 1998, according to both indices.

A 2-month series was also evaluated for evaluating meteorological dryness in addition to examining drought at 1-month time scales; at 3- and 6-month time scales, agricultural drought was demonstrated. Once more, Table 12 shows that, as reported by both SPI and SPEI at 1-month time series indexes, both index at 2-month time scale suggested increased frequencies of the meteorological drought nearly occurred in the same years. Furthermore, extreme meteorological frequencies occurred from 1998 to 2000 years (as SPI-2) and from 1998 to 2001 years, including 2022 year (as SPEI-2). These 2-month scale indices likewise show increased frequencies of meteorological drought, ranging from 7 to 12 from 1995 to 2022.

Similarly, Figure 10 describes the frequency and magnitudes of meteorological drought in the research area. It displays the Yabello Station SPI and SPEI graph at two time scales. The 2-month SPI's maximum negative value, 3.02 in 1999, is shown in Figure 10. Similar to the SPEI-2, it also shows the high positive value of the wet period in 1997 and the highest value of the meteorological drought (2.81) in 2019. In 2013, the 2-month SPEI recorded its lowest negative reading of -3.65. The continual occurrences of meteorological droughts between 1998 and 2001 are depicted on these 2-month timescales.

Table 12 SPI and SPEI at 2-Month time scale.

2-month SPI														
years	jan	feb	mar	apr	may	jun	jul	aug	sep	oct	nov	dec	negat_SUM	Frequency
1994	-0.43	-2.57	-0.72	0.06	0.66	0.28	-0.87	0.17	-0.26	-0.50	0.50	0.67	-5.35	6
1995	-0.35	0.47	0.96	0.98	0.08	-1.05	0.28	-0.82	0.61	0.52	-0.02	-0.98	-3.22	5
1996	-0.50	-0.37	-0.08	0.37	0.54	0.45	0.89	0.07	1.26	0.48	-0.10	-0.27	-1.32	5
1997	-1.93	-1.88	-0.89	0.66	0.54	-1.30	0.29	-0.11	-1.01	1.53	2.39	1.80	-5.82	5
1998	1.52	1.52	-0.41	-2.12	-0.64	0.22	-0.05	-0.15	-1.08	-0.94	-0.71	-1.03	-7.14	9
1999	-0.78	-1.29	1.16	0.06	-3.02	-2.81	-0.30	-0.12	-0.58	-0.30	-0.42	-0.77	-10.39	10
2000	-0.17	-1.15	-1.52	-1.02	-0.39	-1.08	-1.16	-0.06	-0.20	-0.39	0.02	-0.05	-4.95	9
2001	0.86	0.61	0.43	0.05	-1.26	-2.80	-0.32	0.54	-0.02	-0.53	-0.54	-1.33	-6.80	7
2002	-0.16	-0.07	1.02	0.81	0.21	0.43	-0.14	-0.75	0.35	0.46	0.16	1.22	-1.12	4
2003	1.77	-0.28	0.08	0.64	1.24	1.02	-1.80	0.73	0.05	-2.22	-0.58	0.46	-4.89	4
2004	1.18	1.17	0.09	1.29	1.74	0.44	-1.17	-1.09	0.62	0.34	1.12	1.23	-2.27	2
2005	-0.18	0.30	0.13	0.38	0.96	0.92	0.25	-0.38	-1.61	-0.14	0.34	-0.25	-2.55	5
2006	-1.68	0.48	0.34	-0.30	-0.93	-2.78	-1.09	0.70	0.07	1.17	1.23	0.56	-6.78	5
2007	0.63	-0.51	-0.21	0.48	0.68	0.02	1.04	1.31	0.79	-0.09	-0.10	-0.24	-1.15	5
2008	-0.77	-0.77	0.02	-0.57	-1.43	-1.08	-1.21	0.02	1.06	1.77	-0.34	0.20	-3.88	5
2009	0.09	0.04	0.01	-0.03	0.56	0.77	-1.42	-1.09	0.37	0.38	-0.03	0.26	-2.57	4
2010	0.97	1.14	2.44	2.03	0.67	0.96	-0.53	0.77	0.53	-1.20	-1.28	-1.22	-4.23	4
2011	-1.47	0.02	-0.39	-1.48	-0.65	0.01	0.58	0.04	-1.00	-0.30	1.02	1.19	-5.28	6
2012	-0.56	0.41	-1.91	-0.21	0.57	0.28	-0.04	-1.29	-0.11	0.41	-2.15	-0.67	-6.27	7
2013	0.27	0.02	-1.08	0.66	-0.59	-1.76	0.01	-0.05	1.27	1.02	-2.01	-0.02	-6.34	7
2014	-0.02	-2.13	0.22	-0.70	-1.07	-0.46	-0.88	2.57	1.88	0.40	0.47	-0.80	-6.15	7
2015	-1.81	-1.20	-0.27	-0.28	-0.12	0.52	1.00	-0.81	-0.96	-0.04	0.64	0.89	-5.48	8
2016	0.59	0.44	-0.08	1.20	1.30	0.12	0.95	0.99	-0.99	-1.83	-0.53	0.28	-3.43	4
2017	-0.37	-0.44	-0.04	-1.92	-1.51	-0.38	-0.25	1.08	1.65	1.89	1.16	1.29	-4.93	7
2018	1.47	0.42	1.37	1.69	1.04	0.09	-0.95	-1.32	-1.22	-0.90	-0.53	-0.11	-5.03	6
2019	0.23	-0.96	-1.17	-1.33	-0.60	1.79	2.81	-0.02	-0.02	1.19	1.66	1.63	-4.11	6
2020	1.66	1.09	0.91	0.71	0.26	0.30	1.06	1.03	0.71	1.16	0.70	-0.81	-0.81	1
2021	-0.22	-0.08	-1.08	-0.88	0.71	1.22	0.88	1.87	1.32	0.07	1.10	1.45	-2.26	4
2022	-0.33	0.73	-1.52	-1.02	-0.39	0.27	0.27	-0.06	-0.20	-0.39	0.02	-0.05	-3.96	8

2-month SPEI														
years	jan	feb	mar	apr	may	jun	jul	aug	sep	oct	nov	dec	Negsum	Frequency
1994	0.42	-0.78	-0.66	-0.11	0.45	0.17	-0.14	0.15	-0.16	-0.71	0.40	0.49	-2.56	6
1995	-0.31	0.41	0.90	0.77	-0.08	-0.56	-0.08	-0.07	0.41	0.35	-0.16	-0.57	-1.84	7
1996	-0.33	-0.21	-0.08	0.18	0.32	0.37	0.55	0.13	0.62	0.23	-0.31	-0.31	-1.24	5
1997	-0.63	-0.74	-0.87	0.40	0.36	-0.61	0.03	-0.79	-2.04	0.83	2.20	2.04	-5.69	6
1998	1.27	1.19	-0.88	-1.81	-1.30	-0.66	-0.93	-1.42	-1.65	-1.55	-1.33	-0.81	-12.35	10
1999	-0.76	-1.23	0.62	-0.66	-2.06	-1.14	-0.07	0.06	-0.37	-0.51	-0.64	-0.54	-7.98	10
2000	-0.23	-0.77	-1.59	-1.36	-1.20	-2.02	-2.88	-2.14	-1.34	-1.11	-0.46	-0.38	-15.47	12
2001	0.32	0.17	-0.11	-0.56	-1.42	-1.43	-1.24	-2.06	-1.31	-1.27	-1.11	-0.83	-11.34	10
2002	-0.38	-0.14	0.85	0.53	0.06	0.26	-0.03	-0.16	0.19	0.28	0.01	1.07	-0.70	4
2003	1.50	-0.17	-0.08	0.31	0.89	0.58	-0.08	0.45	-0.01	-1.62	-0.92	0.23	-2.87	6
2004	0.99	1.05	0.00	0.91	1.29	0.19	-0.29	-0.44	0.14	0.00	1.12	1.20	-0.73	2
2005	-0.13	0.26	0.05	0.10	0.61	0.53	0.22	0.00	-0.56	-0.35	0.22	-0.29	-1.32	4
2006	-0.63	0.47	0.30	-0.29	-0.73	-0.87	-0.22	0.43	0.12	1.01	1.26	0.43	-2.73	5
2007	0.49	-0.19	-0.26	0.16	0.42	0.11	0.47	0.72	0.59	-0.23	-0.30	-0.28	-1.27	5
2008	-0.45	-0.35	-0.04	-0.47	-0.93	-1.81	-1.58	0.30	0.61	1.41	-0.90	-1.68	-8.21	9
2009	-0.02	0.20	-0.01	-0.12	0.38	0.34	-0.30	-0.30	0.11	0.18	-0.18	0.10	-0.94	6
2010	0.79	1.05	1.89	1.60	0.50	0.57	0.08	0.58	0.40	-1.01	-1.32	-0.69	-3.02	3
2011	-0.58	0.06	-0.36	-1.11	-0.62	0.06	0.16	-0.13	-0.42	-0.42	1.04	1.20	-3.65	7
2012	-0.29	-0.67	-1.18	-0.34	0.35	0.13	-0.01	-0.31	-0.17	0.20	-1.77	-1.62	-6.36	9
2013	0.14	-3.65	-0.51	0.50	-0.48	-0.58	0.04	0.08	0.66	0.78	-1.70	-2.22	-9.15	6
2014	-2.81	-0.56	0.18	-0.60	-0.85	-0.33	-0.22	1.22	1.13	0.32	0.45	-0.51	-5.86	7
2015	-0.67	-0.65	-0.33	-0.35	-0.18	0.18	0.18	-0.57	-0.89	-0.41	0.60	0.75	-4.05	8
2016	0.38	0.35	0.08	0.97	0.96	0.11	0.31	-0.36	-0.48	-1.44	-0.78	0.05	-3.05	4
2017	-0.39	-0.27	-0.15	-1.27	-1.12	-0.28	-0.11	0.50	0.97	1.74	1.18	-1.30	-4.90	8
2018	-2.58	0.37	1.20	1.36	0.77	0.15	0.10	0.03	-0.51	-0.98	-0.74	-0.21	-5.02	5
2019	-0.15	-1.17	-1.62	-1.46	-0.84	0.99	1.27	-0.19	-0.29	0.92	1.68	1.76	-5.71	7
2020	1.34	0.71	0.39	-0.09	-0.31	-0.09	-0.06	-0.47	-0.60	0.37	0.35	-0.72	-2.35	7
2021	-0.54	-0.50	-1.51	-1.24	-0.04	0.15	-0.49	-0.28	-0.22	-0.76	0.71	1.11	-5.57	9
2022	-0.49	-1.36	-1.85	-1.43	-1.17	-1.80	-2.64	-2.72	-1.51	-1.28	-0.81	-0.45	-17.50	12

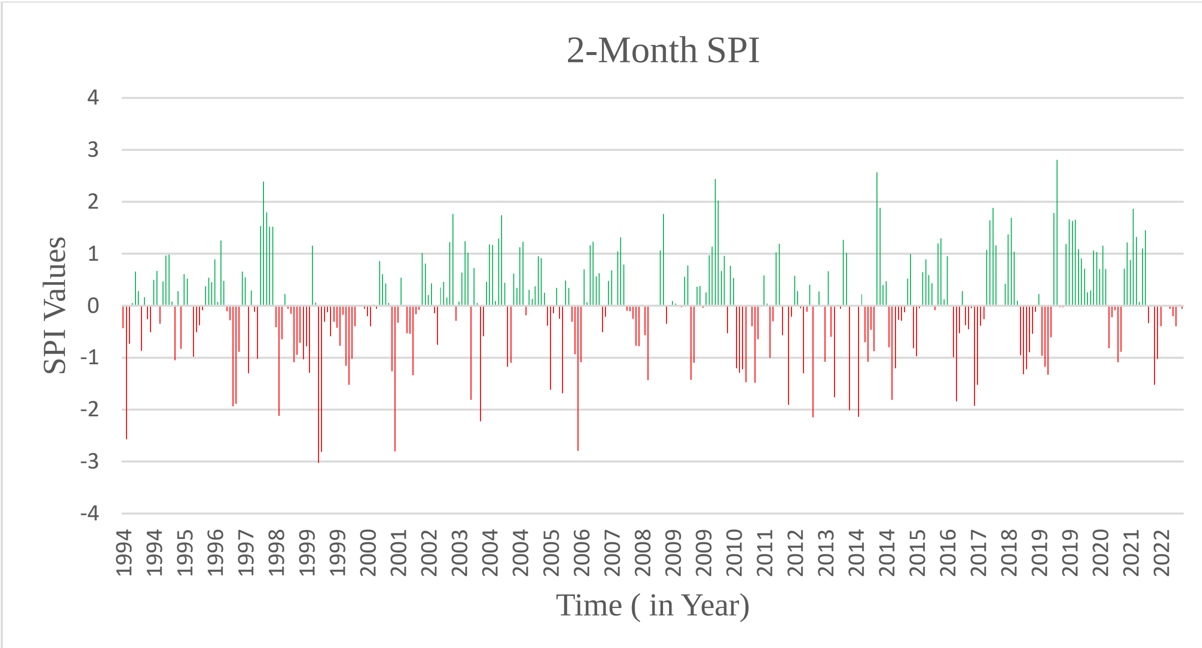

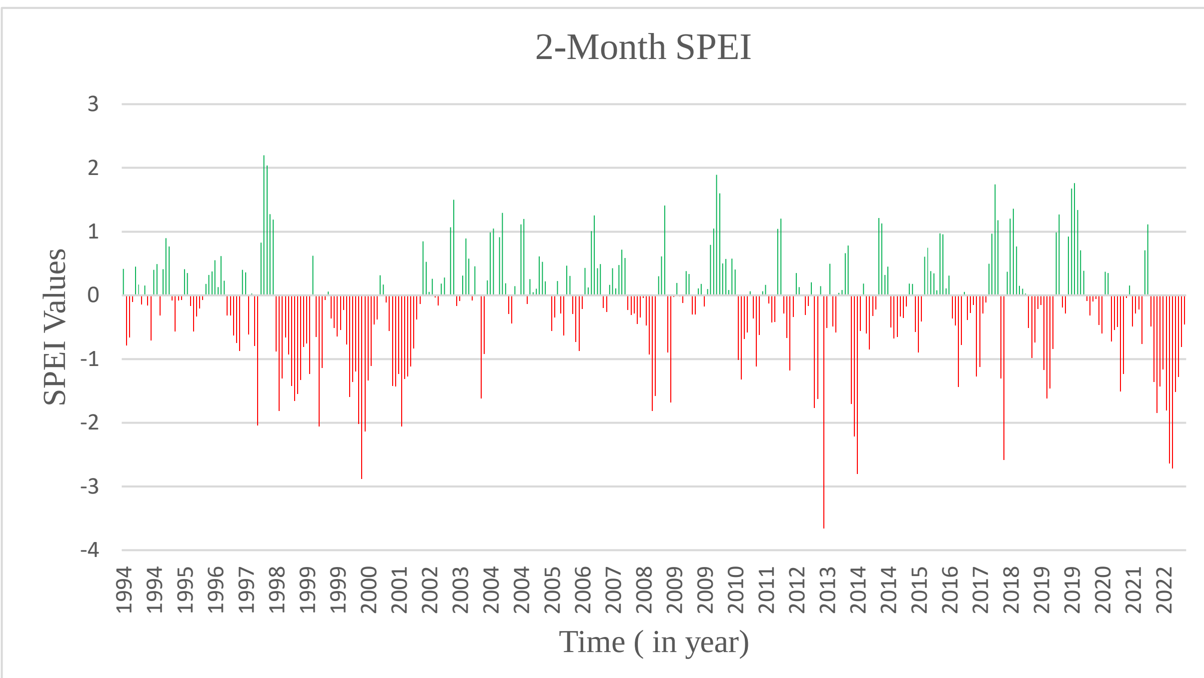

Figure 9. SPI and SPEI graph of yabello station at 2 time scales.

Extreme drought was experienced at SPI/SPEI-2 time scales in February (1994, 2013, 204), May 1999, June to July (2000 and 2001), and August (2000 and 2022). Furthermore Events of severe and moderate drought occurred in the months of January, February, June, and July.

.

Also, Agricultural drought was demonstrated for the purpose of characterizing drought during the study periods at the 3- and 6-month scales of both SPI and SPEI. The values of SPI and SPEI at a 3-month time frame are shown in Table 13 below. The years with the highest frequencies of agricultural drought were 1994, 1998, 1999, 2000, 2001, 2008, 2011, 20012, 2013, 2015, 2021, and 2022. The agricultural droughts in 1998–2001 and 2021–2022 are more frequent on both 3-month timeframes. The agricultural drought in the study area during the chosen study period was also detailed in Figure 1, which shows the SPI and SPEI graph of the Yabello station at three time periods. The patterns of drought are similar for both 3-month scale indices, with the maximum agricultural magnitude (lowest value) occurring in 2006 and 2008. Additionally, indexes show that there were ongoing agricultural drought situations in 1998–2001 and in 2021–2022.

Table 13 SPI and SPEI at 3-Month time scale

3-Month SPI														
years	jan	feb	mar	apr	may	jun	jul	aug	sep	oct	nov	dec	negsum	Freq.
1994	-0.98	-0.84	-1.00	-0.12	0.26	0.58	0.12	-0.33	-0.51	-0.37	0.25	0.43	-4.15	7
1995	0.37	0.43	0.74	1.09	0.38	0.25	-1.21	-0.13	0.40	0.37	0.22	-0.24	-1.57	3
1996	-0.91	-0.63	-0.17	0.23	0.37	0.69	0.53	0.49	1.27	0.32	0.48	-0.36	-2.07	4
1997	-0.52	-2.39	-1.14	0.43	0.09	0.54	-1.10	-0.23	-0.56	1.35	2.25	2.35	-5.95	6
1998	2.10	1.46	0.55	-1.36	-1.32	-0.47	0.17	-0.31	-0.95	-0.99	-1.06	-0.85	-7.30	9
1999	-1.26	-1.01	0.94	-0.08	-0.70	-2.67	-2.30	-0.83	-0.34	-0.47	-0.55	-0.44	-10.67	11
2000	-0.90	-0.58	-1.59	-1.09	-1.02	-1.71	-1.34	-1.39	-0.50	-0.32	-0.19	-0.05	-10.67	12
2001	0.44	0.51	0.73	-0.07	-0.73	-1.11	-2.40	-0.08	0.04	-0.41	-0.70	-0.82	-6.32	8
2002	-0.83	-0.44	0.98	0.60	0.90	0.24	0.36	-0.71	0.24	0.27	0.30	1.08	-1.98	3
2003	1.05	1.35	0.04	0.44	1.13	1.05	0.88	0.03	-0.20	-1.35	-0.96	-0.40	-2.92	4
2004	0.85	1.20	0.53	1.27	1.38	1.50	0.33	-1.89	0.44	0.15	1.28	0.92	-1.89	1
2005	1.09	0.01	0.14	0.37	0.75	0.92	0.90	-0.25	-1.12	-0.32	0.05	0.10	-1.68	3
2006	-0.48	0.14	0.12	0.07	-1.09	-0.82	-2.97	0.08	-0.17	1.29	0.98	1.42	-5.52	6
2007	0.27	0.44	-0.46	0.39	0.38	0.69	0.48	0.98	1.24	-0.02	0.09	-0.36	0.24	3
2008	-0.33	-1.18	-0.10	-0.68	-1.17	-4.57	-0.01	-0.01	1.11	1.58	0.22	-0.61	-13.05	9
2009	-0.46	-0.32	0.17	-0.19	0.50	0.46	0.63	-1.79	0.13	0.22	0.12	0.35	-2.31	3
2010	0.22	1.44	2.32	2.11	2.20	0.58	0.89	0.18	0.42	-0.77	-1.23	-1.53	-3.54	3
2011	-1.46	-0.28	-0.65	-1.05	-1.19	-0.39	0.13	0.09	-0.45	-0.49	0.83	0.91	-5.96	8
2012	0.88	-0.97	-2.23	-0.36	-0.07	0.61	0.11	-0.53	-0.37	0.24	-1.74	-2.25	-8.53	8
2013	-0.03	-0.03	-0.55	-0.54	-0.04	-0.40	-1.80	-0.12	1.11	0.94	-0.74	-0.06	-7.00	9
2014	-0.06	-0.06	-0.02	-0.80	-0.73	-0.90	-0.67	1.94	1.64	1.50	0.21	0.24	-3.12	5
2015	-1.05	-1.52	-0.52	-0.38	-0.32	0.33	0.34	0.69	-1.29	-0.14	0.39	0.85	-5.22	7
2016	0.62	0.85	-0.29	1.23	0.80	1.42	-0.07	0.49	-1.32	-2.04	-0.75	-0.57	-5.04	6
2017	0.01	-0.31	-0.27	-1.63	-1.49	-1.36	-0.28	0.38	1.61	1.96	1.49	0.01	-5.34	6
2018	0.05	0.05	1.15	1.66	1.56	0.91	-0.10	-1.36	-1.55	-1.04	-0.83	-0.34	-5.21	6
2019	-0.33	-0.10	-1.35	-1.31	-1.19	0.80	1.82	2.52	0.13	1.02	1.62	1.91	-4.29	5
2020	1.75	1.52	1.17	0.74	0.62	0.42	0.57	0.98	1.00	1.13	0.79	0.52	0.00	0
2021	-0.66	-0.31	-0.90	-0.83	0.12	0.68	1.52	1.38	1.63	0.47	1.19	1.02	-2.70	4
2022	1.12	-0.74	-1.82	-1.09	-1.02	-1.71	0.39	0.39	-0.50	-0.32	-0.19	-0.05	-8.83	11

3-month SPEI													
years	jan	feb	mar	apr	may	jun	jul	aug	sep	oct	nov	dec	negsum	Freq.
1994	0.33	0.16	-0.82	-0.15	0.16	0.27	0.12	0.00	-0.15	-0.40	0.01	0.29	-1.53	5
1995	0.23	0.34	0.65	0.86	0.27	-0.08	-0.51	-0.05	0.25	0.29	0.08	-0.32	-0.96	4
1996	-0.50	-0.30	-0.15	0.15	0.24	0.42	0.42	0.35	0.60	0.09	0.27	-0.48	-1.43	4
1997	-0.38	-0.72	-0.97	0.26	0.02	0.18	-0.38	-0.49	-1.17	0.14	1.76	2.10	-4.12	6
1998	2.00	1.14	0.09	-1.61	-1.65	-1.21	-0.78	-1.09	-1.71	-1.76	-1.71	-1.20	-12.72	9
1999	-0.90	-0.95	0.32	-0.71	-1.19	-1.59	-0.88	-0.15	-0.10	-0.50	-0.75	-0.53	-8.26	11
2000	-0.57	-0.43	-1.54	-1.41	-1.54	-1.75	-2.33	-2.86	-1.92	-1.25	-0.96	-0.51	-17.06	12
2001	-0.01	0.02	0.15	-0.59	-1.12	-1.32	-1.66	-1.34	-1.79	-1.45	-1.42	-1.13	-11.82	10
2002	-0.68	-0.42	0.74	0.40	0.59	0.03	0.19	-0.08	0.10	0.18	0.11	0.96	-1.17	3
2003	0.83	1.08	-0.10	0.24	0.70	0.62	0.48	0.18	0.02	-1.06	-1.15	-0.58	-2.88	4
2004	0.67	1.03	0.40	0.91	0.88	0.93	0.09	-0.35	-0.01	-0.11	1.09	0.83	-0.47	3
2005	0.95	0.07	0.05	0.19	0.44	0.50	0.48	0.09	-0.28	-0.36	-0.15	-0.05	-0.84	4
2006	-0.35	0.15	0.10	0.09	-0.69	-0.64	-0.74	0.09	0.08	0.97	0.87	1.36	-2.42	4
2007	0.22	0.44	-0.41	0.20	0.19	0.36	0.32	0.51	0.70	0.04	-0.06	-0.48	-0.95	3
2008	-0.26	-0.48	-0.13	-0.44	-0.71	-1.49	-1.46	-1.30	0.62	1.04	-0.27	-0.93	-7.48	10
2009	-1.49	-0.08	0.12	-0.10	0.32	0.17	0.23	-0.32	-0.01	0.07	-0.07	0.26	-2.07	6
2010	0.15	1.24	1.76	1.52	1.46	0.34	0.53	0.30	0.40	-0.48	-1.14	-1.19	-3.32	3
2011	-0.71	-0.14	-0.53	-0.83	-0.81	-0.41	0.11	0.00	-0.21	-0.48	0.74	0.85	-4.13	9
2012	0.77	-0.38	-1.24	-0.34	-0.12	0.26	0.08	-0.13	-0.17	0.05	-1.46	-1.45	-5.28	8
2013	-1.42	-1.53	-0.26	-0.23	0.01	-0.34	-0.48	0.07	0.49	0.64	-0.93	-2.43	-7.62	8
2014	-2.36	-2.81	-0.04	-0.54	-0.52	-0.72	-0.28	0.71	0.85	1.15	0.15	0.16	-7.28	7
2015	-0.58	-0.65	-0.54	-0.33	-0.24	0.02	0.07	-0.01	-0.81	-0.50	0.09	0.76	-3.65	8
2016	0.47	0.66	-0.10	0.96	0.62	0.91	0.02	0.16	-0.47	-1.35	-0.93	-0.67	-3.52	5
2017	-0.11	-0.19	-0.37	-1.11	-1.04	-0.93	-0.15	0.12	0.80	1.42	1.40	-0.04	-3.94	8
2018	-1.33	-1.48	0.97	1.25	1.08	0.58	0.17	0.04	-0.29	-0.85	-0.97	-0.45	-5.14	6
2019	-0.38	-0.40	-1.74	-1.55	-1.22	0.22	0.81	0.93	-0.16	0.58	1.44	1.81	-5.45	6
2020	1.58	1.09	0.60	0.03	-0.08	-0.23	-0.12	-0.21	-0.52	0.13	0.02	0.03	-1.16	5
2021	-0.67	-0.62	-1.36	-1.25	-0.54	-0.25	0.10	-0.49	-0.22	-0.72	0.49	0.50	-6.13	9
2022	0.65	-0.82	-1.88	-1.59	-1.52	-1.66	-2.08	-2.79	-2.08	-1.56	-1.19	-0.75	-17.93	11

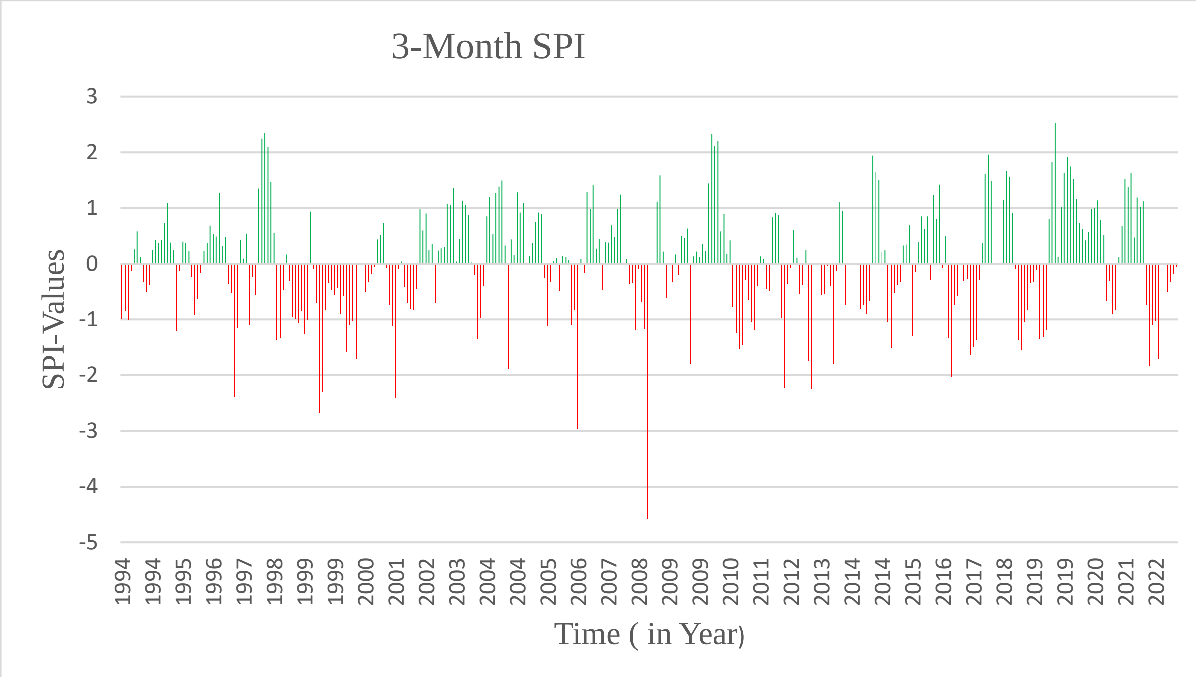

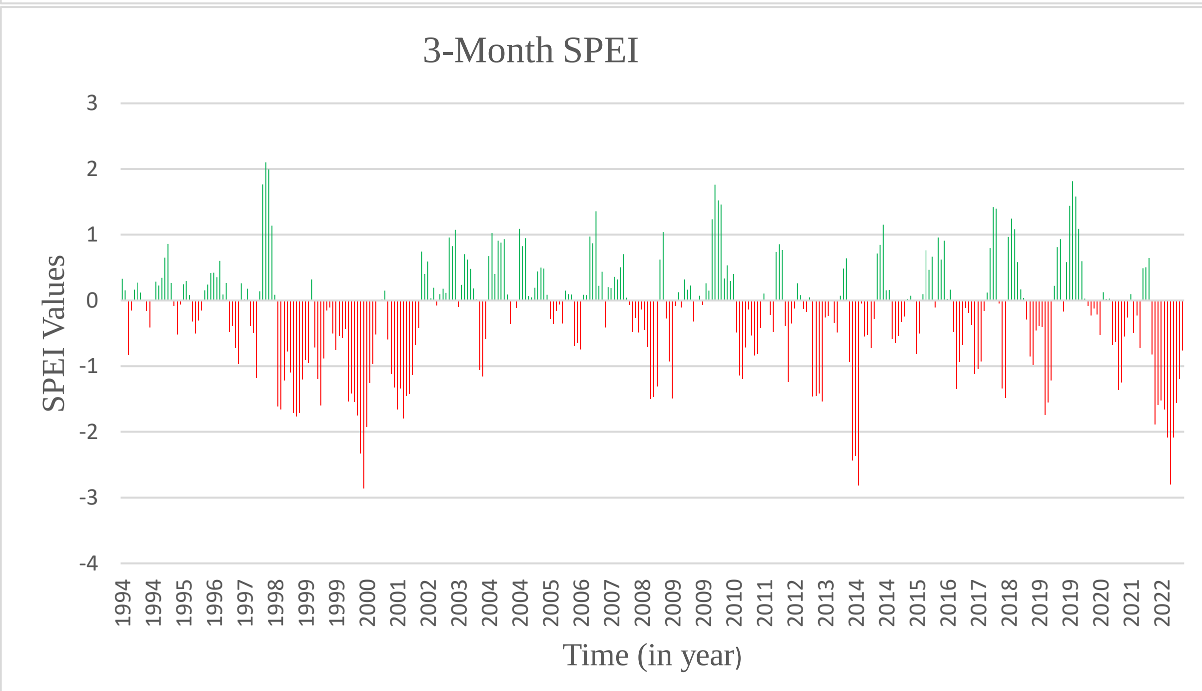

Figure 10. SPI and SPEI graph of yabello station at 3 time scales.

SPI and SPEI at 6-month scales, in addition to 3-month scales, also described the state of the agricultural drought. Table: displays the frequency of agricultural droughts; the results are nearly identical to those obtained with the previously described 3-month scales.

With the exception of the start of the study period, Figure 12's SPI and SPEI graph of the Yabello station at six time scales once more displays comparable patterns. There were ongoing periods of agricultural drought in 1998–2002 and 2020–2022 (ending at the end of the latter year). In addition, SPEI-6 displays a higher number of ongoing drought occurrences compared to lesser time scales

Table 14 SPI and SPEI at 6-Month time scale

6-month SPI														
years	jan	feb	mar	apr	may	jun	jul	aug	sep	oct	nov	dec	negsum	Freq.
1994	-1.83	-1.91	-1.52	-0.44	0.03	-0.04	0.03	0.20	0.36	-0.18	0.20	0.24	-5.92	6
1995	0.14	0.31	0.72	1.06	0.47	0.50	0.59	0.35	0.27	-0.27	0.22	-0.05	-0.32	2
1996	-0.06	-0.11	-0.29	-0.12	0.16	0.34	0.44	0.49	1.04	0.63	0.57	0.28	-0.58	4
1997	0.06	-0.05	-0.84	0.17	-0.21	-0.11	0.05	0.07	0.31	0.78	1.84	2.01	-1.21	5
1998	2.28	2.35	1.98	0.83	-0.02	-0.11	-0.74	-1.21	-0.87	-0.58	-0.79	-1.01	-5.34	8
1999	-1.19	-1.33	0.19	-0.49	-0.77	-0.81	-0.65	-0.77	-2.73	-1.58	-0.53	-0.48	-11.32	11
2000	-0.66	-0.76	-1.05	-1.21	-0.93	-2.29	-2.35	-2.44	-2.00	-2.58	-1.52	-0.19	-17.98	12
2001	0.21	0.03	0.43	0.23	-0.28	-0.36	-0.66	-0.63	-1.19	-1.55	-0.46	-0.64	-5.77	8
2002	-0.59	-0.83	0.24	0.22	0.62	0.67	0.64	0.73	0.20	0.49	0.18	1.00	-1.42	2
2003	0.97	0.90	0.78	0.95	1.44	0.75	0.73	1.07	0.94	-0.19	-0.61	-0.41	-1.21	3
2004	0.08	0.04	0.08	1.43	1.54	1.34	1.14	1.10	1.57	0.37	0.90	0.92	0.00	0
2005	0.93	0.98	0.71	0.93	0.62	0.68	0.69	0.67	0.63	0.43	0.06	-0.19	-0.19	1
2006	-0.36	0.02	0.11	-0.11	-0.71	-0.66	-0.61	-0.89	-1.00	0.25	0.86	1.21	-4.34	7
2007	1.10	0.89	0.85	0.47	0.48	0.23	0.53	0.66	1.03	0.33	0.45	0.26	0.00	0
2008	-0.09	-0.34	-0.33	-0.63	-1.18	-2.41	-2.26	-2.63	-2.13	-0.21	-0.92	0.03	-13.13	11
2009	0.07	-0.02	-0.31	-1.58	0.33	0.33	0.20	0.26	0.40	0.62	-0.08	0.34	-1.99	4
2010	0.38	0.84	1.93	1.83	2.24	1.94	1.98	2.08	0.61	0.14	-0.74	-0.93	-1.67	2
2011	-1.10	-1.17	-1.44	-1.38	-0.96	-0.77	-0.58	-0.98	-0.66	-0.26	0.75	0.68	-9.30	10
2012	0.46	0.37	0.06	0.32	-0.25	-0.20	-0.14	-0.14	0.42	0.30	-1.34	-1.83	-3.90	6
2013	-1.33	-0.58	-1.74	-1.93	-0.84	-0.73	-0.94	-0.03	-0.02	0.12	-0.50	-3.00	-11.64	11
2014	-3.34	-4.23	-3.61	-0.58	-2.05	-0.81	-0.77	0.22	-0.11	1.10	0.90	0.87	-15.50	8
2015	0.77	-0.27	-0.12	-0.68	-0.52	-0.11	-0.05	-0.03	-0.05	0.15	0.56	0.50	-1.84	8
2016	0.43	0.64	0.46	1.29	0.96	0.93	0.99	0.87	1.17	-1.36	-0.30	-0.85	-2.51	3
2017	-0.91	-0.81	-0.58	-1.06	-1.19	-1.31	-1.13	-1.11	-0.45	1.73	1.32	0.70	-8.55	9
2018	0.50	0.53	0.78	0.56	0.73	1.25	1.33	1.30	0.58	-0.81	-0.84	-0.66	-2.32	3
2019	-0.71	-0.78	-0.89	-1.08	-0.89	0.09	0.22	0.26	0.75	2.05	2.05	1.72	-4.36	5
2020	1.86	1.91	1.97	1.60	1.19	0.92	0.82	0.86	0.68	1.35	0.94	0.79	0.00	0
2021	0.60	0.47	-0.04	-0.90	0.03	0.08	0.27	0.59	1.20	1.43	1.35	1.44	-0.94	2
2022	1.12	0.73	0.21	0.09	-0.97	-2.36	-2.35	-2.44	-2.00	-2.58	-1.52	-0.19	-14.42	8

6-Month SPEI														
years	jan	feb	mar	apr	may	jun	jul	aug	sep	oct	nov	dec	negsum	Freq.
1994	1.17	0.55	-0.06	0.12	0.29	-0.03	0.01	0.09	0.15	-0.09	-0.01	0.04	-0.19	4
1995	-0.06	0.14	0.63	0.86	0.43	0.29	0.29	0.14	0.05	-0.20	0.00	-0.10	-0.36	4
1996	-0.10	-0.14	-0.30	-0.10	0.20	0.29	0.33	0.30	0.54	0.35	0.34	0.07	-0.64	4
1997	-0.16	-0.19	-0.92	0.06	-0.13	-0.15	-0.03	-0.21	-0.22	-0.19	0.76	0.98	-2.20	9
1998	1.30	1.58	1.41	0.21	-0.66	-0.89	-1.34	-1.58	-1.54	-1.46	-1.60	-1.74	-10.81	8
1999	-1.94	-1.73	-0.59	-1.01	-1.38	-1.13	-0.89	-0.84	-1.36	-0.89	-0.48	-0.46	-12.70	12
2000	-0.74	-0.77	-1.26	-1.28	-1.52	-2.17	-2.22	-2.17	-2.14	-2.49	-2.01	-1.29	-20.06	12
2001	-0.79	-0.68	-0.22	-0.39	-0.88	-0.96	-1.27	-1.32	-1.66	-2.02	-1.56	-1.71	-13.46	12
2002	-1.50	-1.25	-0.12	0.02	0.46	0.41	0.34	0.34	0.07	0.23	0.00	0.59	-2.86	3
2003	0.67	0.65	0.57	0.65	1.01	0.45	0.41	0.52	0.46	-0.08	-0.47	-0.42	-0.97	3
2004	-0.13	-0.11	-0.07	1.08	1.10	0.81	0.59	0.45	0.67	0.02	0.38	0.45	-0.31	3
2005	0.58	0.71	0.56	0.68	0.48	0.41	0.39	0.31	0.28	0.21	-0.03	-0.25	-0.28	2
2006	-0.46	-0.07	0.04	-0.06	-0.42	-0.39	-0.33	-0.40	-0.44	0.08	0.48	0.83	-2.57	8
2007	0.85	0.72	0.71	0.33	0.41	0.16	0.30	0.34	0.55	0.25	0.29	0.15	0.00	0
2008	-0.11	-0.32	-0.40	-0.43	-0.70	-1.28	-1.07	-1.03	-0.88	-0.32	-0.88	-0.19	-7.61	12
2009	-0.25	-0.27	-0.54	-0.97	0.33	0.21	0.09	0.06	0.13	0.20	-0.23	0.10	-2.04	5
2010	0.19	0.68	1.58	1.44	1.54	1.22	1.17	1.09	0.40	0.20	-0.38	-0.55	0.29	2
2011	-0.85	-0.89	-1.23	-0.98	-0.66	-0.47	-0.36	-0.52	-0.38	-0.14	0.36	0.37	8.93	10
2012	0.27	0.28	-0.02	0.22	-0.13	-0.16	-0.12	-0.14	0.14	0.08	-0.86	-1.16	-2.07	7
2013	-1.14	-1.78	-1.27	-1.01	-0.38	-0.31	-0.38	0.03	-0.02	0.02	-0.43	-1.48	-8.21	10
2014	-1.83	-1.82	-2.07	-2.07	-1.29	-0.52	-0.44	0.05	-0.09	0.47	0.52	0.60	-10.13	8
2015	0.57	-0.24	-0.20	-0.52	-0.34	-0.13	-0.12	-0.17	-0.24	-0.17	0.03	0.05	-2.14	9
2016	0.05	0.37	0.44	1.04	0.80	0.64	0.60	0.46	0.52	-0.60	-0.37	-0.77	-1.73	3
2017	-0.93	-0.77	-0.70	-0.81	-0.90	-0.84	-0.67	-0.60	-0.28	0.72	0.79	0.46	-6.52	9
2018	0.34	0.43	0.71	0.51	0.66	0.84	0.85	0.73	0.33	-0.25	-0.48	-0.52	-1.25	3
2019	-0.82	-0.91	-1.30	-1.26	-1.17	-0.32	-0.21	-0.20	0.11	0.83	1.22	1.05	-6.19	8
2020	1.27	1.37	1.42	0.89	0.51	0.16	-0.03	-0.16	-0.35	-0.02	-0.12	-0.32	-1.00	6
2021	-0.36	-0.32	-0.73	-1.24	-0.61	-0.61	-0.58	-0.58	-0.26	-0.26	-0.03	0.14	-5.58	11
2022	0.05	-0.07	-0.58	-0.69	-1.68	-2.17	-2.17	-2.14	-2.08	-2.47	-2.13	-1.53	-17.70	11

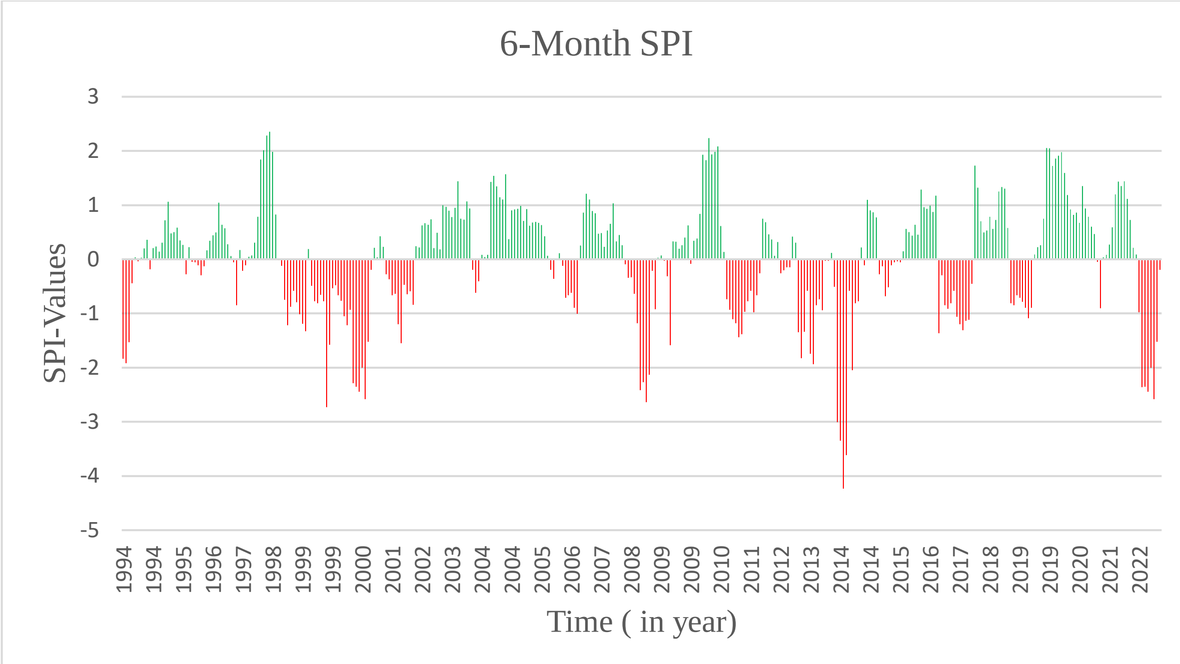

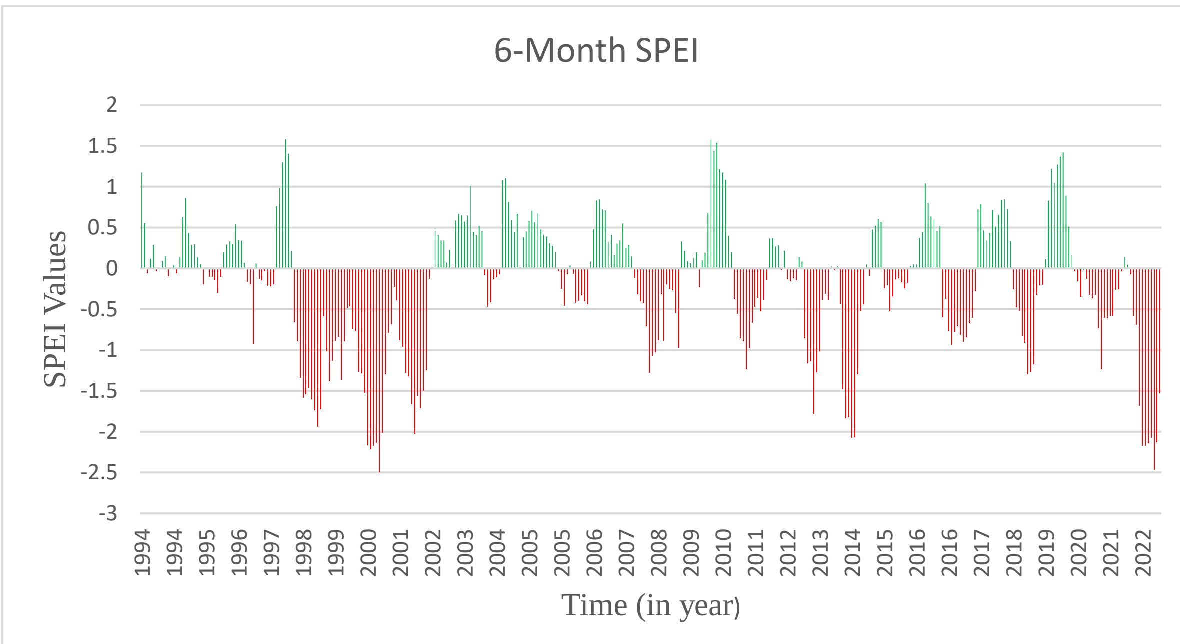

Figure 11. SPI and SPEI graph of yabello station at 6 time scales.

Additionally, very long-term dry periods that could be classified as hydrological droughts were shown at the 9- and 12-month stages. After 1999, the majority of hydrological drought occurrences became noticeable. Table 15: shows Long-term hydrological drought occurrences in 1994, 1999, 200, 2001, 2006, 2007; 20011, 2013, 2014, 2017; 2019, 2021, and 2022 years are shown by SPI and SPEI at a 9-month time scale.

. According to the figure, at the 9- and 12-month timescales, the hydrological drought patterns were different at the start of the study period. The nine-month SPI and nine-month SPEI patterns exhibit extremely high frequencies of ongoing hydrological droughts from 1998 to 2002, 2008 to 2009, 2011 to 2014, and 2022. The graphic depicting nine-month scales likewise demonstrates continuous drought over this time period. Comparing SPEI to lesser scales, this scale also exhibits more consistent dry patterns.

Table 15 SPI and SPEI at 9-Month time scale

9-month SPI														
years	jan	feb	mar	apr	may	jun	jul	aug	sep	oct	nov	dec	neg sum	Freq.
1994	-0.14	-1.60	-2.10	-1.12	-0.70	-0.50	-0.14	0.00	-0.24	-0.33	0.20	0.47	-6.86	9
1995	0.17	0.29	0.54	0.77	0.40	0.57	0.70	0.44	0.53	0.69	0.31	0.03	0.00	0
1996	-0.47	-0.02	-0.26	0.07	0.16	0.17	0.22	0.28	0.64	0.50	0.60	0.57	-0.75	3
1997	0.28	0.17	-0.36	0.27	0.03	-0.22	-0.01	-0.21	-0.32	0.75	1.64	1.78	-1.12	5
1998	1.84	2.05	1.86	1.25	1.24	1.27	0.79	-0.04	-0.40	-1.52	-1.77	-1.13	-4.86	5
1999	-0.80	-1.03	-0.09	-0.80	-1.13	-0.95	-0.76	-0.83	-1.00	-1.14	-1.09	-2.00	-11.62	12
2000	-1.35	-0.69	-1.21	-1.16	-1.03	-1.70	-1.95	-2.04	-2.51	-2.65	-2.03	-1.32	-19.63	12
2001	-1.01	-0.87	0.23	0.06	-0.37	-0.27	-0.16	-0.24	-0.45	-1.11	-1.07	-1.34	-6.89	10
2002	-1.30	-0.59	0.15	0.01	0.14	0.23	0.40	0.51	0.66	0.70	0.68	0.78	-1.88	2
2003	0.96	0.74	0.74	0.89	1.18	1.05	1.08	1.37	0.65	0.14	0.38	0.47	0.00	0
2004	0.46	0.13	-0.06	0.86	0.86	0.91	1.29	1.33	1.41	1.22	1.61	1.60	-0.06	1
2005	0.92	0.74	0.72	0.83	1.03	0.93	1.07	0.56	0.45	0.47	0.48	0.47	0.00	0
2006	0.15	0.06	-0.20	-0.23	-0.55	-0.40	-0.52	-0.60	-0.81	0.11	-0.05	0.38	-3.35	8
2007	0.37	0.84	0.73	0.96	0.78	0.89	0.62	0.69	0.52	0.42	0.49	0.56	0.00	0
2008	0.14	0.10	0.04	-0.51	-0.84	-1.71	-1.61	-2.39	-1.73	-0.78	-1.75	-1.81	-13.14	9
2009	-1.48	-0.93	0.00	-0.12	0.28	0.02	-0.63	0.15	0.28	0.18	0.18	0.45	-3.15	4
2010	0.58	0.62	1.90	1.64	1.78	1.64	1.74	2.15	2.03	1.90	1.28	-0.21	-0.21	1
2011	-0.33	-0.76	-1.25	-1.43	-1.36	-1.17	-0.73	-0.82	-0.99	-1.07	-0.23	0.15	-10.14	11
2012	0.44	0.41	-0.13	0.07	0.20	0.34	0.40	-0.30	-0.38	-0.18	-1.08	-0.55	-2.62	6
2013	-0.91	-3.52	-1.86	-1.21	-1.44	-1.32	-1.79	-0.77	-0.42	-0.44	-0.55	-1.89	-16.11	12
2014	-3.19	-2.47	-1.92	-2.18	-1.89	-2.33	-4.09	-0.83	-0.23	0.15	0.19	0.03	-19.12	9
2015	0.46	0.51	0.39	0.31	-0.33	0.05	-0.22	-0.27	-0.43	-0.30	0.11	0.47	-1.55	5
2016	0.50	0.76	0.15	1.04	0.84	1.07	1.09	1.01	0.71	0.30	0.28	0.59	0.00	0
2017	-0.73	-0.40	-0.95	-1.65	-1.31	-1.17	-0.69	-0.94	-0.63	0.28	0.26	-0.34	-8.81	10
2018	0.33	0.60	1.16	1.37	1.22	0.97	0.53	0.56	1.04	1.00	0.65	0.22	0.00	0
2019	-0.60	-0.77	-1.32	-1.32	-1.13	-0.06	0.18	0.20	0.03	0.70	1.24	1.70	-5.20	6
2020	2.28	2.23	1.95	1.72	1.61	1.61	1.48	1.31	1.12	1.39	1.09	0.74	0.00	0
2021	0.73	0.70	0.19	-0.05	0.36	0.31	0.13	0.42	0.54	0.40	1.15	1.40	-0.05	1
2022	1.55	1.01	0.66	0.27	0.00	-0.67	-0.65	-2.10	-2.58	-2.65	-2.03	-1.32	-12.00	8

9-month SPEI														
years	jan	feb	mar	apr	may	jun	jul	aug	sep	oct	nov	dec	Negsum	Freq.
1994	1.78	1.40	1.12	0.74	0.46	0.18	0.22	0.22	-0.07	-0.16	0.03	0.18	-0.23	2
1995	0.02	0.09	0.44	0.54	0.29	0.35	0.44	0.31	0.30	0.31	0.09	-0.10	-0.10	1
1996	-0.38	-0.12	-0.10	0.04	0.12	0.16	0.24	0.31	0.42	0.28	0.29	0.29	-0.60	3
1997	0.15	0.07	-0.32	0.08	-0.05	-0.29	-0.07	-0.28	-0.43	-0.02	0.47	0.69	-1.45	7
1998	0.67	0.96	0.86	0.21	0.34	0.33	-0.15	-0.92	-1.22	-1.77	-1.89	-1.67	-7.62	6
1999	-1.70	-1.93	-1.38	-1.59	-1.75	-1.38	-1.10	-0.98	-0.95	-0.96	-0.98	-1.30	-16.00	12
2000	-1.01	-0.60	-1.17	-1.30	-1.41	-1.84	-2.14	-2.35	-2.55	-2.33	-2.06	-1.84	-20.61	12
2001	-2.01	-1.95	-1.04	-0.84	-1.07	-0.97	-1.04	-1.19	-1.30	-1.61	-1.59	-1.74	-16.36	12
2002	-2.05	-1.67	-0.88	-0.56	-0.19	0.00	0.19	0.32	0.35	0.31	0.28	0.36	-5.35	6
2003	0.49	0.40	0.49	0.56	0.82	0.71	0.71	0.83	0.36	0.03	0.09	0.18	0.00	0
2004	0.21	0.02	-0.04	0.54	0.57	0.59	0.82	0.76	0.65	0.45	0.67	0.78	-0.04	1
2005	0.38	0.32	0.44	0.48	0.70	0.64	0.73	0.39	0.26	0.20	0.18	0.18	0.00	0
2006	0.04	0.00	-0.10	-0.21	-0.42	-0.35	-0.33	-0.23	-0.28	0.07	-0.07	0.15	-1.99	9
2007	0.16	0.51	0.59	0.66	0.57	0.64	0.45	0.51	0.36	0.24	0.23	0.29	0.00	0
2008	0.12	0.09	0.12	-0.33	-0.59	-1.20	-0.97	-1.05	-0.73	-0.44	-0.98	-1.07	-7.36	9
2009	-1.05	-0.85	-0.03	-0.21	0.11	-0.12	-0.43	0.14	0.17	0.06	-0.01	0.15	-2.72	7
2010	0.23	0.31	1.23	1.15	1.29	1.21	1.21	1.29	1.07	0.92	0.69	-0.08	-0.08	1
2011	-0.13	-0.41	-0.74	-1.02	-1.00	-0.84	-0.51	-0.43	-0.44	-0.50	-0.22	-0.03	-6.28	12
2012	0.20	0.18	-0.12	-0.02	0.14	0.19	0.26	-0.13	-0.18	-0.12	-0.64	-0.42	-1.62	7
2013	-0.61	-1.33	-1.23	-0.81	-0.93	-0.81	-0.88	-0.21	-0.06	-0.11	-0.31	-0.97	-8.28	12
2014	-1.43	-1.23	-1.43	-1.42	-1.34	-1.43	-1.60	-0.41	-0.05	0.08	0.04	-0.06	-10.34	10
2015	0.19	0.26	0.35	0.19	-0.24	-0.05	-0.22	-0.22	-0.33	-0.29	-0.16	0.04	-1.52	7
2016	0.06	0.24	0.05	0.66	0.63	0.81	0.77	0.66	0.41	0.15	0.09	0.21	0.00	0
2017	-0.53	-0.42	-0.87	-1.24	-1.08	-0.94	-0.55	-0.52	-0.31	0.07	0.01	-0.28	-6.74	10
2018	0.11	0.34	0.88	1.01	0.95	0.77	0.49	0.51	0.62	0.52	0.35	0.10	0.00	0
2019	-0.37	-0.59	-1.34	-1.43	-1.28	-0.43	-0.23	-0.19	-0.31	0.00	0.32	0.75	-6.17	9
2020	1.14	1.26	1.07	0.89	0.86	0.85	0.61	0.32	-0.01	-0.02	-0.17	-0.31	-0.51	4
2021	-0.30	-0.33	-0.92	-0.96	-0.48	-0.49	-0.70	-0.62	-0.56	-0.77	-0.36	-0.07	-6.58	12
2022	0.07	-0.30	-0.60	-0.88	-0.96	-1.42	-1.50	-2.47	-2.61	-2.42	-2.11	-1.89	-17.16	12

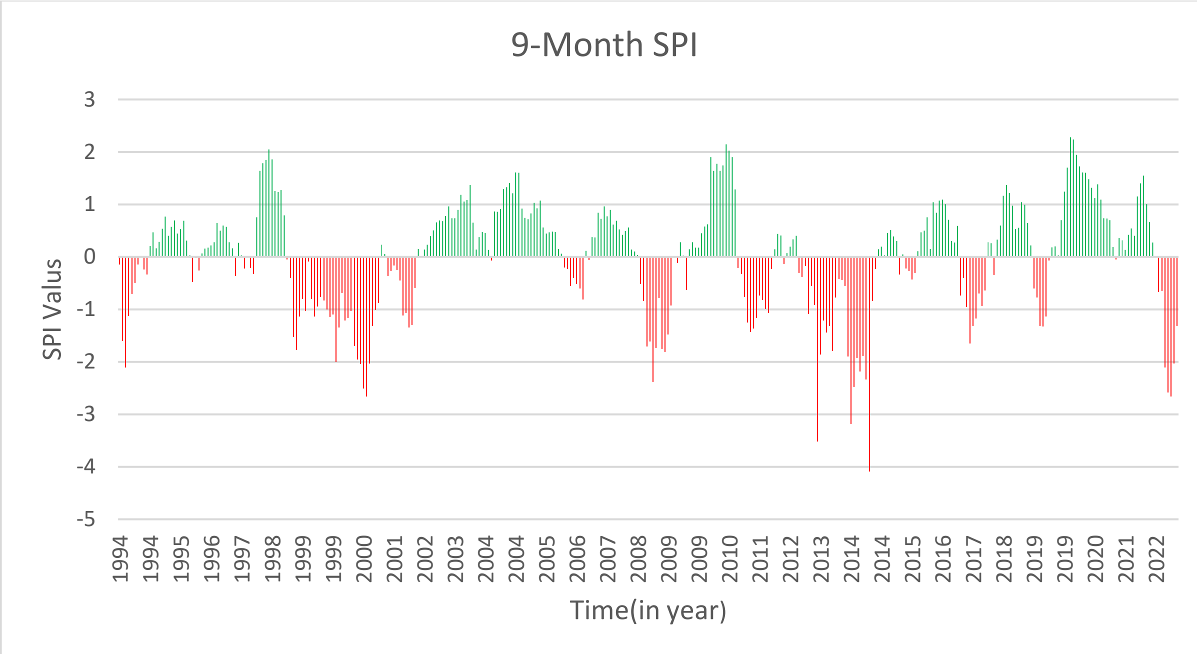

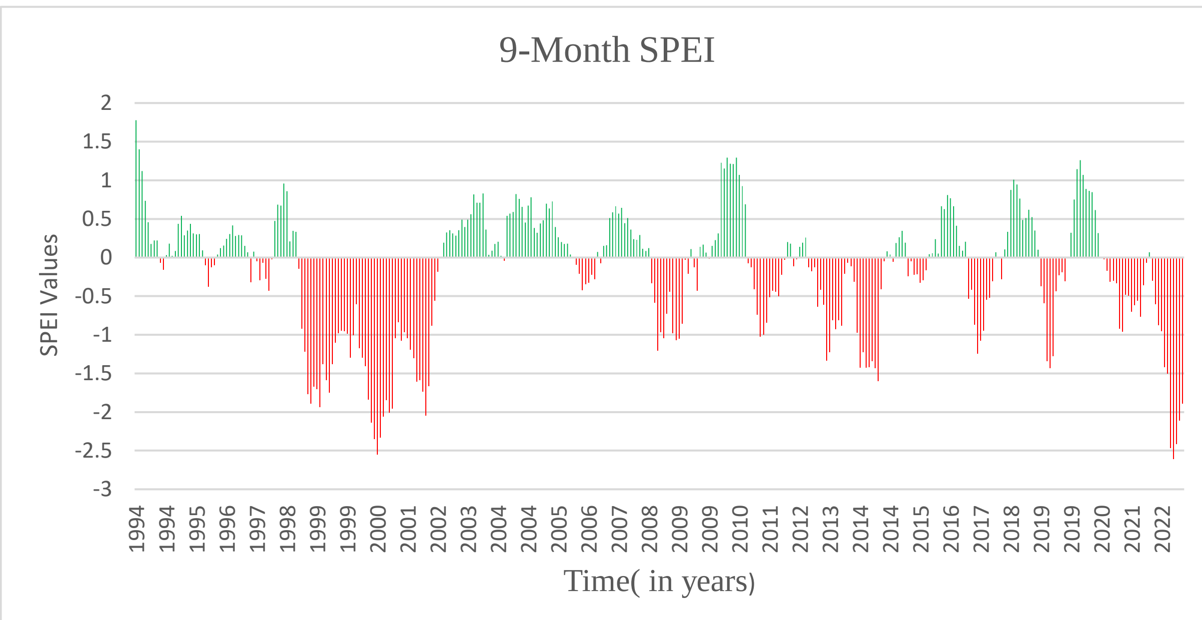

Figure 12 SPI and SPEI graph of yabello station at 9 time scales.

In addition to the 9-month scales, the 12-month SPI and SPEI were also analyzed to describe hydrological drought. According to table 16 and figure 14, these indices (12-month SPI and 12-month SPEI) showed that there were comparable increases in the frequency of hydrological droughts in the years 1999 to 2002, 2013 to 2014, and 2021 to 2022. However, the initial year indexes also display different patterns (frequency) of drought outcomes.

Table 16 SPI and SPEI at 12-Month time scale

12-month SPI														
years	jan	feb	mar	apr	may	jun	jul	aug	sep	oct	nov	dec	sum neg	Freq.
1994	-0.01	-0.30	-0.18	-0.20	-0.76	-0.81	-0.80	-0.71	-0.67	-0.49	0.02	0.00	-4.95	11
1995	-0.06	0.25	0.67	0.73	0.35	0.45	0.46	0.39	0.61	0.82	0.41	0.29	-0.06	1
1996	0.30	0.08	-0.18	-0.22	0.14	0.19	0.25	0.25	0.41	0.24	0.40	0.34	-0.41	2
1997	0.24	0.23	0.07	0.40	0.11	0.03	0.03	0.01	-0.39	0.56	1.24	1.31	-0.39	1
1998	1.66	1.86	1.78	0.94	1.16	1.18	1.14	1.19	1.18	0.46	-0.65	-0.79	-1.44	2
1999	-1.55	-1.84	-0.52	-0.63	-1.11	-1.18	-1.12	-1.20	-1.11	-1.25	-1.16	-1.12	-13.79	12
2000	-1.15	-1.16	-2.65	-1.60	-1.08	-1.82	-1.92	-1.85	-1.92	-2.40	-1.89	-1.93	-21.37	12
2001	-1.58	-1.52	-0.82	-0.76	-1.04	-0.42	-0.35	-0.35	-0.34	-0.54	-0.69	-0.83	-9.23	12
2002	-1.11	-1.10	-0.64	-0.46	0.12	0.18	0.16	0.07	0.22	0.43	0.51	1.08	-3.31	4
2003	1.01	1.04	0.62	0.91	1.07	1.05	1.02	1.17	1.02	0.75	0.85	0.33	0.00	0
2004	0.51	0.72	0.56	1.03	0.82	0.84	0.85	0.72	0.97	1.46	1.77	1.60	0.00	0
2005	1.39	1.35	1.45	0.84	0.87	0.95	0.97	0.99	0.79	1.02	0.43	0.37	0.00	0
2006	0.23	0.40	0.36	0.11	-0.56	-0.63	-0.66	-0.51	-0.51	0.03	0.00	0.27	-2.86	5
2007	0.22	0.04	0.04	0.44	0.75	0.83	0.97	0.93	1.12	0.56	0.56	0.23	0.00	0
2008	0.23	0.18	0.35	-0.28	-0.56	-1.29	-1.43	-1.61	-1.39	-0.66	-1.77	-1.79	-10.78	9
2009	-1.68	-1.66	-1.63	-1.12	-0.31	0.21	0.14	0.14	-0.02	-0.75	0.08	0.36	-7.17	7
2010	0.24	0.69	1.78	1.66	1.60	1.63	1.64	1.77	1.73	1.75	1.61	1.32	0.00	0
2011	1.20	1.01	-0.59	-0.81	-1.22	-1.11	-1.02	-1.26	-1.36	-1.23	-0.26	-0.24	-9.12	10
2012	-0.29	-0.45	-0.51	0.11	0.20	0.21	0.14	0.14	0.23	0.41	-1.15	-1.22	-3.62	5
2013	-1.05	-1.83	-0.89	-0.98	-1.44	-1.46	-1.41	-1.39	-1.05	-1.31	-1.20	-2.13	-16.13	12
2014	-2.54	-1.58	-1.83	-2.44	-1.77	-1.84	-1.87	-1.07	-1.61	-1.85	-0.71	-0.11	-19.21	12
2015	-0.17	-0.12	-0.31	0.11	0.16	0.39	0.39	-0.18	-0.18	-0.48	-0.13	0.12	-1.56	7
2016	0.08	0.34	0.19	1.04	0.90	0.91	0.91	0.90	0.94	0.63	0.54	0.31	0.00	0
2017	0.26	0.11	0.32	-1.40	-1.11	-1.46	-1.33	-1.15	-0.71	0.34	0.16	-0.57	-7.73	7
2018	-0.63	-0.39	0.26	1.20	1.21	1.25	1.19	1.10	0.82	0.10	0.05	0.71	-1.03	2
2019	0.68	0.48	-0.33	-1.15	-1.23	-0.31	-0.22	-0.24	-0.11	0.56	1.06	1.19	-3.59	7
2020	1.40	1.57	2.00	2.07	2.00	1.60	1.64	1.72	1.79	2.08	1.50	1.15	0.00	0
2021	0.91	0.83	0.28	0.14	0.51	0.46	0.50	0.63	0.66	0.22	0.94	0.96	0.00	0
2022	0.84	0.82	0.83	0.75	0.28	-0.25	-0.44	-0.63	-0.85	-1.06	-1.94	-1.97	-7.15	7

12-monthSPEI														
years	jan	feb	mar	apr	may	jun	jul	aug	sep	oct	nov	dec	negsum	Freq.
1994	1.80	1.71	1.62	1.46	1.15	0.90	0.62	0.41	0.15	0.08	0.13	-0.03	-0.03	1
1995	-0.08	0.08	0.39	0.45	0.23	0.25	0.25	0.26	0.40	0.48	0.23	0.13	-0.08	1
1996	0.13	-0.01	-0.12	-0.16	0.09	0.20	0.27	0.27	0.36	0.24	0.28	0.20	-0.30	3
1997	0.14	0.10	0.04	0.26	0.10	-0.05	-0.05	-0.16	-0.52	-0.02	0.38	0.39	-0.78	5
1998	0.57	0.66	0.64	0.02	0.13	0.03	-0.10	0.00	-0.02	-0.68	-1.39	-1.46	-3.64	5
1999	-2.06	-2.19	-1.65	-1.60	-1.98	-1.75	-1.52	-1.47	-1.29	-1.19	-1.10	-1.01	-18.79	12
2000	-1.10	-1.08	-1.89	-1.40	-1.22	-1.78	-2.01	-2.21	-2.34	-2.48	-2.09	-2.11	-21.70	12
2001	-2.20	-2.13	-1.96	-1.76	-1.94	-1.36	-1.31	-1.35	-1.32	-1.47	-1.48	-1.49	-19.78	12
2002	-1.79	-1.71	-1.46	-1.17	-0.60	-0.39	-0.23	-0.12	0.06	0.22	0.26	0.51	-7.48	8
2003	0.49	0.49	0.31	0.50	0.63	0.61	0.63	0.74	0.64	0.40	0.44	0.13	0.00	0
2004	0.21	0.32	0.30	0.59	0.51	0.50	0.47	0.40	0.54	0.72	0.92	0.74	0.00	0
2005	0.63	0.59	0.71	0.40	0.46	0.53	0.58	0.62	0.52	0.58	0.25	0.16	0.00	0
2006	0.08	0.16	0.21	0.11	-0.30	-0.38	-0.41	-0.25	-0.24	0.08	0.04	0.16	-1.57	5
2007	0.12	0.01	0.04	0.24	0.48	0.55	0.64	0.65	0.77	0.41	0.38	0.15	0.00	0
2008	0.14	0.09	0.25	-0.05	-0.24	-0.78	-0.81	-0.89	-0.80	-0.40	-0.99	-0.96	-5.94	9
2009	-1.00	-0.99	-1.02	-0.78	-0.32	0.10	0.02	0.03	-0.07	-0.37	0.04	0.16	-4.55	7
2010	0.09	0.31	0.94	0.93	0.98	1.01	1.05	1.14	1.13	1.03	0.99	0.74	0.00	0
2011	0.68	0.57	-0.21	-0.41	-0.66	-0.60	-0.60	-0.75	-0.79	-0.63	-0.17	-0.15	-4.98	10
2012	-0.21	-0.32	-0.33	0.05	0.11	0.10	0.08	0.12	0.16	0.25	-0.63	-0.65	-2.14	5
2013	-0.63	-0.95	-0.47	-0.52	-0.80	-0.77	-0.74	-0.66	-0.50	-0.53	-0.53	-0.91	-8.03	12
2014	-1.16	-0.82	-0.98	-1.29	-1.06	-1.11	-1.09	-0.66	-0.89	-0.87	-0.36	-0.05	-10.34	12
2015	-0.11	-0.12	-0.19	0.05	0.11	0.24	0.22	-0.15	-0.21	-0.37	-0.22	-0.09	-1.46	8
2016	-0.13	-0.01	0.02	0.52	0.50	0.53	0.54	0.59	0.63	0.40	0.32	0.15	-0.14	2
2017	0.10	0.01	0.11	-0.87	-0.79	-0.99	-0.89	-0.76	-0.47	0.15	0.03	-0.33	-5.11	7
2018	-0.40	-0.30	0.15	0.71	0.78	0.84	0.83	0.81	0.63	0.22	0.14	0.41	-0.70	2
2019	0.37	0.21	-0.30	-0.93	-1.02	-0.47	-0.46	-0.47	-0.39	0.00	0.29	0.33	-4.05	7
2020	0.45	0.52	0.83	0.94	0.96	0.67	0.65	0.68	0.66	0.59	0.22	-0.05	-0.05	1
2021	-0.24	-0.32	-0.66	-0.73	-0.46	-0.58	-0.56	-0.52	-0.47	-0.90	-0.41	-0.36	-6.22	12
2022	-0.48	-0.54	-0.51	-0.56	-0.97	-1.38	-1.54	-1.72	-1.87	-1.96	-2.24	-2.24	-16.02	12

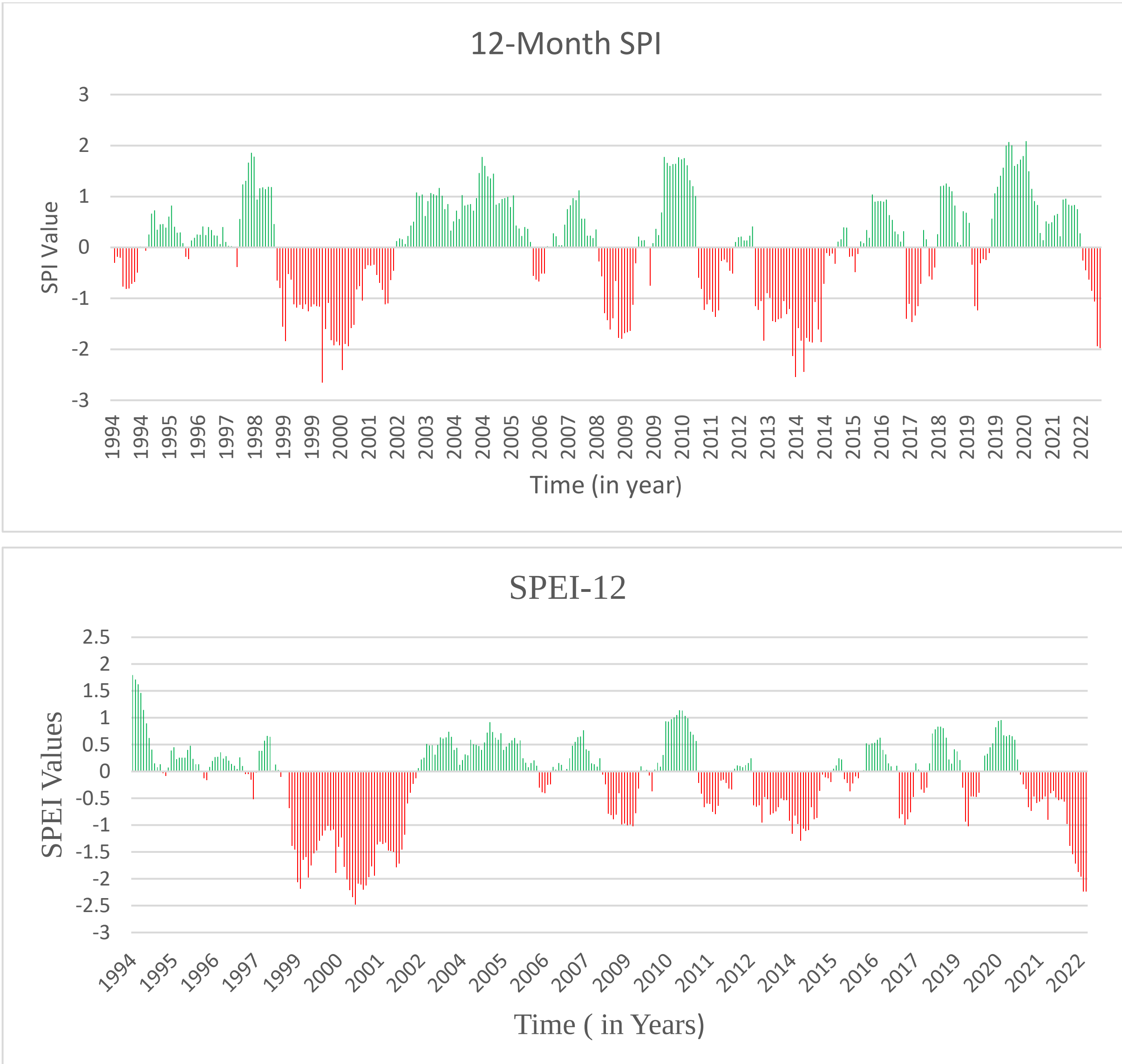

Figure 13 SPI and SPEI graph of yabello station at 12 time scales.

In general, wet and dry episodes did not always occur in the same months at the station, as can be seen from the statistics and tables. The annual accumulated (total) negative values of both SPI and SPEI at each of the previous 28 years showed the classifications of all drought severity levels (Meteorological drought, Agricultural drought, and hydrological drought), based on the classification standard given in the Table 2.In addition to differing in magnitude and length, both indices displayed comparable patterns at shorter time scales as compared to longer ones. While at longer time scales, higher frequency of drought was seen. The lowest period studied one month showed a lower frequency of drought. Thus, there was significant variance in meteorological, agricultural, and hydrological droughts according to both indexes.

Notes: Both indices display extreme (SPI/SPEI values less than or equal to -2) severe (SPI/SPEI values between -1.5 and -1.99) and moderate (SPI/SPEI values between -1 and -1.49) droughts at estimated time scales in various months or years (see tables 11 to 16 and figures 9 to 14).

The driest years over the studied periods were 1999, 1998, 2000, 2001, 2008, 2009, 2010, and 2022. The majority of droughts occurred in the months of January, February, June, July, September, and December.

4.1.2 Drought magnitude results based on SPEI

Additionally, this study used the multi-scalar drought index, SPEI, calculated at 1, 2, 3, 6, 9 and 12 month scale for the investigated period to analyze drought characteristics (duration and magnitude or severity). SPEI provides a more reliable measure of drought severity than SPI because it uses both precipitation and evapotranspiration to quantify drought frequency, duration, and severity.

The meteorological drought indices (SPEI-1 and SPEI-2) have extreme observed values (values less than or equal to -2) mostly throughout the study period from 1994 to 2022 years. Table 17 shows that, based on the drought severity categorization tables 1 and 2, at 1-month and 2-month SPEI, mild meteorological droughts occurred in the years 1996, 2005, 2007, and 2001 based on SPEI-2 and SPEI-1. PEI-3 and SPEI-6 show exceptionally low values of agricultural drought for the research periods of 1997 to 2001 and 2008 to 2022, with the exception of 2020. The 9-month and 12-month SPEIs indicate the hydrological drought severity from 1994 to 1997 years, and the extreme hydrological drought severity from 1998 – 2002, 2008 – 2009, 2023 – 2015, and 209 – 2022 years. These indices also show the severities of the agricultural drought from near normal to severe from 1994 to 1996 years. Furthermore, table 17 below illustrates that during the study period, drought occurrences happened at various time scales (1–12 month SPEI). The effects of drought may worsen if the SPI and SPEI values consistently remain negative for several months in a row. Researcher computed the magnitude of the drought to quantify this effect. Table 17 displays the amount and length of the drought for the Yabello district. The studied years had the highest observed meteorological, agricultural, and hydrological drought magnitudes during the analyzed period. Please note that, each values listed under 1 -12 SPEI in column shows magnitudes of droughts in respective to time of years and the values in months indicated duration or frequencies of drought in months along the rows with the each years (Table 17).But, overall drought frequencies were calculated at selected time scales as general for 28 years of study.

Table 17 drought magnitudes and durations (in months) based on SPEI time scales.

years	SPEI-1	Months	SPEI-2	Months	SPEI-3	Months	SPEI-6	Months	SPEI-9	Months	SPEI-12	Months
1994	-3.2989	8	-2.5616	6	-1.5348	5	-0.1912	4	-0.2272	2	-0.0333	1
1995	-2.9037	6	-1.8424	7	-0.9593	4	-0.3556	4	-0.1001	1	-0.0805	1
1996	-1.7680	6	-1.2363	5	-1.4314	4	-0.6383	4	-0.6000	3	-0.2955	3
1997	-7.6877	7	-5.6887	6	-4.1150	6	-2.2026	9	-1.4535	7	-0.7845	5
1998	-13.1513	12	-12.3455	10	-12.7249	9	-10.8054	8	-7.6224	6	-3.6389	5
1999	-7.6976	11	-7.9813	10	-8.2608	11	-12.6951	12	-15.9961	12	-18.7871	12
2000	-13.9629	12	-15.4674	12	-17.0583	12	-20.0561	12	-20.6067	12	-21.7046	12
2001	-11.5379	10	-11.3410	10	-11.8227	10	-13.4644	12	-16.3555	12	-19.7778	12
2002	-1.2070	5	-0.7043	4	-1.1671	3	-2.8640	3	-5.3492	6	-7.4754	8
2003	-3.1235	4	-2.8703	6	-2.8830	4	-0.9683	3	0.0000	0	0.0000	0
2004	-2.2152	6	-0.7300	2	-0.4747	3	-0.3123	3	-0.0443	1	0.0000	0
2005	-1.5576	4	-1.3227	4	-0.8430	4	-0.2789	2	0.0000	0	0.0000	0
2006	-3.1372	7	-2.7339	5	-2.4216	4	-2.5700	8	-1.9874	9	-1.5737	5
2007	-2.1996	7	-1.2719	5	-0.9508	3	0.0000	0	0.0000	0	0.0000	0
2008	-7.0166	8	-8.2120	9	-7.4828	10	-7.6075	12	-7.3587	9	-5.9404	9
2009	-1.6128	6	-0.9354	6	-2.0695	6	-2.0397	5	-2.7186	7	-4.5543	7
2010	-2.6017	5	-3.0177	3	-3.3205	3	0.2903	2	-0.0760	1	0.0000	0
2011	-3.4287	7	-3.6528	7	-4.1347	9	8.9259	10	-6.2762	12	-4.9828	10
2012	-5.3314	7	-6.3555	9	-5.2839	8	-2.0739	7	-1.6233	7	-2.1445	5
2013	-6.0395	4	-9.1540	6	-7.6240	8	-8.2087	10	-8.2815	12	-8.0327	12
2014	-3.8398	9	-5.8594	7	-7.2796	7	-10.1338	8	-10.3429	10	-10.3407	12
2015	-3.7625	8	-4.0532	8	-3.6545	8	-2.1363	9	-1.5175	7	-1.4600	8
2016	-4.3081	8	-3.0491	4	-3.5239	5	-1.7337	3	0.0000	0	-0.1391	2
2017	-5.8386	7	-4.8995	8	-3.9410	8	-6.5162	9	-6.7368	10	-5.1075	7
2018	-2.8341	5	-5.0228	5	-5.1354	6	-1.2466	3	0.0000	0	-0.6965	2
2019	-5.3446	7	-5.7111	7	-5.4531	6	-6.1927	8	-6.1740	9	-4.0496	7
2020	-2.9621	7	-2.3451	7	-1.1604	5	-0.9954	6	-0.5140	4	-0.0528	1
2021	-5.1578	10	-5.5743	9	-6.1320	9	-5.5769	11	-6.5758	12	-6.2187	12
2022	-15.4857	12	-17.5037	12	-17.9302	11	-17.6954	11	-17.1614	12	-16.0154	12

4.1.3 Drought classes and its frequencies results based on SPI and SPEI.

At the station, different droughts with different lengths, frequencies, and magnitudes were noted throughout the examined years. At the various timescales taken into consideration for this study, researchers examined this phenomena. The largest and lowest drought durations, as indicated by SPI-3 and SPI-12 from table 18, were moderate droughts (43 months) and extreme droughts (2 months), respectively, based on table 2 from the literature. The SPI showed that the overall duration of extreme drought occurrences within the 1–12 month time frame was 7, 9, 9, 20, 13, and 2 months. Furthermore, data on moderate drought episodes (9,36,43,20,33, and 43 months) and severe drought durations (10,11,10,7, 16 and 26 months) were gathered from lower to higher SPI time scales.

Similarly, utilizing particular SPEI time scales, distinct drought events for extreme, severe, and moderate drought were also made. From lower to higher SPEI time scales, extreme drought durations (6, 9, 5, 16, 11 and 7) and severe drought durations (9, 17, 17, 13, 16, and 15) as well as moderate drought occurrences (19, 20, 30, 26, 38, and 29 months) were obtained (see table 18). Table 18 further shows that different results were achieved when the drought frequencies were studied at 1, 2, 3, 6, 9, and 12-month timeframes of both SPI/SPEI. At the Yabello station, SPI/SPEI-1 displays meteorological drought frequencies ranging from 2% to 19%. Additionally, the 2-month SPI/SPE indicates the frequency of droughts ranging from 3% to 11%. for the purpose of characterizing agricultural droughts Over a 28-year period of study, the frequency of extreme, severe, and moderate agricultural droughts ranged from 1% to 13%, according to the 3- and 6-month SPI/SPEI. Furthermore, the SPI/SPEI for 9 and 12 months indicates that the frequency of hydrological droughts ranged from 1% to 13%.

Generally, SPI indicates that the range of drought frequencies over the study period was 13% (moderate drought) to 1% (severe drought). At Yabello station, SPI-3 and SPI-12 were used to detect the majority of extreme drought episodes, with 43 occurrences each indicating a moderate drought class. On the other hand, SPEI indicates that the frequency of extreme, severe, and moderate drought varied from 1% to 11% and that the total number of drought events at the station ranged from 5 to 38. According to SPEI-9 and SPEI-3, the number of drought occurrences was 38 and 30, respectively. As a result, Table 18 shows that the frequency and occurrences of drought periods in the Yabello district range from 1% to 13% and 2 to 43 months, respectively.

Table 18: over all durations and frequencies for drought classes using SPI/SPEI

Duration(in months) from 1994-2022							
Station	Drought classes	SPI-1	SPI-2	SPI-3	SPI-6	SPI-9	SPI-12
	Moderate	9	36	43	20	33	43
	severe	10	11	10	7	16	26
	Extreme	7	9	9	20	13	2
	Total	28	58	62	47	62	71
	Duration(in months) from 1994-2022						
Station	Drought classes	SPEI-1	SPEI-2	SPEI-3	SPEI-6	SPEI-9	SPEI-12
	Moderate	19	20	30	26	38	29
	severe	9	17	17	13	16	15
	Extreme	6	9	5	16	11	7
	Total	34	46	52	55	64	51
SPI based drought Frequency from 1994 -2022(%)							
Station	Drought classes	SPI-1	SPI-2	SPI-3	SPI-6	SPI-9	SPI-12
	Moderate	3	11	13	6	10	13
	severe	3	3	3	3	5	8
	Extreme	2	3	3	6	4	1
	Total	8	17	19	15	19	22
	SPEI based drought Frequency from 1994 -2022(%)						
Station	**Drought classes**	**SPEI-1**	**SPEI-2**	**SPEI-3**	**SPEI-6**	**SPEI-9**	**SPEI-12**
	Moderate	6	6	9	8	11	9
	severe	3	5	5	4	5	4
	Extreme	2	3	1	5	3	2
	Total	11	14	15	17	19	15

Total number of months for 28 years = 336. Frequency = (number of drought months/336)*100

From above table 18, highest value of drought duration (71 months) and highest value of frequency of drought (22) was showed at 12-months SPI for 28 years of study. Lower durations and frequencies of drought were indicated at both 1-monthSPI/SPEI. It implies longer time scale shows higher durations and frequencies of drought than lower time scales.

4.1.4 Linear relationship results between SPI and SPEI.

Table 18, which is seen below, shows Correlation Analysis Findings for the study were obtained using Pearson's correlation coefficient with a 95% confidence interval. The correlation coefficient's findings lead to the following observations.

There was a high, positive, and statistically significant association between SPI and SPEI, with correlations ranging from 0.554 to 0.912 when using the correlation limit given by Adler & Parmryd (2010).This indicates that the linear relationship between SPI and SPEI at various time scales was investigated using Pearson's correlation coefficient. The test result showed that, at the 1-month ($r = 0.764$, $p < 0.01$), 2-month ($r = 0.762$, $p < 0.01$), 3-month ($r = 0.792$, $p < 0.01$), 6-month ($r = 0.880$, $p < 0.01$), 9-month ($r = 0.819$, $p < 0.01$), and 12-month ($r = 0.798$, $p < 0.01$) timescales, SPI and SPEI demonstrated a strong and significant relationships. As can be shown from Table 18, the Pearson’s correlation values for the 1- to 2-month SPI and SPEI for meteorological drought conditions across the study period range from 0.554 to 0.764, indicating the different forms of drought. The correlation values for agricultural drought assessment on the 3- to 6-month SPI and SPEI scales ranged from 0.553 to 0.880. On the other hand, the longer time scales (from 9 to 12 months) also demonstrated very strong and significant relationships (Pearson’s correlation ranging from 0.684 to 0.12, $p<0.01$) for the presence of hydrological drought during the study periods.

Table 18 Correlations Analysis between SPI and SPEI

		1-Month SPI	2-Month SPI	1-Month SPEI	2- month SPEI
1-Month SPI	Pearson Correlation	1	.697**	.764**	.554**
	Sig. (2-tailed)		<.001	<.001	<.001
	N	348	348	348	348
2-Month SPI	Pearson Correlation	.697**	1	.614**	.762**
	Sig. (2-tailed)	<.001		<.001	<.001
	N	348	348	348	348
1-Month SPEI	Pearson Correlation	.764**	.614**	1	.759**
	Sig. (2-tailed)	<.001	<.001		<.001
	N	348	348	348	348

2- month SPEI	Pearson Correlation	.554**	.762**	.759**	1
	Sig. (2-tailed)	<.001	<.001	<.001	
	N	348	348	348	348

		3-Month SPI	6-Month SPI	3-month SPEI	6-Month SPEI
3-Month SPI	Pearson Correlation	1	.587**	.792**	.553**
	Sig. (2-tailed)		<.001	<.001	<.001
	N	348	348	348	348
6-Month SPI	Pearson Correlation	.587**	1	.702**	.880**
	Sig. (2-tailed)	<.001		<.001	<.001
	N	348	348	348	348
3-month SPEI	Pearson Correlation	.792**	.702**	1	.770**
	Sig. (2-tailed)	<.001	<.001		<.001
	N	348	348	348	348
6-Month SPEI	Pearson Correlation	.553**	.880**	.770**	1
	Sig. (2-tailed)	<.001	<.001	<.001	
	N	348	348	348	348

		9-Month SPI	12-Month SPI	9-Month SPEI	12- Month SPEI
9-Month SPI	Pearson Correlation	1	.860**	.819**	.684**
	Sig. (2-tailed)		<.001	<.001	<.001
	N	348	348	348	348
12-Month SPI	Pearson Correlation	.860**	1	.744**	.798**
	Sig. (2-tailed)	<.001		<.001	<.001
	N	348	348	348	348
9-Month SPEI	Pearson Correlation	.819**	.744**	1	.912**
	Sig. (2-tailed)	<.001	<.001		<.001
	N	348	348	348	348
12- Month SPEI	Pearson Correlation	.684**	.798**	.912**	1
	Sig. (2-tailed)	<.001	<.001	<.001	
	N	348	348	348	348
**. Correlation is significant at the 0.01 level (2-tailed).					

4.1.5 Kappa statistics test results

This study implemented Cohen's Kappa statistics (Viera & Garrett, 2005) to test degree of agreement between SPI and SPEI. The results of Cohen's Kappa Statistics for SPI and SPEI on a 1- and 2-month time scale range from 0.381 to 0.647, indicating a reasonable to moderate degree of agreement about meteorological drought. For the 3- and 6-month time scales, the value of Cohen's Kappa Statistics ranged from 0.395 to 0.669, indicating a degree of agreement from fair to substantial to demonstrate the existence of an agricultural drought. Similarly, for the 9- and 12-month time scales, the kappa results between SPI and SPEI ranged from 0.513 to 0.717, indicating a moderate to substantial degree of agreement to demonstrate hydrological drought.

Generally, the Cohen's Kappa Statistics result indicated a statistically fair to substantial ((0.2–0.8) degree of agreement between SPI and SPEI in all investigated time scales at $p < 0.01$ (see Table 19).

Table 19 Cohen's Weighted Kappa statistics analysis

Cohen's Weighted Kappa						
		Asymptotic			95% Confidence Interval	
Ratings	Weighted Kappa[a]	Std. Error[b]	z[c]	Sig.	Lower Bound	Upper Bound
1-Month SPI - 2-Month SPI	.521	.027	15.378	<.001	.467	.574
1-Month SPI - 1-Month SPEI	.640	.023	19.071	<.001	.595	.685
1-Month SPI - 2-month SPEI	.381	.029	11.397	<.001	.324	.438
2-Month SPI - 1-Month SPEI	.458	.029	13.753	<.001	.402	.514
2-Month SPI - 2-month SPEI	.647	.020	19.480	<.001	.608	.687
1-Month SPEI - 2-month SPEI	.589	.025	17.407	<.001	.540	.638

3-Month SPI - 6-Month SPI	.473	.028	14.005	<.001	.419	.528
3-Month SPI - 3-month SPEI	.659	.019	19.901	<.001	.622	.695
3-Month SPI - 6-Month SPEI	.395	.028	12.008	<.001	.341	.450
6-Month SPI - 3-month SPEI	.477	.028	14.580	<.001	.422	.532
6-Month SPI - 6-Month SPEI	.669	.018	20.603	<.001	.633	.705
3-month SPEI - 6-Month SPEI	.544	.026	16.075	<.001	.493	.595
9-Month SPI - 12-Month SPI	.687	.020	20.306	<.001	.648	.727
9-Month SPI - 9-Month SPEI	.622	.022	19.136	<.001	.579	.665
9-Month SPI - 12-Month SPEI	.485	.026	14.884	<.001	.434	.536
12-Month SPI - 9-Month SPEI	.513	.026	15.885	<.001	.462	.563
12-Month SPI - 12-Month SPEI	.584	.022	18.067	<.001	.541	.626
9-Month SPEI - 12-Month SPEI	.717	.018	21.191	<.001	.682	.753
a. The estimation of the weighted kappa uses linear weights.						

Additionally, the following table shows summery of the test of the degree of agreements between SPI and SPEI

Time scale	Kappa statistics	Pearson's correlation(r)
1-month	0.64	0.764
2-month	0.647	0.762
3-month	0.659	0.792
6-month	0.669	0.880
9- month	0.622	0.819
12-month	0.568	0.798

Significant at p <0.001

Overall, Higher degree of agreement were observed for all corresponded timescales

4.2 Spatial analysis of Meteorological drought results based on SPI and SPEI.

The researcher classified the data in accordance with Tables 1 and 2 after using the IDW method of interpolation for spatial analysis of meteorological drought. They then computed the area under hazard classes based on SPI and SPEI at 2-month and 12-month time scales.

For the purpose of characterizing meteorological drought in the research area, Figure 15 displays a classified 2-month SPI and SPEI-2 severity maps of meteorological drought from 1994 to 2022 years of study. According to SPI-2, the district's moderately dry, severely dry, and extremely dry land dominance are shown as 65.75 %(20478.46 km2), 23.39 %(7284.471 km2), and 10.87 %(3385.3 km2), respectively (see table 20). Similarly, reclassified SPEI-2 map of 1994 -2022 exhibits drought impacts from 1994–2022 years of study. This map (reclassified SPEI-2 map of 1994 -2022), indicated that the district's total area was affected by moderately dry, severely dry, and extremely dry severities of droughts covering 66.086% (20584.71 km2), 23.38647% (7202.529km2), and 10.79032% (3360.995km2) of the total area (see table 21).

The map produced by SPI-2 was determined to be the most serious of the hazard maps included in the IDW model, displaying a greater region of the district impacted by severely dry conditions of droughts, based on the aforementioned 2-month time frames. However, the SPEI-2 map shows that a greater portion of the district had moderately dry drought conditions.

.

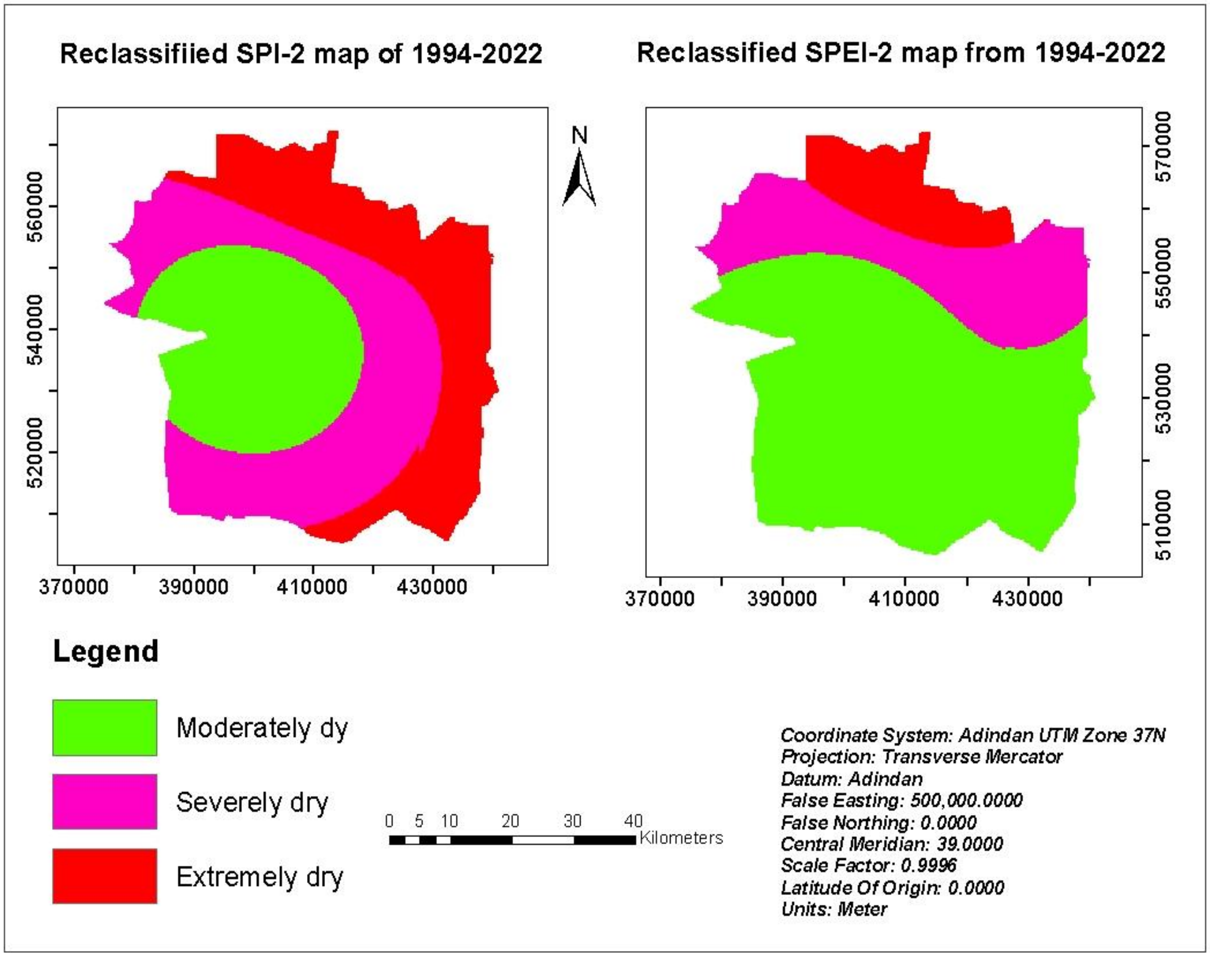

Figure 15: 2-months SPI/SPEI based spatial pattern of Meteorological drought severity maps for the year 1994 -2022.

Table 20: SPI-2 based drought severity classes from 1994- 2022

Value	Count	Severity-classes	Area	%
1	29490	Moderately dry	20478.46	65.74518
2	10490	Severely dry	7284.471	23.38647
3	4875	Extremely dry	3385.3	10.86835
Total			31148.23	100

Table 21**:** SPEI-2 based drought severity classes from 1994- 2022

Value	Count	Severity-Classes	Area	%
1	29643	Moderately dry	20584.71	66.08628
2	10372	Severely dry	7202.529	23.1234
3	4840	Extremely dry	3360.995	10.79032
Total			31148.23	100

A different result was found when the spatial severities of drought were examined using SPI/SPEI-12 at a 12-month timescale (figure 16). Particularly for severe and extreme dryness, the longer timescale SPI/SPEI-12 showed more severity than the shorter timescale SPI/SPEI-2. Shorter timeline SPI/SPEI-2 indices, however, showed greater drought severity throughout the study region for moderate dryness. Similar patterns of moderately dry drought conditions are shown in the district's western portions on SPI/SPEI-12 maps.

Reclassified SPI-12 map suggested that mostly North West parts of the district was affected by both extreme and moderate dryness conditions. In this map, about 30.04 %(9357.316 km2), 37.83%(11782.93km2) and 32.13%(10007.99km2) of the area falls under the moderately dry, severely dry, and extremely dry severities of droughts classes, indicating that most parts of the study area have experienced the worst droughts during the study period(table 22).

Also figure 16 provide a visual representation of the SPEI-12 hazard maps prepared using the IDW interpolation model. SPIEI-12 revealed moderate, severe and extreme dryness classes of the drought covered 32.20%(10028.82km2), 52.6%(16385.55km2) and 15.2%(4733.865km2) respectively(table 23a).

Overall, the shorter and longer durations show different spatial distributions of drought in different parts of the district. Consequently, any plan pertaining to drought management should take into account this internal variability as well as potential countermeasures for the effects of the drought in this research area's district.

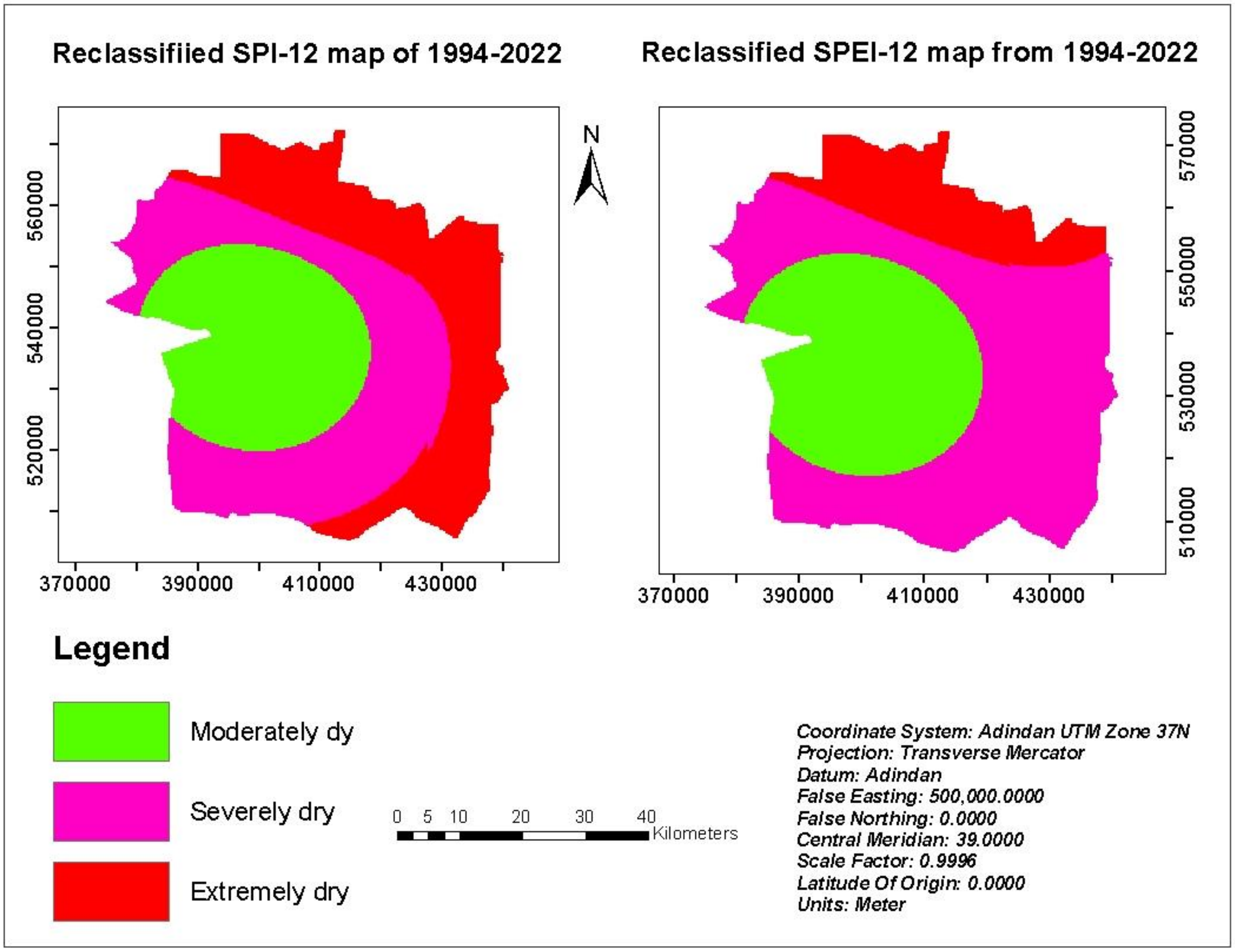

Figure 16: 12-months SPI/SPEI based spatial pattern of Meteorological drought severity maps for the year 1994 -2022.

Table 22: SPI-12 based drought severity classes from 1994- 2022

VALUE	COUNT	SEVERITY-CLASSES	AREA	%
1	13475	Moderately dry	9357.316	30.04
2	16968	Severely dry	11782.93	37.83
3	14412	Extremely dry	10007.99	32.13
Total area			31148.23	100

Table 23a: SPEI-12 based drought severity classes from 1994- 2022

Value	Count	Severity-Classes	Area	%
1	14442	Moderately dry	10028.82	32.20
2	23596	Severely dry	16385.55	52.60
3	6817	Extremely dry	4733.865	15.20
Total area			31148.23	100

4.3 Satellite Image based spatial analysis results of agricultural drought.

The remote sensing or Satellite images based method of identifying drought hazard areas gives spatial information on the area based on variations in vegetation development. The agricultural drought was determined by analyzing temporal images from NDVI, DEVNDVI, and VCI, and the meteorological drought was determined by using rainfall auxiliary data. To determine the hazards resulting from agricultural droughts, temporal images from the NDVI, DEVNDVI, and VCI were analyzed based on the criteria provided. It includes an explanation of the demonstrated connection between vegetation and rainfall.

. The various categories of drought severity level showed varying degrees of NDVI change. The change of NDVI, DevNDVI, and VCI for the district of the study region was used by the researcher to identify agricultural drought risk area.

4.3.1 Normalized Difference Vegetation Index (NDVI) anomaly results.

The research area's spatial patterns of agricultural drought from 1994 to 2022 are depicted in Figure 15. From reclassified Landsat images from 1994 to 2004 and from 2014 to 2022, the level of drought intensity varied from slight to very severe. Between 1994 and 2004, a greater portion of the district was not affected by a drought; this coverage gradually decreased until the year 2022. It suggests that the district experienced the drought from 1994 and 2022. Based on reclassified Landsat image data from 1994 to 2004, a significant portion of the research region experienced severe (10.72%) and very severe (4.03%) agricultural drought, with moderate and slight drought affecting 2.7% and 1.95% of the area, respectively.

However, the majority of the research area 80.62%, or 25137.11 km2 was unaffected by the drought (table 20). Table 21 shows that from 2004 to 2014, the percentage of the total area affected by extremely severe, severe, moderate, and slight agricultural droughts was 17.54% (5471.397 km2), 10.97% (3429.873 km2), 5.893% (1867.527 km2), and 3.893% (1214.084 km2), respectively.

On the other hand, over the years 2014–2022, the corresponding agricultural drought severity was 94.15% (29364.77 km2), 2.305 % (718.854 km2), 0.895 % (279.027 km2), and 0.464 % (144.684 km2) of the total area (31188.64 km2) respectively (table 22).

The map presented in Figure 15 illustrates that the research area experienced extreme drought from 1994 to 2022, with a decrease in the percentages and areas no drought from the start to the end of the study years.

Table 20 NDVI anomaly based drought severity classes from from1994 -2004

Value	Count	Area	Drought Severity	%
1	371309	3341.781	Very severe drought	10.71728
2	139611	1256.499	Severe drought	4.029662
3	93154	838.386	Moderate drought	2.688751
4	67497	607.473	Slight drought	1.9482
5	2793012	25137.11	no drought	80.61611
total		31188.64		100

Table 21 NDVI anomaly based drought severity classes from 2004- 2014

VALUE	Count	Area	Drought-Severity	%
1	607933	5471.397	Very severe drought	17.54292
2	381097	3429.873	Severe drought	10.99719
3	207503	1867.527	Moderate drought	5.987844
4	134898	1214.082	Slight drought	3.892706
5	2133973	19205.76	no drought	61.57934
total		31188.64		100

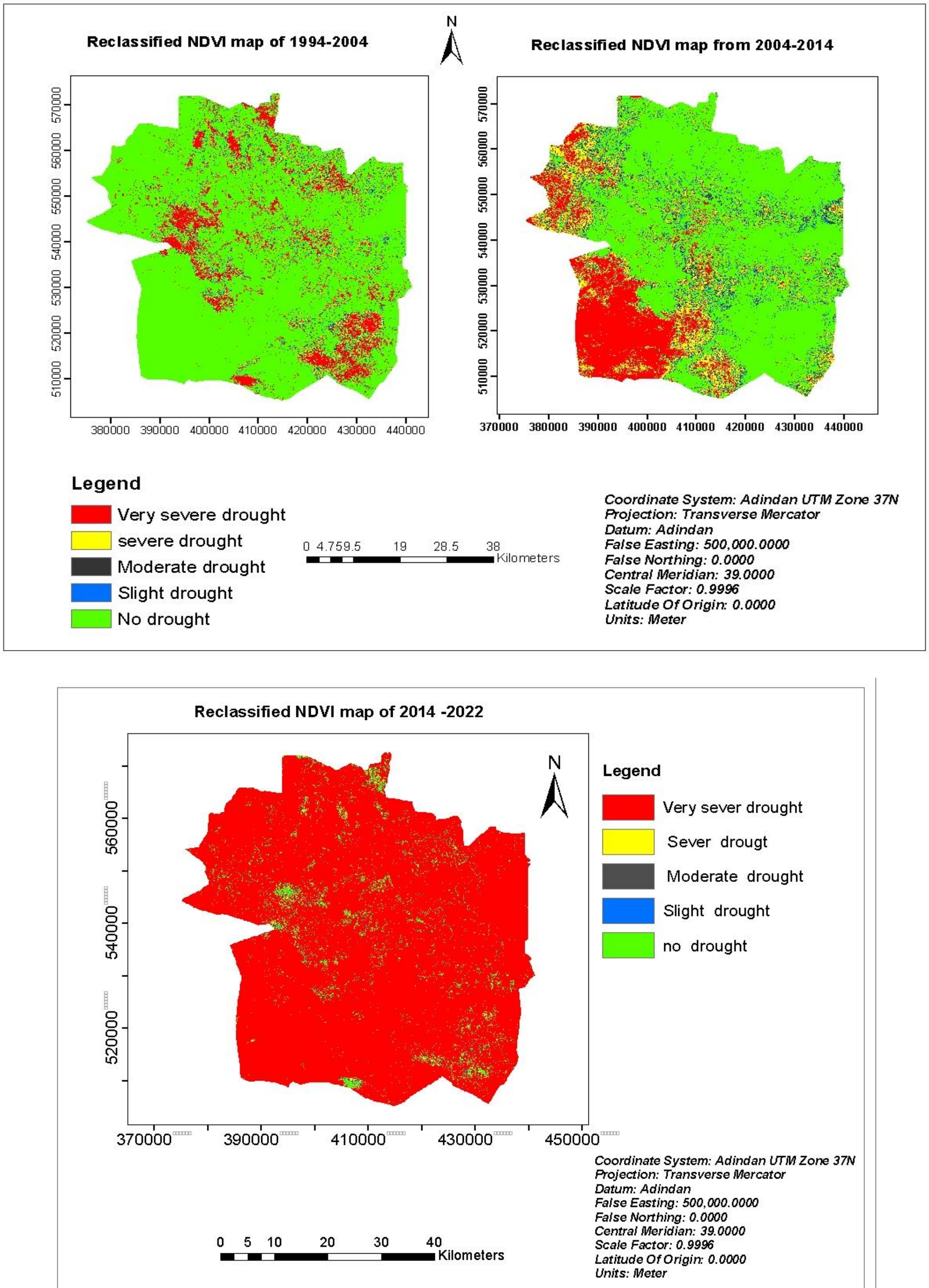

Figure 14: NDVI anomaly based spatial pattern of agricultural drought severity for the year 1994-2004, 2004 -2014 and 2014 -2022.

Table 22 NDVI anomaly based drought severity classes from 2014 -20022

VALUE	COUNT	AREA	DROUGHT_SEVERITY	%
1	3262752	29364.77	Very severe drought	94.15214
2	79873	718.857	Severe drought	2.304868
3	31003	279.027	Moderate drought	0.894643
4	16076	144.684	Slight drought	0.4639
5	75700	681.3	no drought	2.184449
total		31188.64		100

4.3.2 DEVNDVI analysis results.

Figure 16 depicts the variability of the agricultural drought in the research area using three LandSAT images and related indices DEVNDVI for the years 1994–2022.

The vegetation is in a normal state when the DEVNDVI values are higher than zero. An index indicates drought conditions when it deviates from zero. The size of the deviation below the norm is directly correlated with the severity of a drought. In this case, the difference between the long-term mean NDVI from two decadal NDVI and one eight-year NDVI is used to further examine the severity of the agricultural drought. Four classifications were identified using DevNDVI (Figure 16). For the purpose of characterizing agricultural drought in the research area, Figure 16 displays a classified DevNDVI image. The district's extreme dry, moderate dry, near normal, and extreme wet land dominance are shown as 0.025%, 0.155%, 91.432, and 8.396%, respectively, on the DEVNDVI map for the years 1994–2004 (see table 23). Furthermore, the 2004–2014 DEVNDVI map exhibits greater drought impacts than the 1994–2004 categorized map. This year, the district's total area was affected by near-normal, moderate-dry, and extreme dry agricultural droughts, covering 0.030% (9.454 km2), 0.064% (21.456 km2), and 99.361% (30989.3 km2) of the total area (see table 24). It suggests that from 2004 to 2014, a near-normal agricultural drought affected 99.361% of the district's land. In certain areas of the Yabello district, moderately dry and nearly typical conditions are also reported for the years 2014–2022. Near-normal drought severity was also present throughout most of the district, as shown by figures 16 and 25. A moderate dry and near-normal agricultural drought harmed 97.593% (30437.97 km2) of the district's total area (739.683 km2). Overall, the district had a more severe drought between 1994 and 2022 (however the percentage and area of the district's wet areas occasionally decreased). Figure 16 below depicts the spatial pattern of the agricultural drought severity map for the years 1994–2004, 2004–2014, and 2014–2022, based on the NDVI deviation.

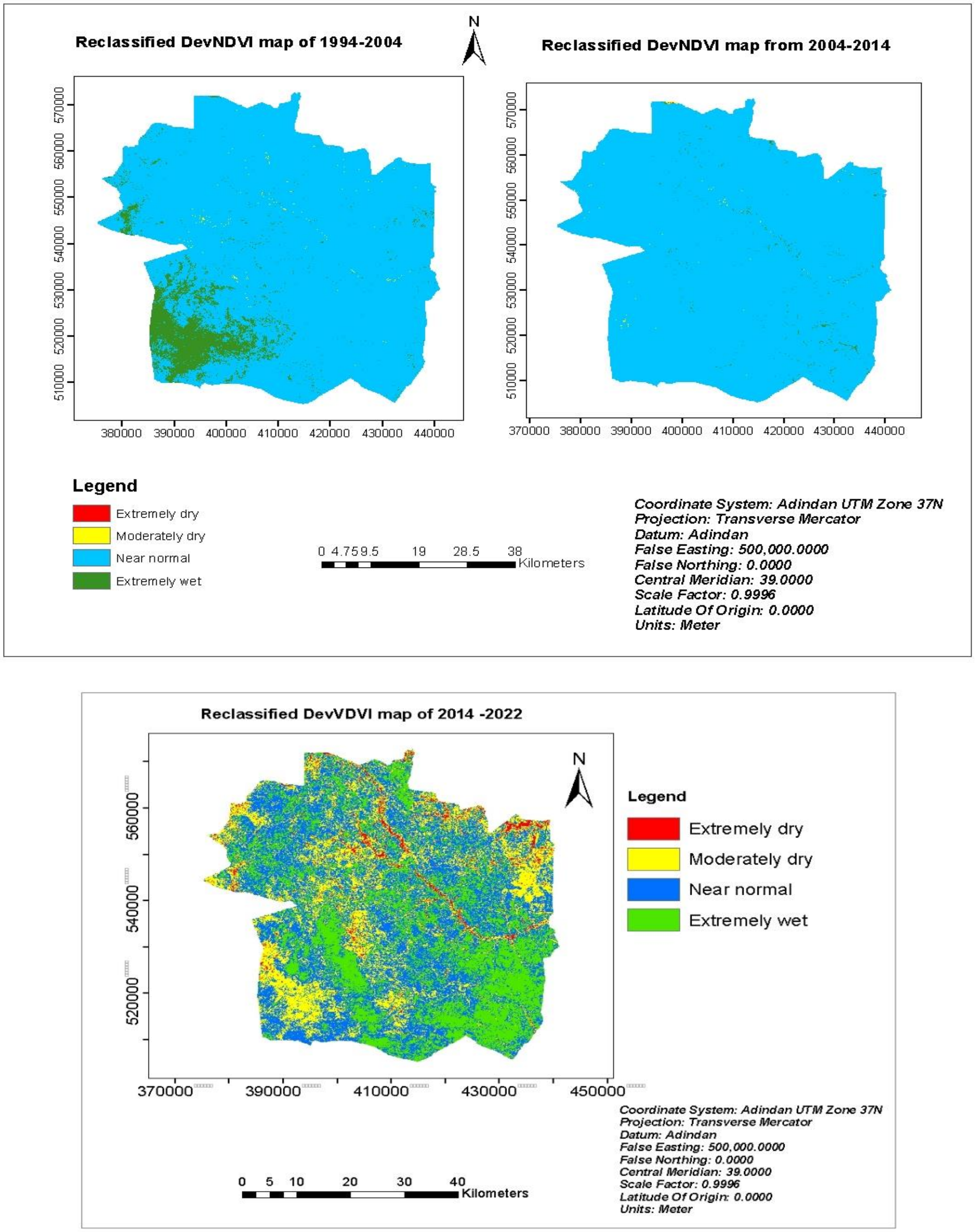

Figure 15: NDVI deviation based spatial pattern of agricultural drought severity map for the year 1994-2004, 2004 -2014 and 2014 -2022.

Table 23 DEVNDVI from1994 -2004

VALUE	COUNT	AREA	SEVERITY	%
1	10	7.924	extremely dry	0.025
2	5372	48.348	moderately dry	0.155
3	3168193	28513.74	near normal	91.423
4	290959	2618.631	Extremely wet	8.396
Total		31188.64		100

Table 24 drought severity area based on DEVNDVI from 2004 - 2014.

Value	Count	Severity	Area	%
1	180	extremely dry	9.454	0.030
2	2384	moderately dry	21.456	0.069
3	3443255	near normal	30989.3	99.361
4	18715	extremely wet	168.435	0.540
Total			31188.64	100

Table 25; drought severity area based on DEVNDVI from 2014 -2022.

VALUE	COUNT	SEVERITY	AREA	%
1	189	Extremely dry	9.535	0.031
2	82187	Moderately dry	739.683	2.372
3	3381997	Near normal	30437.97	97.593
4	161	extremely wet	1.449	0.005
Total			31188.64	100

4.3.3 VCI analysis results

Using VCI from Landsat images, the best performing remote sensing-based agricultural drought indicator from the appropriate sensor, the research area's agricultural drought situation was also monitored during the study period. The drought severity level has been classified as extreme, severe, moderate, no drought, and wet based on the VCI criterion. Figure 17 was used to display the spatial patterns of agricultural drought for the years 1994–2004, 2004–2014, and 2014–2022 years.

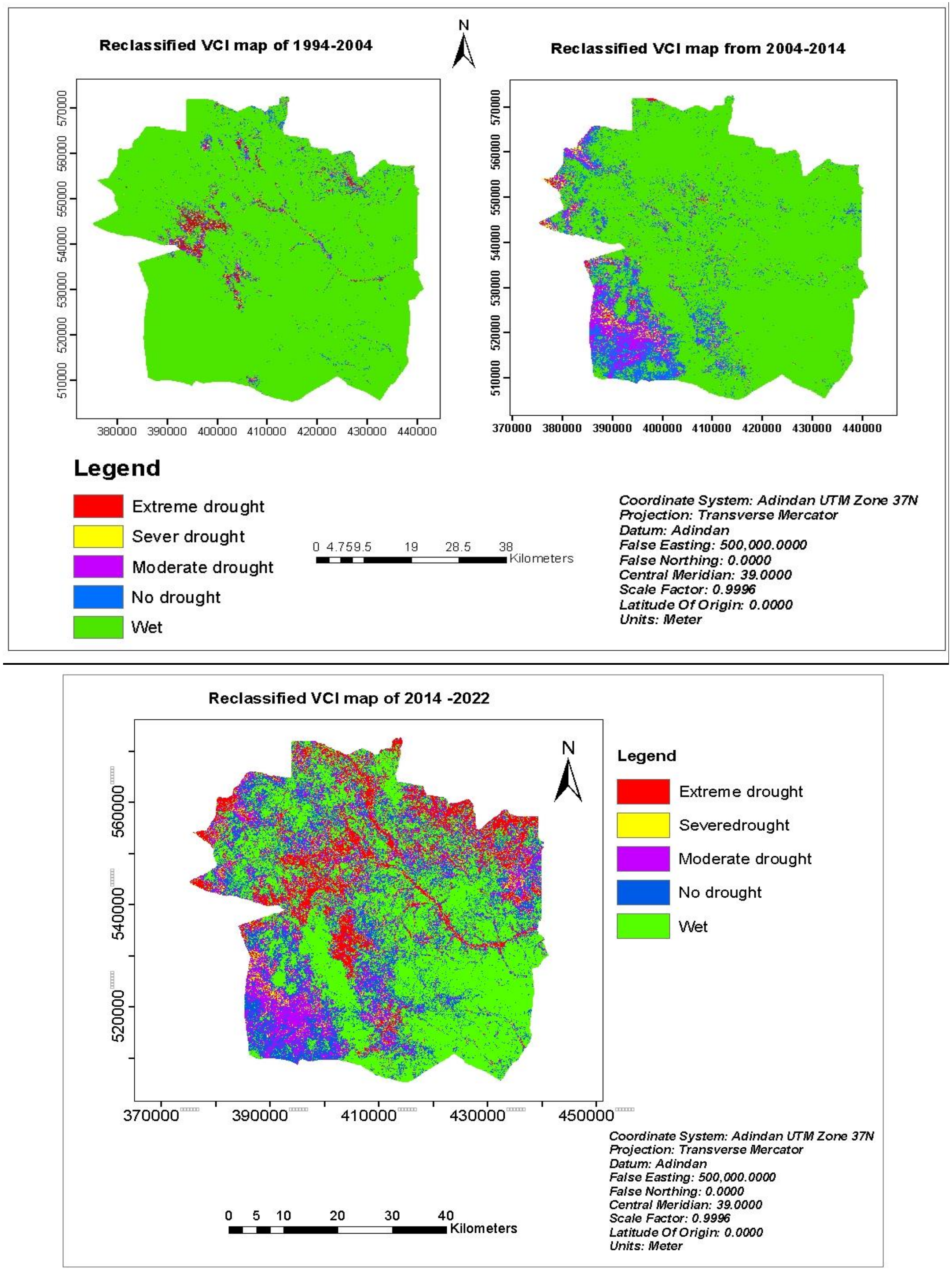

Figure 16: VCI based spatial pattern of agricultural drought severity maps for the year 1994-2004, 2004 -2014 and 2014 -2022.

In the year 1994 -2004, 2%, 94% percent of the study area was covered by extreme and wet severity condition of the drought respectively (figure 17 and table 26).

Table 26: drought severity area based on Vegetation Condition Index (VCI) from 1994 -2004

VALUE	COUNT	DROUGHT SEVERITY	AREA(Sq-km)	%.
<10%	54587	Extreme drought	491.283	2%
10%-20%	18579	Severe drought	167.211	1%
20%-35%	43146	Moderate drought	388.314	1%
35%-50%	81512	No drought	733.608	2%
>50%	3266710	Wet	29400.39	94%

Table 27: drought severity area based on Vegetation Condition Index (VCI) from 2004 -2014

VALUE	COUNT	DROUGHT SEVERITY	AREA(Sq-km)	.%
<10%	17089	Extreme drought	153.801	0.5%
10%-20%	41733	Severe drought	375.597	1%
20%-35%	189803	Moderate drought	1708.227	4.5%
35%-50%	323299	No drought	2909.691	9%
>50%	2892610	Wet	26033.49	83%

Table 28: drought severity area based on Vegetation Condition Index (VCI) from 2014 – 2022.

VALUE	COUNT	DROUGHT SEVERITY	AREA(sq.km)	%
<10%	382270	Extreme drought	3440.43	11%
10%-20%	171629	Severe drought	1544.66	5%
20%-35%	529950	Moderate drought	4769.55	15%
35%-50%	757277	No drought	6815.49	22%
>50%	1623408	Wet	14610.7	47%

In 2004 -2014, the area impacted by extreme agricultural drought decreased as compared to 1994 -2004 year and also the percent of wet area also decreased from94% to 83% (figure 17, table26 and table 27).

From the VCI classification of 2014 – 2022((Figure17 and table 28), around 11,5,15 and 22 percent of the research area showed extreme, severe, moderate and no drought conditions of study area respectively. this mean, drought hit the district more in this year than other years.

At here before obtaining drought risk map from above classifications of NDVI, DevNDVI and Classifications of VCI researcher tried to see the correlations between extracted values of DevNDVI and VCI with SPEI and precipitation values respectively using SPSS software. The values of NDVI, DevNDVI and VCI was obtained using ArcGIS in arc toolbox.

Table 29: correlation between VCI and Precipitation

Pearson Correlation		precipitation	vci_1994-2004	vci_2004-2014	vci_2014-2022
precipitation	Pearson Correlation	1	-.050	.008	.020
	Sig. (2-tailed)		.357	.888	.712
	N	348	348	348	348
vci_1994-2004	Pearson Correlation	-.050	1	-.583**	-.323**
	Sig. (2-tailed)	.357		.000	.000
	N	348	348	348	348
vci_2004-2014	Pearson Correlation	.008	-.583**	1	.807**
	Sig. (2-tailed)	.888	.000		.000
	N	348	348	348	348
vci_2014-2022	Pearson Correlation	.020	-.323**	.807**	1
	Sig. (2-tailed)	.712	.000	.000	
	N	348	348	348	348
**. Correlation is significant at the 0.01 level (2-tailed).					

Pearson Correlation between VCI and Precipitation in 1994 -2004, in 2004-2014, in 2014 -2022 have no strong and significant relationships (table 29)

Table: correlation between DevNDVI and SPEI

Correlations										
		DEV1994-2004	DEV2004-2014	DEV2014-2022	1-Month SPEI	2- month SPEI	3-MonthSPEI	6-Month SPEI	9-Month SPEI	12- Month SPEI
DEV1994-2004	Pearson Correlation	1	-.611**	-.438**	-.016	-.119*	-.099	-.012	-.038	-.047
	Sig. (2-tailed)		.000	.000	.770	.027	.066	.824	.478	.379
	N	348	348	348	348	348	348	348	348	348
DEV2004-2014	Pearson Correlation	-.611**	1	.643**	.038	.057	.058	.011	-.054	-.036
	Sig. (2-tailed)	.000		.000	.475	.291	.283	.843	.319	.505
	N	348	348	348	348	348	348	348	348	348
DEV2014-2022	Pearson Correlation	-.438**	.643**	1	.072	.067	.100	.076	.002	.002
	Sig. (2-tailed)	.000	.000		.179	.213	.062	.157	.964	.974
	N	348	348	348	348	348	348	348	348	348

**. Correlation is significant at the 0.01 level (2-tailed).

*. Correlation is significant at the 0.05 level (2-tailed).

From the table above, Dev NDVI and SPEI have negative and less correlation, but there was some significant correlation between DevNDVI of the different years.

4.4 Combined drought hazard map results

Overall drought hazard map of the yabello district produced from generated meteorological and agricultural drought severities maps. Meteorological drought maps (SPI and SPEI maps) generated at 2 and 12-month time scales and NDVI anomaly, DevNDVI, and VCI drought frequency maps were integrated to create the combined drought hazard map of the district (Figure 18), which provides an overview of the drought conditions from 1994 to 2022. A weighted overlay analysis was used to create the map.

Yabello District was categorized as having low, moderate, and high levels of drought based on the findings. According to the combined hazard map shown in Figure 18 and Table 30, the percentages of the Yabello District's total area impacted by low, moderate, and high drought are 30.46418% (9498.978km2), 66.48492% (20730.54km2), and 3.050904% (951.2966km2), respectively. The hazardous areas with low drought observed in western while high drought hazards were seen in the northern parts of the district.

The majority of this hazard map falls under the moderate hazard class (66.48492%), particularly, from north to east as well as from east to south parts of the district.

In general, drought affected nearly the whole study region between 1994 and 2022. As a result, local and governmental drought mitigation plans ought to be created to address this hazard. Figure 13 displays the Yabello District's overall drought hazard map from 1994 to 2022..

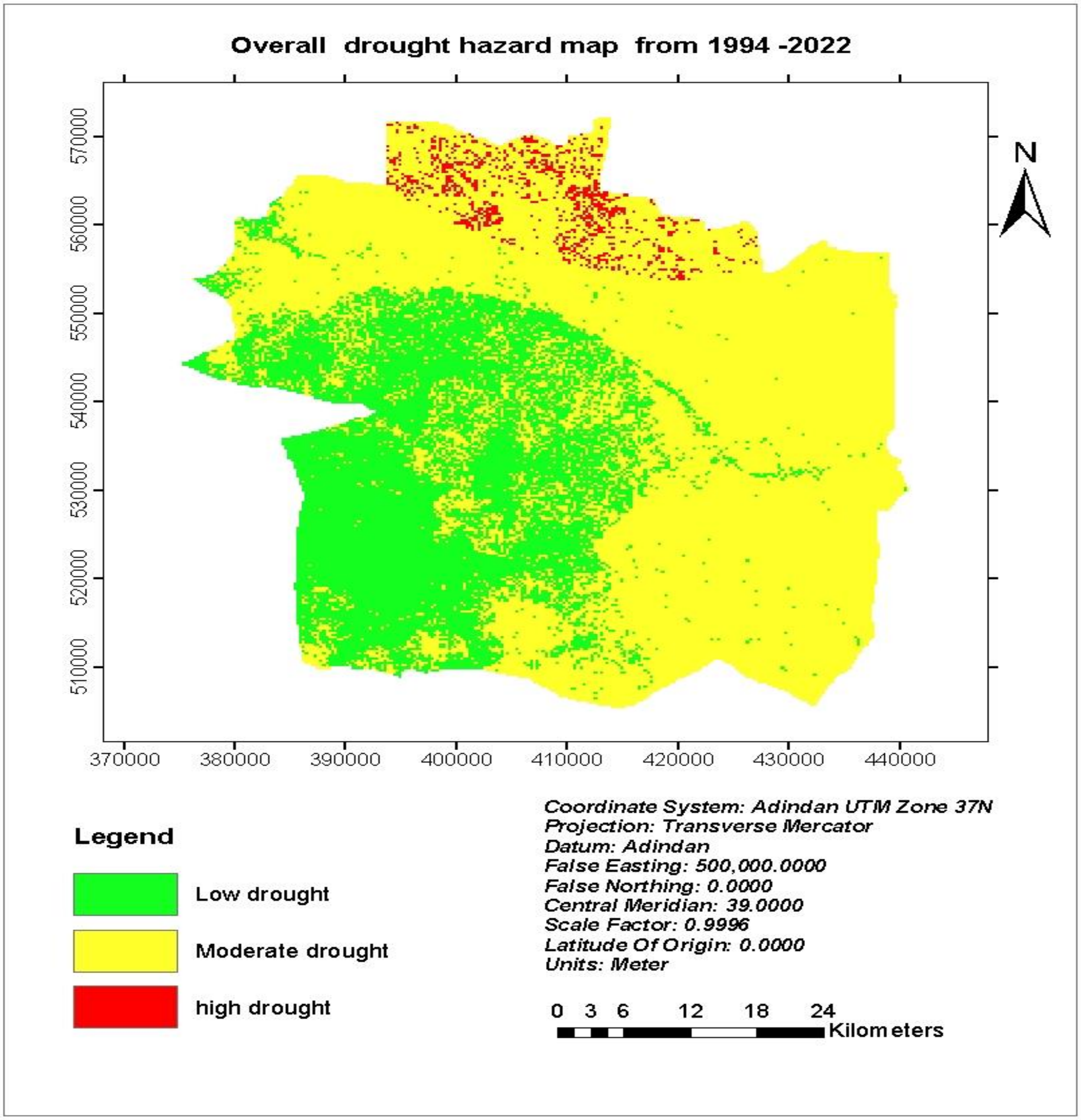

Figure 17: Overall drought hazards map

Table 30 : Overall drought hazard from 1994-2022

Value	Count	Severity Classes	Area	%
2	13679	Low drought	9498.978	30.46418
3	29853	Moderate drought	20730.54	66.48492
4	935	high drought	951.2966	3.050904
Total			31180.81	100

4.5 Discussion

The effectiveness of drought indices based on meteorological data and the availability of agricultural drought indices based on remote sensing make it possible to investigate drought in a particular area. It is essential to choose a suitable drought index for a certain area in order to support meteorological and agricultural drought monitoring. This study evaluated the meteorological, and agricultural drought in the study area using meteorological data and Landsat satellite imagery. Through the development of SPI and SPEI indices using total monthly precipitation, maximum and minimum temperature data, meteorological and agricultural drought were evaluated. Three Landsat images were utilized to evaluate agricultural drought conditions in the study district from 1994 to 2022. NDVI, DevNDVI, and VCI are employed to characterize agricultural droughts. SPI and SPEI were calculated at 1, 2, 3, 6, 9, and 12 time periods in order to examine the temporal features of the drought at the Yabello district station. In this district, drought is a common occurrence, and it frequently affects the study area.

The time scales drought indices that were examined in January, February, June, July, August, September, and December were recognized for their frequent occurrences of varying degrees of drought at the station. This result agreed with(Worku, 2024), who reported that the timescale (SPI/SPEI) showed the existence of a range of moderate to extreme drought events throughout the study area. In particular, Worku (2024) explained that, among other years in Borana, 1994, 1999, 2000, 2001, and 2011 were identified as severe to extreme drought years.

This study looked at the numerous occasions between 1994 and 2022 when the study area suffered by both agricultural and meteorological droughts. Abera et al. (2020) report that Ethiopia had drought between 2011 and 2016. Additionally, he clarified that the droughts that happened between 1999 and 2017 were more severe, more frequent, and stayed longer. This study so agreed to these showing more frequent drought occurred from 1994 to 2022 years. Also as indicated by Worku (2024), Worku (2024) also points out that Yimer et al. (2018) determined that the worst drought years in Ethiopia were 1999, 2003–2004, and 2007–2008. As a result, , Duba et al.(2021)also determined that the research area (Yabello District) experienced droughts in 1998, 2002, 2003, 2006, 2015, and 2016 based on consistent findings with this paper.

The degree of agreement and correlations between the used indices were examined using the Kappa statistics test and Pearson's correlation coefficient.

. The results of this study show that when SPI was related to SPEI, there was the greatest agreement (highest correlation coefficient values) and the highest degree of agreement. Low correlation coefficient values were also found between DevNDVI and SPEI, as well as between VCI and the precipitation values in the study area.

According to JV (2014), as indicated in Tefera et al.(2019), Even though some disagreements between SPI and SPEI were reported in some parts of Central Africa, the obtained Cohen's Kappa Statistics results between SPI and SPEI ranged for Fair level of agreement (0.2–0.6)achieved in the total study years. Their results were in agreement with drought comparison studies in the Horn of Africa in which this study also consistent to it. It implies, in this study research the Cohen’s Kappa Statistics result indicated a statistically fair to substantial ((0.2–0.8) degree of agreement between SPI and SPEI in all investigated time scales. Hence, the study result were in agreement to (Tefera et al., 2019). So, Standard precipitation index (SPI) and SPEI, which are obtained from meteorological data, and remote sensing indices like NDVI anomaly, DevNDVI, and vegetation condition index (VCI), which are produced from vegetation data for the study region, can be used to assess the state of drought.

.

.

CHAPTER FIVE: CONCLUSION AND RECOMMENDATIONS

5.1 Conclusions

According to the study, drought conditions can be assessed using the standard precipitation index (SPI) and SPEI generated from meteorological data, and remote sensing indices such as the vegetative condition index (VCI), the DevNDVI and NDVI anomaly derived from Remote sensing data. This study came to the conclusion that, depending on SPI/SPEI values, different drought classes were identified as severe (SPI/SPEI values between -1.5 and -1.99) and moderate (SPI/SPEI values between -1 and -1.49) droughts in different months or years at each estimated time scale. January, February, June, July, September, and December are the months and years when the majority of droughts occurs. Particularly, 1998, and 1999 years was absolutely continuous driest year among the others. The frequencies of droughts during the study period ranged from 1% (severe drought) to 13% (moderate drought), according on SPI time periods. At Yabello station, SPI-3 and SPI-12 were used to detect the majority of extreme drought episodes, with 43 occurrences each indicating a moderate drought class. The frequency of extreme, severe, and moderate drought varied from 1% to 11% at SPEI time scales, and the total number of drought events at the station varied from 5 to 38 months. According to SPEI-9 and SPEI-3, the number of drought events was 38 and 30, respectively. As a result, the Yabello District had varying frequencies and numbers of drought events, ranging from 1% to 13% and 2 to 43, respectively. Throughout the study period, there was a substantial correlation and greater level of agreement between the corresponding SPI and SPEI indices. Yet, during the study period, there were low relationships found between the agricultural and meteorological indices. DevNDVI, VCI, and the drought NDVI anomaly were utilized to characterize the spatial patterns. The majority of the research region was hit by a severe agricultural drought from 1994 to 2022, according to the results of the drought risk map.

The overall drought hazards map indicated that, of the entire Yabello district, 30.46418% (9498.978km2), 66.48492% (20730.54km2), and 3.050904% (951.2966km2) were affected by low, moderate, and extreme drought, respectively. This indicates that between 1994 and 2022, drought situation affected nearly the whole research region. Generally, these revealed that study area is frequently affected to agricultural and meteorological droughts.

5.2 Recommendations

The following recommendations for further research are made based on the findings of this study:

- Remote sensing based drought study is better than conventional based for assessment of spatial distribution of drought over an area.
- It would be beneficial for future research to investigate the potential of utilizing additional remote sensing-based drought indices, such as the Temperature Condition Index (TCI) in conjunction with the Vegetable Health Index (VHI), to measure agricultural and meteorological dryness and create a vegetation health index (VHI) that can be used as a drought indicator in a given area.
- In future study for Agricultural drought evaluations, other high spatial resolution images such as sentinel should be examined.
- Meteorological, Agricultural and hydrological droughts have to study spatially rather than temporarily for selected study area.
- Future research on the effects of drought on socioeconomic systems, adaptation, and mitigation techniques such as identifying drought-prone areas and mapping drought-affected areas, as well as involving local communities in preparation plans and responses is also recommended.

REFRENCE

A, K. R., & A, N. N. (2020). *Hydrometeorological Drought Hazard and Vulnerability Assessment for Northern Bulgaria*. *24*(2), 112–123. https://doi.org/10.5937/gp24-25074

Abara, M., Komariah, & Budiastuti, S. (2020). Drought Frequency, Severity, and Duration Monitoring Based on Climate Change in Southern and Southeastern Ethiopia. *IOP Conference Series: Earth and Environmental Science*, *477*(1). https://doi.org/10.1088/1755-1315/477/1/012011

Adler, J., & Parmryd, I. (2010). Quantifying colocalization by correlation: The pearson correlation coefficient is superior to the Mander's overlap coefficient. *Cytometry Part A*, *77*(8), 733–742. https://doi.org/10.1002/cyto.a.20896

Amin, M., Khan, M. R., Hassan, S. S., Khan, A. A., Imran, M., & Goheer, M. A. (2020). *No Title*. 203–216. https://doi.org/10.2166/wcc.2020.232

Aziz, A., Umar, M., Mansha, M., Khan, M. S., Javed, M. N., Gao, H., Farhan, S. Bin, Iqbal, I., & Abdullah, S. (2018). Assessment of drought conditions using HJ-1A/1B data: A case study of Potohar region, Pakistan. *Geomatics, Natural Hazards and Risk*, *9*(1), 1019–1036. https://doi.org/10.1080/19475705.2018.1499558

Birhanu Gedi.f, Legesse Hadish, Solomon Addisu, & Suryabhagavan, K. V. (2014). Drought Risk Assessment using Remote Sensing and GIS: The Case of Southern Zone, Tigray Region, Ethiopia. *Journal of Natural Sciences Research*, *4*(23), 87−94.

Danandeh Mehr, A., & Vaheddoost, B. (2020). Identification of the trends associated with the SPI and SPEI indices across Ankara, Turkey. *Theoretical and Applied Climatology*, *139*(3–4), 1531–1542. https://doi.org/10.1007/s00704-019-03071-9

Das, J. (2021). *Spatio-temporal characterization of rainfall in Bangladesh : an innovative trend and discrete wavelet transformation approaches*.

Dilawar, A., Chen, B., Arshad, A., Guo, L., Ehsan, M. I., Hussain, Y., Kayiranga, A., Measho, S., Zhang, H., Wang, F., Sun, X., & Ge, M. (2021). Towards understanding variability in droughts in response to extreme climate conditions over the different agro-ecological zones of Pakistan. *Sustainability (Switzerland)*, *13*(12). https://doi.org/10.3390/su13126910

Duba, G. W., Demissie, S. T., & Emiru, T. S. (2021). *Gelgelo Wako Duba, Solomon Tekalign Demissie, Tegegne Sishaw Emiru [1]*. *The Ethiop*(1).

Durowoju, O. S., Ologunorisa, T. E., & Akinbobola, A. (2022). Assessing agricultural and hydrological drought vulnerability in a savanna ecological zone of Sub-Saharan Africa. *Natural Hazards*, *111*(3), 2431–2458. https://doi.org/10.1007/s11069-021-05143-4

Faheem, Z., Hasan, J., Shaikh, S., Arshad, S., & Mohammed, S. (2024). Random forest-based analysis of land cover / land use LCLU dynamics associated with meteorological droughts in the desert ecosystem of Pakistan. *Ecological Indicators*, *159*(January), 111670. https://doi.org/10.1016/j.ecolind.2024.111670

Haile, B. T., Bekitie, K. T., Zeleke, T. T., Ayal, D. Y., Feyisa, G. L., & Anose, F. A. (2022). Drought Analysis Using Standardized Evapotranspiration and Aridity Index at Bilate Watershed: Sub-Basins of Ethiopian Rift Valley. *Scientific World Journal*, *2022*. https://doi.org/10.1155/2022/1181198

Hill, S., & Atnafu, S. (2011). *Using Satellite Images for Drought Monitoring : A Knowledge Discovery Approach Using Satellite Images for Drought Monitoring : A Knowledge Discovery Approach Getachew Berhan University of Pennsylvania Tsegaye Tadesse University of Nebraska-Lincoln*. *July*.

Iwata, T., Nishiyama, N., Nagano, K., Izumi, N., Tsukioka, T., Chung, K., Hanada, S., Inoue, K., Kaji, M., & Suehiro, S. (2012). Preoperative serum value of sialyl Lewis X predicts pathological nodal extension and survival in patients with surgically treated small cell lung cancer. *Journal of Surgical Oncology*, *105*(8), 818–824. https://doi.org/10.1002/jso.23002

J.A., C. (1960). A coefficient of agreement for nominal scales. *Educational And Psychological Measurement*, *XX*(1), 37–46.

Keith, L. (2017). *Environmental sampling and analysis: a practical guide*. Routledge.

Kim, H., Park, J., Yoo, J., & Kim, T. (2013). *ScienceDirect Assessment of drought hazard , vulnerability , and risk : A case study for administrative districts in South Korea*. 1–8.

Legesse, G., & Suryabhagavan, K. V. (2014). Remote sensing and GIS based agricultural drought assessment in East Shewa zone, Ethiopia. *Tropical Ecology*, *55*(3), 349–363.

Mera, G. A. (2018). Drought and its impacts in Ethiopia. *Weather and Climate Extremes*, *22*(September), 24–35. https://doi.org/10.1016/j.wace.2018.10.002

Montes-Vega, M. J., Guardiola-Albert, C., & Rodríguez-Rodríguez, M. (2023). Calculation of the SPI, SPEI, and GRDI Indices for Historical Climatic Data from Doñana National Park: Forecasting Climatic Series (2030–2059) Using Two Climatic Scenarios RCP 4.5 and RCP 8.5 by IPCC. *Water (Switzerland)*, *15*(13). https://doi.org/10.3390/w15132369

Negassa, W. (2017). Www.Shutturstock.Com. *Agricultural Drought Risk Area Assessment and Mapping Using Remote Sensing and Gis: A Case Study of West Hararge Zone, Ethiopia A*.

Qaisrani, Z. N., Nuthammachot, N., Techato, K., & Asadullah. (2021). Drought monitoring based on Standardized Precipitation Index and Standardized Precipitation Evapotranspiration Index in the arid zone of Balochistan province, Pakistan. *Arabian Journal of Geosciences*, *14*(1). https://doi.org/10.1007/s12517-020-06302-w

Queensland, S. (2021). *Drought Vulnerability Assessment Using Geospatial Techniques in Southern Queensland, Australia*. 13–15.

Saha, A., Pal, S. C., Chowdhuri, I., Roy, P., Chakrabortty, R., & Shit, M. (2022). *Gondwana Research*. *xxxx*, 1–17.

Shah, S., & Iqbal, J. (2023). *Spatial – temporal variations of vegetation and drought severity across Tharparkar , Pakistan , using remote sensing-derived indices Sami Ullah Shah*. *August*. https://doi.org/10.1117/1.JRS.10.036005.

Svoboda, M., Hayes, M., & Wood, D. (2012). Spi Index for Diferent Locations. *World Meteorological Organization*, *1090*. https://digitalcommons.unl.edu/droughtfacpub

Tareke, K. A., & Awoke, A. G. (2022). Hydrological Drought Analysis using Streamflow Drought Index (SDI) in Ethiopia. *Advances in Meteorology*, *2022*. https://doi.org/10.1155/2022/7067951

Tefera, A. S., Ayoade, J. O., & Bello, N. J. (2019). Comparative analyses of SPI and SPEI as drought assessment tools in Tigray Region, Northern Ethiopia. *SN Applied Sciences*, *1*(10), 1–14. https://doi.org/10.1007/s42452-019-1326-2

Todisco, L. V. F., & Lena, B. Di. (2021). Evaluation of the similarity between drought indices by correlation analysis and Cohen ' s Kappa test in a Mediterranean area. *Natural Hazards*, *108*(2), 2187–2209. https://doi.org/10.1007/s11069-021-04775-w

Uttaruk, Y., & Laosuwan, T. (2017). *DROUGHT DETECTION BY APPLICATION OF REMOTE SENSING*. *18*(6), 115–121. https://doi.org/10.12911/22998993/76326

Viera, A. J., & Garrett, J. M. (2005). Anthony J. Viera, MD; Joanne M. Garrett, PhD (2005). Understanding interobserver agreement: the kappa statistic. Fam Med 2005;37(5):360-63. *Family Medicine*, *37*(5), 360–363. http://www1.cs.columbia.edu/~julia/courses/CS6998/Interrater_agreement.Kappa_statistic.pdf

Vries, D. (2010). *IVM Institute for Environmental Studies*.

Wako Duba, G., Tekalign, S., & Sishaw, T. (2021). Determinants Choices of Drought Coping Strategies Among Boorana Pastoral Communities: The Case of Yabello Woreda, Oromiya Region, Southern Ethiopia. *American Journal of Life Sciences*, *9*(4), 73. https://doi.org/10.11648/j.ajls.20210904.13

Wangwongchai, A., Waqas, M., Dechpichai, P., Hlaing, P. T., Ahmad, S., & Humphries, U. W. (2023). Imputation of missing daily rainfall data; A comparison between artificial intelligence and statistical techniques. *MethodsX*, *11*(September), 102459. https://doi.org/10.1016/j.mex.2023.102459

Wilhite, D. A. (2000). *Drought Preparedness and Response in the Context of Sub-Saharan Africa*.

Wondimu, M. A., Erena, S. H., Reddy, R. U., Gebreselassie, T. A., Rao, P. P. J., Abraha, M. E., Rohland, E., García-Acosta, V., Government India, Imagery, S. R. G. B., Legesse, G., Suryabhagavan, K. V., Tamiru, H., Wagari, M., Abebe, W. T., Endalie, D., Muñoz, P., Orellana-Alvear, J., Bendix, J., … Segele, Z. T. (2022). Evaluation of the Performance of Remote Sensing-based Drought Indices for Agricultural Drought Characterization: The case of Tigray Region, Northern Ethiopia By. *Natural Hazards and Earth System Sciences*, *10*(3), 446–473. http://dx.doi.org/10.1016/j.procs.2016.09.319%0Ahttps://www.elsevier.com/books/drought-early-warning-and-forecasting/funk/978-0-12-814011-

6%0Ahttp://dx.doi.org/10.22192/ijamr.2018.05.06.006%0Ahttps://doi.org/10.1186/s40537-022-00683-3%0Ahttps://doi.org/10

Worku, M. A. (2024). Spatiotemporal analysis of drought severity using SPI and SPEI: case study of semi-arid Borana area, southern Ethiopia. *Frontiers in Environmental Science*, *12*(March), 1–15. https://doi.org/10.3389/fenvs.2024.1337190

Yuan, S., Quiring, S. M., & Patil, S. (2016). *SPATIAL AND TEMPORAL VARIATIONS IN THE ACCURACY*. *42*(1), 167–183. https://doi.org/10.18172/cig.2916

A, K. R., & A, N. N. (2020). *Hydrometeorological Drought Hazard and Vulnerability Assessment for Northern Bulgaria*. *24*(2), 112–123. https://doi.org/10.5937/gp24-25074

Abara, M., Komariah, & Budiastuti, S. (2020). Drought Frequency, Severity, and Duration Monitoring Based on Climate Change in Southern and Southeastern Ethiopia. *IOP Conference Series: Earth and Environmental Science*, *477*(1). https://doi.org/10.1088/1755-1315/477/1/012011

Adler, J., & Parmryd, I. (2010). Quantifying colocalization by correlation: The pearson correlation coefficient is superior to the Mander's overlap coefficient. *Cytometry Part A*, *77*(8), 733–742. https://doi.org/10.1002/cyto.a.20896

Amin, M., Khan, M. R., Hassan, S. S., Khan, A. A., Imran, M., & Goheer, M. A. (2020). *No Title*. 203–216. https://doi.org/10.2166/wcc.2020.232

Aziz, A., Umar, M., Mansha, M., Khan, M. S., Javed, M. N., Gao, H., Farhan, S. Bin, Iqbal, I., & Abdullah, S. (2018). Assessment of drought conditions using HJ-1A/1B data: A case study of Potohar region, Pakistan. *Geomatics, Natural Hazards and Risk*, *9*(1), 1019–1036. https://doi.org/10.1080/19475705.2018.1499558

Birhanu Gedi.f, Legesse Hadish, Solomon Addisu, & Suryabhagavan, K. V. (2014). Drought Risk Assessment using Remote Sensing and GIS: The Case of Southern Zone, Tigray Region, Ethiopia. *Journal of Natural Sciences Research*, *4*(23), 87−94.

Danandeh Mehr, A., & Vaheddoost, B. (2020). Identification of the trends associated with the SPI and SPEI indices across Ankara, Turkey. *Theoretical and Applied Climatology*, *139*(3–

4), 1531–1542. https://doi.org/10.1007/s00704-019-03071-9

Das, J. (2021). *Spatio-temporal characterization of rainfall in Bangladesh : an innovative trend and discrete wavelet transformation approaches*.

Dilawar, A., Chen, B., Arshad, A., Guo, L., Ehsan, M. I., Hussain, Y., Kayiranga, A., Measho, S., Zhang, H., Wang, F., Sun, X., & Ge, M. (2021). Towards understanding variability in droughts in response to extreme climate conditions over the different agro-ecological zones of Pakistan. *Sustainability (Switzerland)*, *13*(12). https://doi.org/10.3390/su13126910

Duba, G. W., Demissie, S. T., & Emiru, T. S. (2021). *Gelgelo Wako Duba, Solomon Tekalign Demissie, Tegegne Sishaw Emiru [1]*. *The Ethiop*(1).

Durowoju, O. S., Ologunorisa, T. E., & Akinbobola, A. (2022). Assessing agricultural and hydrological drought vulnerability in a savanna ecological zone of Sub-Saharan Africa. *Natural Hazards*, *111*(3), 2431–2458. https://doi.org/10.1007/s11069-021-05143-4

Faheem, Z., Hasan, J., Shaikh, S., Arshad, S., & Mohammed, S. (2024). Random forest-based analysis of land cover / land use LCLU dynamics associated with meteorological droughts in the desert ecosystem of Pakistan. *Ecological Indicators*, *159*(January), 111670. https://doi.org/10.1016/j.ecolind.2024.111670

Haile, B. T., Bekitie, K. T., Zeleke, T. T., Ayal, D. Y., Feyisa, G. L., & Anose, F. A. (2022). Drought Analysis Using Standardized Evapotranspiration and Aridity Index at Bilate Watershed: Sub-Basins of Ethiopian Rift Valley. *Scientific World Journal*, *2022*. https://doi.org/10.1155/2022/1181198

Hill, S., & Atnafu, S. (2011). *Using Satellite Images for Drought Monitoring : A Knowledge Discovery Approach Using Satellite Images for Drought Monitoring : A Knowledge Discovery Approach Getachew Berhan University of Pennsylvania Tsegaye Tadesse University of Nebraska-Lincoln*. *July*.

Iwata, T., Nishiyama, N., Nagano, K., Izumi, N., Tsukioka, T., Chung, K., Hanada, S., Inoue, K., Kaji, M., & Suehiro, S. (2012). Preoperative serum value of sialyl Lewis X predicts pathological nodal extension and survival in patients with surgically treated small cell lung cancer. *Journal of Surgical Oncology*, *105*(8), 818–824. https://doi.org/10.1002/jso.23002

J.A., C. (1960). A coefficient of agreement for nominal scales. *Educational And Psychological*

Measurement, *XX*(1), 37–46.

Keith, L. (2017). *Environmental sampling and analysis: a practical guide*. Routledge.

Kim, H., Park, J., Yoo, J., & Kim, T. (2013). *ScienceDirect Assessment of drought hazard , vulnerability , and risk : A case study for administrative districts in South Korea*. 1–8.

Legesse, G., & Suryabhagavan, K. V. (2014). Remote sensing and GIS based agricultural drought assessment in East Shewa zone, Ethiopia. *Tropical Ecology*, *55*(3), 349–363.

Mera, G. A. (2018). Drought and its impacts in Ethiopia. *Weather and Climate Extremes*, *22*(September), 24–35. https://doi.org/10.1016/j.wace.2018.10.002

Montes-Vega, M. J., Guardiola-Albert, C., & Rodríguez-Rodríguez, M. (2023). Calculation of the SPI, SPEI, and GRDI Indices for Historical Climatic Data from Doñana National Park: Forecasting Climatic Series (2030–2059) Using Two Climatic Scenarios RCP 4.5 and RCP 8.5 by IPCC. *Water (Switzerland)*, *15*(13). https://doi.org/10.3390/w15132369

Negassa, W. (2017). Www.Shutturstock.Com. *Agricultural Drought Risk Area Assessment and Mapping Using Remote Sensing and Gis: A Case Study of West Hararge Zone, Ethiopia A.*

Qaisrani, Z. N., Nuthammachot, N., Techato, K., & Asadullah. (2021). Drought monitoring based on Standardized Precipitation Index and Standardized Precipitation Evapotranspiration Index in the arid zone of Balochistan province, Pakistan. *Arabian Journal of Geosciences*, *14*(1). https://doi.org/10.1007/s12517-020-06302-w

Queensland, S. (2021). *Drought Vulnerability Assessment Using Geospatial Techniques in Southern Queensland, Australia*. 13–15.

Saha, A., Pal, S. C., Chowdhuri, I., Roy, P., Chakrabortty, R., & Shit, M. (2022). *Gondwana Research*. *xxxx*, 1–17.

Shah, S., & Iqbal, J. (2023). *Spatial – temporal variations of vegetation and drought severity across Tharparkar , Pakistan , using remote sensing-derived indices Sami Ullah Shah*. *August*. https://doi.org/10.1117/1.JRS.10.036005.

Svoboda, M., Hayes, M., & Wood, D. (2012). Spi Index for Diferent Locations. *World Meteorological Organization*, *1090*. https://digitalcommons.unl.edu/droughtfacpub

Tareke, K. A., & Awoke, A. G. (2022). Hydrological Drought Analysis using Streamflow

Drought Index (SDI) in Ethiopia. *Advances in Meteorology*, *2022*. https://doi.org/10.1155/2022/7067951

Tefera, A. S., Ayoade, J. O., & Bello, N. J. (2019). Comparative analyses of SPI and SPEI as drought assessment tools in Tigray Region, Northern Ethiopia. *SN Applied Sciences*, *1*(10), 1–14. https://doi.org/10.1007/s42452-019-1326-2

Todisco, L. V. F., & Lena, B. Di. (2021). Evaluation of the similarity between drought indices by correlation analysis and Cohen ' s Kappa test in a Mediterranean area. *Natural Hazards*, *108*(2), 2187–2209. https://doi.org/10.1007/s11069-021-04775-w

Uttaruk, Y., & Laosuwan, T. (2017). *DROUGHT DETECTION BY APPLICATION OF REMOTE SENSING*. *18*(6), 115–121. https://doi.org/10.12911/22998993/76326

Viera, A. J., & Garrett, J. M. (2005). Anthony J. Viera, MD; Joanne M. Garrett, PhD (2005). Understanding interobserver agreement: the kappa statistic. Fam Med 2005;37(5):360-63. *Family Medicine*, *37*(5), 360–363. http://www1.cs.columbia.edu/~julia/courses/CS6998/Interrater_agreement.Kappa_statistic.pdf

Vries, D. (2010). *IVM Institute for Environmental Studies*.

Wako Duba, G., Tekalign, S., & Sishaw, T. (2021). Determinants Choices of Drought Coping Strategies Among Boorana Pastoral Communities: The Case of Yabello Woreda, Oromiya Region, Southern Ethiopia. *American Journal of Life Sciences*, *9*(4), 73. https://doi.org/10.11648/j.ajls.20210904.13

Wangwongchai, A., Waqas, M., Dechpichai, P., Hlaing, P. T., Ahmad, S., & Humphries, U. W. (2023). Imputation of missing daily rainfall data; A comparison between artificial intelligence and statistical techniques. *MethodsX*, *11*(September), 102459. https://doi.org/10.1016/j.mex.2023.102459

Wilhite, D. A. (2000). *Drought Preparedness and Response in the Context of Sub-Saharan Africa*.

Wondimu, M. A., Erena, S. H., Reddy, R. U., Gebreselassie, T. A., Rao, P. P. J., Abraha, M. E., Rohland, E., García-Acosta, V., Government India, Imagery, S. R. G. B., Legesse, G., Suryabhagavan, K. V., Tamiru, H., Wagari, M., Abebe, W. T., Endalie, D., Muñoz, P., Orellana-Alvear, J., Bendix, J., … Segele, Z. T. (2022). Evaluation of the Performance of Remote Sensing-based Drought Indices for Agricultural Drought Characterization: The case of Tigray Region, Northern Ethiopia By. *Natural Hazards and Earth System Sciences*, *10*(3), 446–473. http://dx.doi.org/10.1016/j.procs.2016.09.319%0Ahttps://www.elsevier.com/books/drought-early-warning-and-forecasting/funk/978-0-12-814011-6%0Ahttp://dx.doi.org/10.22192/ijamr.2018.05.06.006%0Ahttps://doi.org/10.1186/s40537-022-00683-3%0Ahttps://doi.org/10

Worku, M. A. (2024). Spatiotemporal analysis of drought severity using SPI and SPEI: case study of semi-arid Borana area, southern Ethiopia. *Frontiers in Environmental Science*, *12*(March), 1–15. https://doi.org/10.3389/fenvs.2024.1337190

Yuan, S., Quiring, S. M., & Patil, S. (2016). *SPATIAL AND TEMPORAL VARIATIONS IN THE ACCURACY*. *42*(1), 167–183. https://doi.org/10.18172/cig.2916

A, K. R., & A, N. N. (2020). *Hydrometeorological Drought Hazard and Vulnerability Assessment for Northern Bulgaria*. *24*(2), 112–123. https://doi.org/10.5937/gp24-25074

Abara, M., Komariah, & Budiastuti, S. (2020). Drought Frequency, Severity, and Duration Monitoring Based on Climate Change in Southern and Southeastern Ethiopia. *IOP Conference Series: Earth and Environmental Science*, *477*(1). https://doi.org/10.1088/1755-1315/477/1/012011

Adler, J., & Parmryd, I. (2010). Quantifying colocalization by correlation: The pearson correlation coefficient is superior to the Mander's overlap coefficient. *Cytometry Part A*, *77*(8), 733–742. https://doi.org/10.1002/cyto.a.20896

Amin, M., Khan, M. R., Hassan, S. S., Khan, A. A., Imran, M., & Goheer, M. A. (2020). *No Title*. 203–216. https://doi.org/10.2166/wcc.2020.232

Aziz, A., Umar, M., Mansha, M., Khan, M. S., Javed, M. N., Gao, H., Farhan, S. Bin, Iqbal, I., & Abdullah, S. (2018). Assessment of drought conditions using HJ-1A/1B data: A case study of Potohar region, Pakistan. *Geomatics, Natural Hazards and Risk*, *9*(1), 1019–1036. https://doi.org/10.1080/19475705.2018.1499558

Birhanu Gedi.f, Legesse Hadish, Solomon Addisu, & Suryabhagavan, K. V. (2014). Drought Risk Assessment using Remote Sensing and GIS: The Case of Southern Zone, Tigray Region, Ethiopia. *Journal of Natural Sciences Research*, *4*(23), 87−94.

Danandeh Mehr, A., & Vaheddoost, B. (2020). Identification of the trends associated with the SPI and SPEI indices across Ankara, Turkey. *Theoretical and Applied Climatology*, *139*(3–4), 1531–1542. https://doi.org/10.1007/s00704-019-03071-9

Das, J. (2021). *Spatio-temporal characterization of rainfall in Bangladesh : an innovative trend and discrete wavelet transformation approaches*.

Dilawar, A., Chen, B., Arshad, A., Guo, L., Ehsan, M. I., Hussain, Y., Kayiranga, A., Measho, S., Zhang, H., Wang, F., Sun, X., & Ge, M. (2021). Towards understanding variability in droughts in response to extreme climate conditions over the different agro-ecological zones of Pakistan. *Sustainability (Switzerland)*, *13*(12). https://doi.org/10.3390/su13126910

Duba, G. W., Demissie, S. T., & Emiru, T. S. (2021). *Gelgelo Wako Duba, Solomon Tekalign Demissie, Tegegne Sishaw Emiru [1]*. *The Ethiop*(1).

Durowoju, O. S., Ologunorisa, T. E., & Akinbobola, A. (2022). Assessing agricultural and hydrological drought vulnerability in a savanna ecological zone of Sub-Saharan Africa. *Natural Hazards*, *111*(3), 2431–2458. https://doi.org/10.1007/s11069-021-05143-4

Faheem, Z., Hasan, J., Shaikh, S., Arshad, S., & Mohammed, S. (2024). Random forest-based analysis of land cover / land use LCLU dynamics associated with meteorological droughts in the desert ecosystem of Pakistan. *Ecological Indicators*, *159*(January), 111670. https://doi.org/10.1016/j.ecolind.2024.111670

Haile, B. T., Bekitie, K. T., Zeleke, T. T., Ayal, D. Y., Feyisa, G. L., & Anose, F. A. (2022). Drought Analysis Using Standardized Evapotranspiration and Aridity Index at Bilate Watershed: Sub-Basins of Ethiopian Rift Valley. *Scientific World Journal*, *2022*. https://doi.org/10.1155/2022/1181198

Hill, S., & Atnafu, S. (2011). *Using Satellite Images for Drought Monitoring : A Knowledge Discovery Approach Using Satellite Images for Drought Monitoring : A Knowledge Discovery Approach Getachew Berhan University of Pennsylvania Tsegaye Tadesse University of Nebraska-Lincoln*. *July*.

Iwata, T., Nishiyama, N., Nagano, K., Izumi, N., Tsukioka, T., Chung, K., Hanada, S., Inoue, K., Kaji, M., & Suehiro, S. (2012). Preoperative serum value of sialyl Lewis X predicts pathological nodal extension and survival in patients with surgically treated small cell lung cancer. *Journal of Surgical Oncology*, *105*(8), 818–824. https://doi.org/10.1002/jso.23002

J.A., C. (1960). A coefficient of agreement for nominal scales. *Educational And Psychological Measurement*, *XX*(1), 37–46.

Keith, L. (2017). *Environmental sampling and analysis: a practical guide*. Routledge.

Kim, H., Park, J., Yoo, J., & Kim, T. (2013). *ScienceDirect Assessment of drought hazard , vulnerability , and risk : A case study for administrative districts in South Korea*. 1–8.

Legesse, G., & Suryabhagavan, K. V. (2014). Remote sensing and GIS based agricultural drought assessment in East Shewa zone, Ethiopia. *Tropical Ecology*, *55*(3), 349–363.

Mera, G. A. (2018). Drought and its impacts in Ethiopia. *Weather and Climate Extremes*, *22*(September), 24–35. https://doi.org/10.1016/j.wace.2018.10.002

Montes-Vega, M. J., Guardiola-Albert, C., & Rodríguez-Rodríguez, M. (2023). Calculation of the SPI, SPEI, and GRDI Indices for Historical Climatic Data from Doñana National Park: Forecasting Climatic Series (2030–2059) Using Two Climatic Scenarios RCP 4.5 and RCP 8.5 by IPCC. *Water (Switzerland)*, *15*(13). https://doi.org/10.3390/w15132369

Negassa, W. (2017). Www.Shutturstock.Com. *Agricultural Drought Risk Area Assessment and Mapping Using Remote Sensing and Gis: A Case Study of West Hararge Zone, Ethiopia A*.

Qaisrani, Z. N., Nuthammachot, N., Techato, K., & Asadullah. (2021). Drought monitoring based on Standardized Precipitation Index and Standardized Precipitation Evapotranspiration Index in the arid zone of Balochistan province, Pakistan. *Arabian Journal of Geosciences*, *14*(1). https://doi.org/10.1007/s12517-020-06302-w

Queensland, S. (2021). *Drought Vulnerability Assessment Using Geospatial Techniques in Southern Queensland, Australia*. 13–15.

Saha, A., Pal, S. C., Chowdhuri, I., Roy, P., Chakrabortty, R., & Shit, M. (2022). *Gondwana Research*. *xxxx*, 1–17.

Shah, S., & Iqbal, J. (2023). *Spatial – temporal variations of vegetation and drought severity* *across Tharparkar , Pakistan , using remote sensing-derived indices Sami Ullah Shah*. *August*. https://doi.org/10.1117/1.JRS.10.036005.

Svoboda, M., Hayes, M., & Wood, D. (2012). Spi Index for Diferent Locations. *World Meteorological Organization*, *1090*. https://digitalcommons.unl.edu/droughtfacpub

Tareke, K. A., & Awoke, A. G. (2022). Hydrological Drought Analysis using Streamflow Drought Index (SDI) in Ethiopia. *Advances in Meteorology*, *2022*. https://doi.org/10.1155/2022/7067951

Tefera, A. S., Ayoade, J. O., & Bello, N. J. (2019). Comparative analyses of SPI and SPEI as drought assessment tools in Tigray Region, Northern Ethiopia. *SN Applied Sciences*, *1*(10), 1–14. https://doi.org/10.1007/s42452-019-1326-2

Todisco, L. V. F., & Lena, B. Di. (2021). Evaluation of the similarity between drought indices by correlation analysis and Cohen ' s Kappa test in a Mediterranean area. *Natural Hazards*, *108*(2), 2187–2209. https://doi.org/10.1007/s11069-021-04775-w

Uttaruk, Y., & Laosuwan, T. (2017). *DROUGHT DETECTION BY APPLICATION OF REMOTE SENSING*. *18*(6), 115–121. https://doi.org/10.12911/22998993/76326

Viera, A. J., & Garrett, J. M. (2005). Anthony J. Viera, MD; Joanne M. Garrett, PhD (2005). Understanding interobserver agreement: the kappa statistic. Fam Med 2005;37(5):360-63. *Family Medicine*, *37*(5), 360–363. http://www1.cs.columbia.edu/~julia/courses/CS6998/Interrater_agreement.Kappa_statistic.pdf

Vries, D. (2010). *IVM Institute for Environmental Studies*.

Wako Duba, G., Tekalign, S., & Sishaw, T. (2021). Determinants Choices of Drought Coping Strategies Among Boorana Pastoral Communities: The Case of Yabello Woreda, Oromiya Region, Southern Ethiopia. *American Journal of Life Sciences*, *9*(4), 73. https://doi.org/10.11648/j.ajls.20210904.13

Wangwongchai, A., Waqas, M., Dechpichai, P., Hlaing, P. T., Ahmad, S., & Humphries, U. W. (2023). Imputation of missing daily rainfall data; A comparison between artificial intelligence and statistical techniques. *MethodsX*, *11*(September), 102459. https://doi.org/10.1016/j.mex.2023.102459

Wilhite, D. A. (2000). *Drought Preparedness and Response in the Context of Sub-Saharan Africa*.

Wondimu, M. A., Erena, S. H., Reddy, R. U., Gebreselassie, T. A., Rao, P. P. J., Abraha, M. E., Rohland, E., García-Acosta, V., Government India, Imagery, S. R. G. B., Legesse, G., Suryabhagavan, K. V., Tamiru, H., Wagari, M., Abebe, W. T., Endalie, D., Muñoz, P., Orellana-Alvear, J., Bendix, J., … Segele, Z. T. (2022). Evaluation of the Performance of Remote Sensing-based Drought Indices for Agricultural Drought Characterization: The case of Tigray Region, Northern Ethiopia By. *Natural Hazards and Earth System Sciences*, *10*(3), 446–473. http://dx.doi.org/10.1016/j.procs.2016.09.319%0Ahttps://www.elsevier.com/books/drought-early-warning-and-forecasting/funk/978-0-12-814011-6%0Ahttp://dx.doi.org/10.22192/ijamr.2018.05.06.006%0Ahttps://doi.org/10.1186/s40537-022-00683-3%0Ahttps://doi.org/10

Worku, M. A. (2024). Spatiotemporal analysis of drought severity using SPI and SPEI: case study of semi-arid Borana area, southern Ethiopia. *Frontiers in Environmental Science*, *12*(March), 1–15. https://doi.org/10.3389/fenvs.2024.1337190

Yuan, S., Quiring, S. M., & Patil, S. (2016). *SPATIAL AND TEMPORAL VARIATIONS IN THE ACCURACY*. *42*(1), 167–183. https://doi.org/10.18172/cig.2916

A, K. R., & A, N. N. (2020). *Hydrometeorological Drought Hazard and Vulnerability Assessment for Northern Bulgaria*. *24*(2), 112–123. https://doi.org/10.5937/gp24-25074

Abara, M., Komariah, & Budiastuti, S. (2020). Drought Frequency, Severity, and Duration Monitoring Based on Climate Change in Southern and Southeastern Ethiopia. *IOP Conference Series: Earth and Environmental Science*, *477*(1). https://doi.org/10.1088/1755-1315/477/1/012011

Adler, J., & Parmryd, I. (2010). Quantifying colocalization by correlation: The pearson correlation coefficient is superior to the Mander's overlap coefficient. *Cytometry Part A*, *77*(8), 733–742. https://doi.org/10.1002/cyto.a.20896

Amin, M., Khan, M. R., Hassan, S. S., Khan, A. A., Imran, M., & Goheer, M. A. (2020). *No Title*. 203–216. https://doi.org/10.2166/wcc.2020.232

Aziz, A., Umar, M., Mansha, M., Khan, M. S., Javed, M. N., Gao, H., Farhan, S. Bin, Iqbal, I., & Abdullah, S. (2018). Assessment of drought conditions using HJ-1A/1B data: A case study of Potohar region, Pakistan. *Geomatics, Natural Hazards and Risk, 9*(1), 1019–1036. https://doi.org/10.1080/19475705.2018.1499558

Birhanu Gedi.f, Legesse Hadish, Solomon Addisu, & Suryabhagavan, K. V. (2014). Drought Risk Assessment using Remote Sensing and GIS: The Case of Southern Zone, Tigray Region, Ethiopia. *Journal of Natural Sciences Research*, *4*(23), 87−94.

Danandeh Mehr, A., & Vaheddoost, B. (2020). Identification of the trends associated with the SPI and SPEI indices across Ankara, Turkey. *Theoretical and Applied Climatology*, *139*(3–4), 1531–1542. https://doi.org/10.1007/s00704-019-03071-9

Das, J. (2021). *Spatio-temporal characterization of rainfall in Bangladesh : an innovative trend and discrete wavelet transformation approaches*.

Dilawar, A., Chen, B., Arshad, A., Guo, L., Ehsan, M. I., Hussain, Y., Kayiranga, A., Measho, S., Zhang, H., Wang, F., Sun, X., & Ge, M. (2021). Towards understanding variability in droughts in response to extreme climate conditions over the different agro-ecological zones of Pakistan. *Sustainability (Switzerland)*, *13*(12). https://doi.org/10.3390/su13126910

Duba, G. W., Demissie, S. T., & Emiru, T. S. (2021). *Gelgelo Wako Duba, Solomon Tekalign Demissie, Tegegne Sishaw Emiru [1]*. *The Ethiop*(1).

Durowoju, O. S., Ologunorisa, T. E., & Akinbobola, A. (2022). Assessing agricultural and hydrological drought vulnerability in a savanna ecological zone of Sub-Saharan Africa. *Natural Hazards*, *111*(3), 2431–2458. https://doi.org/10.1007/s11069-021-05143-4

Faheem, Z., Hasan, J., Shaikh, S., Arshad, S., & Mohammed, S. (2024). Random forest-based analysis of land cover / land use LCLU dynamics associated with meteorological droughts in the desert ecosystem of Pakistan. *Ecological Indicators*, *159*(January), 111670. https://doi.org/10.1016/j.ecolind.2024.111670

Haile, B. T., Bekitie, K. T., Zeleke, T. T., Ayal, D. Y., Feyisa, G. L., & Anose, F. A. (2022). Drought Analysis Using Standardized Evapotranspiration and Aridity Index at Bilate Watershed: Sub-Basins of Ethiopian Rift Valley. *Scientific World Journal*, *2022*. https://doi.org/10.1155/2022/1181198

Hill, S., & Atnafu, S. (2011). *Using Satellite Images for Drought Monitoring : A Knowledge Discovery Approach Using Satellite Images for Drought Monitoring : A Knowledge Discovery Approach Getachew Berhan University of Pennsylvania Tsegaye Tadesse University of Nebraska-Lincoln*. *July*.

Iwata, T., Nishiyama, N., Nagano, K., Izumi, N., Tsukioka, T., Chung, K., Hanada, S., Inoue, K., Kaji, M., & Suehiro, S. (2012). Preoperative serum value of sialyl Lewis X predicts pathological nodal extension and survival in patients with surgically treated small cell lung cancer. *Journal of Surgical Oncology*, *105*(8), 818–824. https://doi.org/10.1002/jso.23002

J.A., C. (1960). A coefficient of agreement for nominal scales. *Educational And Psychological Measurement*, *XX*(1), 37–46.

Keith, L. (2017). *Environmental sampling and analysis: a practical guide*. Routledge.

Kim, H., Park, J., Yoo, J., & Kim, T. (2013). *ScienceDirect Assessment of drought hazard , vulnerability , and risk : A case study for administrative districts in South Korea*. 1–8.

Legesse, G., & Suryabhagavan, K. V. (2014). Remote sensing and GIS based agricultural drought assessment in East Shewa zone, Ethiopia. *Tropical Ecology*, *55*(3), 349–363.

Mera, G. A. (2018). Drought and its impacts in Ethiopia. *Weather and Climate Extremes*, *22*(September), 24–35. https://doi.org/10.1016/j.wace.2018.10.002

Montes-Vega, M. J., Guardiola-Albert, C., & Rodríguez-Rodríguez, M. (2023). Calculation of the SPI, SPEI, and GRDI Indices for Historical Climatic Data from Doñana National Park: Forecasting Climatic Series (2030–2059) Using Two Climatic Scenarios RCP 4.5 and RCP 8.5 by IPCC. *Water (Switzerland)*, *15*(13). https://doi.org/10.3390/w15132369

Negassa, W. (2017). Www.Shutturstock.Com. *Agricultural Drought Risk Area Assessment and Mapping Using Remote Sensing and Gis: A Case Study of West Hararge Zone, Ethiopia A*.

Qaisrani, Z. N., Nuthammachot, N., Techato, K., & Asadullah. (2021). Drought monitoring based on Standardized Precipitation Index and Standardized Precipitation Evapotranspiration Index in the arid zone of Balochistan province, Pakistan. *Arabian Journal of Geosciences*, *14*(1). https://doi.org/10.1007/s12517-020-06302-w

Queensland, S. (2021). *Drought Vulnerability Assessment Using Geospatial Techniques in*

Southern Queensland, Australia. 13–15.

Saha, A., Pal, S. C., Chowdhuri, I., Roy, P., Chakrabortty, R., & Shit, M. (2022). *Gondwana Research*. *xxxx*, 1–17.

Shah, S., & Iqbal, J. (2023). *Spatial – temporal variations of vegetation and drought severity across Tharparkar , Pakistan , using remote sensing-derived indices Sami Ullah Shah*. *August*. https://doi.org/10.1117/1.JRS.10.036005.

Svoboda, M., Hayes, M., & Wood, D. (2012). Spi Index for Diferent Locations. *World Meteorological Organization*, *1090*. https://digitalcommons.unl.edu/droughtfacpub

Tareke, K. A., & Awoke, A. G. (2022). Hydrological Drought Analysis using Streamflow Drought Index (SDI) in Ethiopia. *Advances in Meteorology*, *2022*. https://doi.org/10.1155/2022/7067951

Tefera, A. S., Ayoade, J. O., & Bello, N. J. (2019). Comparative analyses of SPI and SPEI as drought assessment tools in Tigray Region, Northern Ethiopia. *SN Applied Sciences*, *1*(10), 1–14. https://doi.org/10.1007/s42452-019-1326-2

Todisco, L. V. F., & Lena, B. Di. (2021). Evaluation of the similarity between drought indices by correlation analysis and Cohen ' s Kappa test in a Mediterranean area. *Natural Hazards*, *108*(2), 2187–2209. https://doi.org/10.1007/s11069-021-04775-w

Uttaruk, Y., & Laosuwan, T. (2017). *DROUGHT DETECTION BY APPLICATION OF REMOTE SENSING*. *18*(6), 115–121. https://doi.org/10.12911/22998993/76326

Viera, A. J., & Garrett, J. M. (2005). Anthony J. Viera, MD; Joanne M. Garrett, PhD (2005). Understanding interobserver agreement: the kappa statistic. Fam Med 2005;37(5):360-63. *Family Medicine*, *37*(5), 360–363. http://www1.cs.columbia.edu/~julia/courses/CS6998/Interrater_agreement.Kappa_statistic.pdf

Vries, D. (2010). *IVM Institute for Environmental Studies*.

Wako Duba, G., Tekalign, S., & Sishaw, T. (2021). Determinants Choices of Drought Coping Strategies Among Boorana Pastoral Communities: The Case of Yabello Woreda, Oromiya Region, Southern Ethiopia. *American Journal of Life Sciences*, *9*(4), 73.

https://doi.org/10.11648/j.ajls.20210904.13

Wangwongchai, A., Waqas, M., Dechpichai, P., Hlaing, P. T., Ahmad, S., & Humphries, U. W. (2023). Imputation of missing daily rainfall data; A comparison between artificial intelligence and statistical techniques. *MethodsX*, *11*(September), 102459. https://doi.org/10.1016/j.mex.2023.102459

Wilhite, D. A. (2000). *Drought Preparedness and Response in the Context of Sub-Saharan Africa*.

Wondimu, M. A., Erena, S. H., Reddy, R. U., Gebreselassie, T. A., Rao, P. P. J., Abraha, M. E., Rohland, E., García-Acosta, V., Government India, Imagery, S. R. G. B., Legesse, G., Suryabhagavan, K. V., Tamiru, H., Wagari, M., Abebe, W. T., Endalie, D., Muñoz, P., Orellana-Alvear, J., Bendix, J., … Segele, Z. T. (2022). Evaluation of the Performance of Remote Sensing-based Drought Indices for Agricultural Drought Characterization: The case of Tigray Region, Northern Ethiopia By. *Natural Hazards and Earth System Sciences*, *10*(3),446–473. http://dx.doi.org/10.1016/j.procs.2016.09.319%0Ahttps://www.elsevier.com/books/drought-early-warning-and-forecasting/funk/978-0-12-814011-6%0Ahttp://dx.doi.org/10.22192/ijamr.2018.05.06.006%0Ahttps://doi.org/10.1186/s40537-022-00683-3%0Ahttps://doi.org/10

Worku, M. A. (2024). Spatiotemporal analysis of drought severity using SPI and SPEI: case study of semi-arid Borana area, southern Ethiopia. *Frontiers in Environmental Science*, *12*(March), 1–15. https://doi.org/10.3389/fenvs.2024.1337190

Yuan, S., Quiring, S. M., & Patil, S. (2016). *SPATIAL AND TEMPORAL VARIATIONS IN THE ACCURACY*. *42*(1), 167–183. https://doi.org/10.18172/cig.2916

APPENDICES

Appendix I: Rainfall data used in study

year	Jan	Feb	Mar	Apr	May	June	July	August	Sep.	Oct.	Nov.	Dec.
1994	0	0.1	33	170.2	112.1	5	1.3	18.8	8	83.5	94.4	17.5
1995	0	50.6	108.3	190.4	30.7	24.4	2.7	3.1	53	107.5	22.8	3.3

1996	10.6	7	59.3	173.8	95.6	32	16	2.2	86	71	52.8	0
1997	0.8	0	27.2	235.6	34.2	12.6	14.8	0.1	11.8	244.3	198.2	26.2
1998	92	38.8	8.3	56.2	102.4	11.4	7.4	6.8	4.1	65.3	16.1	8.7
1999	0.3	3.1	179.3	24.4	14.1	0.4	13.5	1.1	18.2	84.9	15	17.8
2000	4.5	0	11.3	109.7	69	0	0	15.8	12.6	85.1	48.7	15.4
2001	53.1	5.3	99.7	103.1	12.3	2.3	11.3	17.9	15.6	74.6	17.4	0
2002	22.5	4.1	161	118.5	115.5	10.7	6.3	0.2	45.7	110	35.4	125.5
2003	15.7	4.2	72.7	188.1	166.2	0.1	1	33.5	2.2	24.7	64.4	31.4
2004	59.4	39.4	38.2	298.1	126.9	0	3.8	0	56.7	89.8	158.9	2.6
2005	19.4	22.8	58.1	175.5	142.4	16.3	9.9	0.8	4.6	108.6	54	0
2006	1.5	50	47.6	125	12.2	2.6	1.8	31.9	4.2	213.9	48.5	55
2007	0	14.2	44.3	199.6	85.8	16.3	38.1	17.2	47	69.4	54.2	0
2008	9.2	0	72.9	79.1	26	0	17.2	0	77.6	204.6	0	0
2009	30.8	0	72.2	123.8	147.8	0.6	1.8	2	44.5	105	24.3	58
2010	17.7	78.6	311.1	125.5	158.1	3.6	6.7	29.1	23.9	34.5	17.5	2.4
2011	0	29.9	18.6	75.6	82.7	18.9	17.6	0	12.1	91.3	145.2	12.8
2012	0	0	6	174.1	99	17.9	1.1	1.6	29.1	122.5	0	5.9
2013	32.1	0	120.3	142.9	19.4	14.5	5.8	10.1	78.6	125.9	0	0
2014	0.4	0	87.4	54.9	72.8	5.8	0.4	121.4	6.8	144.2	30.7	1.1
2015	0	4.1	50.9	123.5	79.3	52.4	0	5.9	6.7	112.7	80.1	50.1
2016	2.8	46	20	304.5	57.3	50.5	0	0	12.2	24.6	68.1	15.6
2017	1.2	14.5	54.4	18.3	82.2	0	14.8	31.3	80.7	215.7	37.8	0
2018	0	48	162	227.2	101	5.4	0.1	2.5	6.7	64.9	27.6	33.1
2019	2.9	3.6	15.1	87.4	74.3	155	14.8	1.6	31.7	188.7	133.7	71.1
2020	59.3	33.1	119.8	148.6	90.8	27.1	28.2	16.3	44.1	173.1	26.3	5
2021	15.82	10.55	10.55	119.25	169.71	11.46	36	44.79	47.2	79.76	166.45	17.87
2022	0	0	11.3	109.7	69	0	0	15.8	12.6	85.1	48.7	15.4

Appendix II: monthly total minimum temperature

Year	Jan	Feb	Mar	Apr	May	Jun	Jul	Aug	Sep	Oct	Nov	Dec
1994	12.8	13.7	15.9	15.7	15.7	14.3	13.5	14.1	14.6	15.1	15.4	12.6
1995	12.4	14.6	15.2	15.9	15.4	14.1	14.5	14.2	15.0	15.2	14.2	13.6
1996	14.3	15.3	16.0	15.8	15.4	15.2	13.5	13.5	14.4	14.4	13.4	11.7
1997	13.9	12.9	15.1	15.7	14.6	14.3	14.2	14.0	14.9	16.3	15.7	14.6
1998	11.8	12.6	14.6	15.6	15.4	13.8	13.2	13.8	14.1	14.9	11.9	12.8
1999	11.8	12.5	11.6	14.2	15.3	14.5	14.1	14.5	14.8	15.1	13.1	12.7
2000	12.6	12.9	15.6	15.5	15.0	14.5	13.6	14.0	14.1	15.2	13.2	12.0
2001	13.0	13.2	14.7	15.0	14.8	14.1	13.1	13.5	14.1	14.9	13.5	13.4
2002	13.8	13.4	14.9	15.3	14.8	13.1	14.5	14.2	14.9	15.2	12.7	12.4
2003	9.7	13.8	16.0	15.0	15.3	13.9	13.5	13.6	13.7	14.0	14.3	12.9

2004	14.2	13.5	14.0	15.7	14.7	13.4	12.5	13.1	13.9	15.1	15.0	12.7
2005	11.7	13.3	15.5	15.8	15.0	14.4	13.2	13.2	14.2	14.6	13.0	10.3
2006	13.3	15.0	15.7	15.7	15.7	14.6	14.6	14.7	15.3	15.7	13.9	12.8
2007	12.8	14.8	15.1	15.7	15.8	14.5	14.0	14.5	15.0	14.2	13.6	11.0
2008	13.1	13.5	14.8	15.6	15.2	14.6	14.4	15.2	16.1	15.8	10.8	11.2
2009	12.6	14.9	15.4	16.0	15.2	14.3	13.8	14.3	15.5	16.2	14.1	14.6
2010	12.8	16.3	15.7	16.3	16.3	15.0	14.2	13.9	14.7	15.0	12.8	11.8
2011	13.0	13.7	16.3	16.4	16.3	15.7	15.2	14.5	15.8	15.1	15.7	12.0
2012	11.2	12.1	14.6	15.8	15.6	15.3	14.4	14.4	15.6	15.9	14.4	13.5
2013	13.2	14.6	16.6	16.2	14.1	13.5	12.9	13.3	14.3	14.8	12.2	11.1
2014	12.6	14.4	14.9	15.7	15.8	15.2	15.2	15.3	14.7	15.9	14.4	11.5
2015	11.2	14.2	15.5	16.2	16.2	14.1	13.7	13.0	14.3	16.6	15.0	13.8
2016	14.3	14.3	17.0	17.0	15.1	14.4	13.4	13.9	13.4	15.3	14.2	11.0
2017	9.6	14.8	15.0	16.0	16.6	15.1	15.5	15.1	15.5	15.9	13.8	14.5
2018	11.5	14.4	15.0	15.9	15.1	14.5	13.9	13.6	14.4	15.2	14.6	14.0
2019	12.7	15.1	16.8	17.2	16.5	15.1	14.3	14.4	14.0	15.5	15.5	13.7
2020	12.7	13.9	16.8	16.6	13.3	13.4	13.6	14.7	13.2	15.4	13.0	10.9
2021	11.4	12.0	14.6	16.6	14.3	14.5	13.7	13.7	15.2	14.9	13.6	10.8
2022	13.2	12.7	15.9	16.2	15.7	15.6	13.9	14.5	16.1	14.1	13.8	11.1

Appendix II: Monthly total maximum temperature

Year	Jan	Feb	Mar	Apr	May	Jun	Jul	Aug	Sep	Oct	Nov	Dec
1994	29.59	30.47	29.21	25.91	24.35	24.27	23.59	24.45	26.66	25.95	25.37	27.10
1995	29.32	28.81	25.92	25.60	25.80	25.47	24.57	23.95	25.47	25.07	25.79	27.71
1996	28.89	30.44	28.07	26.07	24.65	22.68	22.69	25.04	25.60	25.35	26.00	27.50
1997	29.14	30.61	29.93	24.57	24.92	25.63	23.22	31.31	31.81	29.80	25.27	25.74
1998	28.80	30.62	33.69	33.88	29.94	29.46	27.26	28.97	31.37	30.08	30.73	30.96
1999	31.97	33.62	32.95	31.05	29.48	25.11	23.37	25.38	26.66	25.30	26.87	27.27
2000	29.50	31.41	34.07	32.82	31.37	30.74	29.55	29.59	31.25	28.48	29.68	31.30
2001	32.26	33.36	33.23	30.12	29.15	29.05	30.13	30.10	31.00	30.01	29.51	31.14
2002	30.25	30.18	27.24	26.22	24.07	23.07	24.73	24.53	25.90	24.48	26.48	26.14
2003	26.85	30.00	30.08	25.70	24.33	23.47	22.91	23.90	26.28	27.29	26.92	26.31
2004	27.23	28.18	28.96	25.11	24.53	23.84	24.19	24.94	26.49	25.88	24.37	26.09
2005	27.82	29.54	28.57	26.93	24.46	23.31	22.88	24.60	25.95	25.01	25.06	27.41
2006	28.76	28.74	28.35	25.26	25.91	25.27	23.92	24.26	26.02	24.67	24.87	25.13
2007	27.62	29.41	29.34	26.55	24.68	23.27	23.59	23.59	25.01	25.40	25.52	27.53
2008	28.23	29.07	28.56	24.96	25.02	28.83	23.01	24.63	26.69	29.40	29.31	27.74
2009	27.42	28.46	29.05	25.29	24.67	24.80	24.38	25.19	26.54	25.20	26.46	26.19
2010	27.41	28.24	26.32	25.60	24.62	24.02	22.81	23.49	25.28	25.55	26.79	27.43
2011	28.61	29.14	29.33	28.49	24.95	24.71	25.19	25.93	25.91	25.53	24.12	24.87

2012	27.99	29.19	29.67	25.98	24.88	24.89	24.16	25.82	26.34	25.36	30.47	26.96
2013	28.17	27.45	27.68	25.36	24.58	23.40	23.40	23.88	26.34	24.74	29.03	31.47
2014	29.04	28.65	28.10	26.25	25.77	25.82	24.25	24.65	24.84	24.45	25.29	27.45
2015	29.18	30.29	29.18	26.23	25.19	25.12	24.61	26.33	28.16	25.91	25.25	26.90
2016	29.20	30.10	26.24	26.24	24.34	23.80	24.21	24.86	26.13	26.67	26.38	27.24
2017	29.04	29.12	29.86	27.23	26.43	25.40	24.69	25.11	25.18	24.95	24.95	27.10
2018	28.95	28.78	25.79	25.07	24.52	23.01	22.55	24.39	26.91	25.84	26.64	28.08
2019	33.37	34.11	35.05	32.44	25.64	23.74	24.75	25.99	26.97	24.81	25.13	26.10
2020	30.88	33.55	34.54	31.71	25.61	25.03	27.28	28.58	31.63	28.95	29.37	31.50
2021	31.12	33.32	33.44	32.40	27.26	28.44	28.00	31.05	30.31	30.74	31.74	29.35
2022	31.19	34.68	34.39	34.47	30.08	29.48	29.55	31.40	31.48	32.18	33.26	30.18

Appendix IV: Potential evapotranspiration (PET)

Year	Jan	Feb	Mar	Apr	May	Jun	Jul	Aug	Sep	Oct	Nov	Dec
1994	55.30	74.74	106.33	115.19	126.81	138.26	136.40	123.49	104.75	72.60	44.94	43.75
1995	55.04	68.20	90.65	112.29	141.02	149.43	140.24	119.61	96.62	68.48	47.84	44.08
1996	52.06	72.41	99.89	116.13	131.42	118.29	128.77	130.74	99.44	71.52	49.61	45.33
1997	53.18	76.18	112.12	105.42	137.39	150.00	129.89	174.62	132.94	86.27	44.07	51.17
1998	38.69	54.39	76.60	132.24	169.87	176.05	184.07	168.65	158.17	132.33	90.21	63.21
1999	51.58	61.70	85.97	133.61	155.14	172.70	144.45	131.43	129.23	104.23	69.73	52.15
2000	43.96	55.30	78.70	132.11	163.07	189.00	192.01	185.79	162.03	131.68	82.96	59.28
2001	52.86	61.46	84.38	129.76	146.54	171.64	179.55	192.09	167.27	130.30	89.86	58.55
2002	51.42	55.94	74.19	98.42	118.96	129.46	133.42	141.57	123.88	99.65	66.00	51.65
2003	41.91	51.70	73.11	110.55	116.57	128.64	132.81	130.53	121.51	105.37	80.63	50.77
2004	41.78	48.15	67.75	109.58	109.48	133.75	138.75	146.16	131.37	106.08	72.29	42.80
2005	41.48	52.24	72.41	103.92	122.13	131.77	128.82	131.84	128.51	102.02	69.70	47.63
2006	46.23	52.85	67.36	102.23	110.82	140.76	145.17	133.95	119.40	98.93	65.47	45.88
2007	39.31	50.59	69.85	108.87	119.77	129.50	128.23	134.01	115.19	93.82	72.37	47.99
2008	45.93	51.84	70.51	105.67	108.69	135.60	175.79	126.90	119.91	100.08	85.64	60.66

2009	46.19	50.33	66.51	106.64	109.27	132.59	142.88	141.67	128.64	101.20	66.49	49.88
2010	39.70	50.18	63.41	91.25	110.29	125.68	131.80	125.89	117.04	96.65	71.12	52.33
2011	45.05	52.83	70.55	105.84	130.59	128.55	134.60	141.75	133.15	96.57	70.63	40.76
2012	39.67	53.06	72.80	111.87	115.19	132.16	138.27	137.08	132.71	99.79	68.03	60.04
2013	42.49	51.60	63.70	95.87	108.88	137.00	134.50	137.66	122.61	104.04	68.01	58.62
2014	53.78	54.19	67.89	102.96	117.64	138.93	147.37	133.72	119.91	94.01	63.69	46.26
2015	45.35	55.77	73.46	107.03	115.41	131.81	146.58	144.04	141.81	114.17	68.39	45.18
2016	42.08	52.90	72.80	86.31	111.77	130.12	133.43	142.27	127.53	105.24	75.05	49.51
2017	45.35	56.66	68.89	111.87	123.58	140.79	144.17	135.90	124.29	93.21	66.00	46.20
2018	41.76	55.03	68.39	90.39	108.52	131.52	125.49	125.44	125.12	106.77	71.72	49.67
2019	44.45	64.27	84.65	134.70	155.58	134.06	129.16	142.80	134.34	108.22	66.53	44.02
2020	40.52	58.41	84.28	132.09	152.33	149.22	148.84	167.00	152.47	135.60	84.50	58.70
2021	53.94	60.08	85.47	130.98	157.09	158.50	172.79	172.93	173.47	124.01	92.86	64.15
2022	49.72	58.70	89.04	133.14	172.23	176.11	177.25	184.98	173.62	128.20	100.09	67.83

Appendix V: Climatic water balance (CWBAL)

Year	Jan	Feb	Mar	Apr	May	Jun	Jul	Aug	Sep	Oct	Nov	Dec
1994	71.8	53.0	16.7	183.1	219.2	14.9	1.0	0.0	0.4	29.7	18.5	15.6
1995	-55.3	-74.6	-73.3	55.0	-14.7	-133.3	-135.1	-104.7	-96.8	10.9	49.5	-26.3
1996	-55.0	-17.6	17.7	78.1	-110.3	-125.0	-137.5	-116.5	-43.6	39.0	-25.0	-40.8
1997	-41.5	-65.4	-40.6	57.7	-35.8	-86.3	-112.8	-128.5	-13.4	-0.5	3.2	-45.3
1998	-52.4	-76.2	-84.9	130.2	-103.2	-137.4	-115.1	-174.5	-121.1	158.0	154.1	-12.5

1999	37.6	-37.8	-123.9	-113.7	-73.6	-172.7	-161.2	-151.4	-128.2	-24.9	-47.1	-42.9
2000	-61.4	-82.9	45.7	-130.7	-158.6	-144.0	-117.9	-128.1	-86.0	15.2	-37.2	-26.2
2001	-50.8	-78.7	-120.8	-53.4	-120.0	-291.0	-185.8	-146.2	-119.1	2.1	-10.6	-37.5
2002	-8.4	-79.1	-30.1	-43.4	-159.3	-177.3	-180.8	-149.4	-114.7	-15.3	-41.1	-51.4
2003	-33.4	-70.1	62.6	-0.5	-14.0	-122.7	-135.3	-123.7	-54.0	44.0	-16.2	83.6
2004	-36.0	-68.9	-37.9	71.5	37.6	-132.7	-129.5	-88.0	-103.2	-55.9	13.6	-10.4
2005	11.2	-28.4	-71.4	188.6	-6.9	-138.7	-142.4	-131.4	-49.4	17.5	116.1	-38.9
2006	-32.8	-49.6	-45.8	53.4	10.6	-112.5	-121.9	-127.7	-97.4	38.9	6.4	-46.2
2007	-51.4	-17.4	-54.6	14.2	-128.6	-142.6	-132.1	-87.5	-94.7	148.4	2.6	15.7
2008	-50.6	-55.7	-64.6	79.8	-43.7	-111.9	-95.9	-98.0	-46.8	-3.0	6.2	-45.9
2009	-42.6	-70.5	-32.8	-29.6	-109.6	-274.8	-109.7	-119.9	-22.5	119.0	-159.7	-46.2
2010	-19.5	-66.5	-34.4	14.5	15.2	-142.3	-139.9	-126.6	-56.7	38.5	-25.6	18.3
2011	-32.5	15.2	219.8	15.2	32.4	-128.2	-119.2	-87.9	-72.8	-36.6	-34.8	-42.6
2012	-52.8	-40.6	-87.2	-55.0	-45.8	-115.7	-124.1	-133.2	-84.5	20.7	104.4	-26.9
2013	-53.1	-72.8	-105.9	58.9	-33.2	-120.4	-136.0	-131.1	-70.7	54.5	-159.0	-36.6
2014	-19.5	-162.7	24.4	34.0	-117.6	-120.0	-131.9	-112.5	-25.4	57.9	-157.6	-152.8

2015	-53.8	-67.9	-15.6	-62.7	-66.1	-141.6	-133.3	1.5	-87.2	80.5	-15.6	-44.3
2016	-55.8	-69.4	-56.1	8.1	-52.5	-94.2	-144.0	-135.9	-107.5	44.3	34.9	8.0
2017	-50.1	-26.8	-66.3	192.7	-72.8	-82.9	-142.3	-127.5	-93.0	-50.5	18.6	-29.8
2018	-55.5	-54.4	-57.5	-105.3	-58.6	-144.2	-121.1	-93.0	-12.5	149.7	-8.4	-140.8
2019	-55.0	-20.4	71.6	118.7	-30.5	-120.1	-125.3	-122.6	-100.1	-6.8	-22.1	-11.3
2020	-61.4	-81.0	-119.6	-68.2	-59.8	25.8	-128.0	-132.7	-76.5	122.2	89.7	30.6
2021	0.9	-51.2	-12.3	-3.7	-58.4	-121.7	-138.8	-136.2	-91.5	88.6	-32.4	-48.9
2022	-44.3	-74.9	-120.4	-37.8	11.2	-161.3	-136.9	-128.7	-76.8	-13.1	102.3	-31.8

Appendix VI: Steps used to calculate SPI

The steps required to calculate SPI values after precipitation data were organized and arranged in Microsoft Excel 2016 and imported to Studio using SPEI Package loaded in console part of Rstudio Software was as follows:

```
>install. Package ("SPEI")
> Library (SPEI)
# Package SPEI (1.8.1) loaded [try SPEINews()].
> Library (SPEI)
> Library (readxl)
> YabelloSPIdata <- read_excel("E:/my research data/yabelo rainfall/spi by Rstudio/YabelloSPIdata.xlsx")
> View (YabelloSPIdata)
> spi3<-spi(YabelloSPIdata$precip,3)
```

Where, YabelloSPI is the data used.

Appendix VII: Steps followed to obtain SPEI

SPEI was calculated using hargreave method using Rstudio software/R-programming typing in R console part as the following below.

>yabelloSPEIdata$PET<-Hargreaves(Tmin=yabelloSPEIdata$Tmin,Tmax= yabelloSPEIdata$Tmax, lat = 45.057)...enter

> YabelloSPEIdata$PET…...enter. At here PET obtained.

Then to Calculate CWBAL:

>CWBAL<-yabelloSPEIdata$precip-yabelloSPEIdata$PET

> CWBAL

Finally after CWBAL Was obtained, to obtain SPEI at different time scales:

>spei3<-spei (CWBAL, 3)

>spi6<-spei(CWBAL, 3) …….follow similar steps to calculate other selected time scales.

Where, yabelloSPEIdata is name of data used to calculate SPEI at required time scales